Analysis of Subsurface Geology, including the Parautochthonous Breccias, Flynn Creek Impact Structure, Tennessee

by

Matthew Christian Adams

A thesis submitted to the Graduate Faculty of
Auburn University
in partial fulfillment of the
requirements for the Degree of
Master of Science

Auburn, Alabama
December 14, 2019

Keywords: impacts, cratering, melts,
carbonate target, subsurface breccias

To be Approved by

David T. King Jr., Chair, Professor of Geology
Willis E. Hames, Professor of Geology
Steven J. Jaret, Kathryn W. Davis Postdoctoral Fellow - American Museum

Abstract

The present study concerns the Flynn Creek impact structure, Tennessee, which is estimated to have formed approximately 382 million years ago in a shallow marine environment. The present crater is about 3.8 km in diameter at its widest part, and has a non-circular, asymmetric outline. The target was the epicontinental shelf of the Chattanooga Sea, which was underlain by Ordovician carbonates that were deformed during the impact. Impact produced a structure with wide, terraced rims formed by extensive post-impact slumping, a shallow bowl-shaped inner crater of about 2 km in diameter, and slump-derived topographic features, including a central slump-produced mound that has been interpreted in the past as a central peak. Twenty-one drill cores with more than 3 km of total core length have been analyzed using high-resolution photographs in order to provide a detailed analysis of the subsurface stratigraphy of this impact structure. For example, an abundance of previously unknown impact-related breccias have been discovered at depths within and below the crater bowl. Observation and description of these drill cores combined with a petrographic analysis of selected samples from some of the deeper breccia zones suggests a new interpretation of Flynn Creek impact structure as a small simple crater of about 2 km diameter that is surrounded by relatively large concentric slump features. In the rocks beneath the simple crater bowl, i.e. in Flynn Creek's parautochthonous breccia zone, otherwise rare melt-bearing textures are found to be relatively common.

Acknowledgements

I would like to thank the National Aeronautics and Space Administration, Planetary Geology and Geophysics Program, for supporting the project proposal (NASA PGG NNH14AY73I) by Justin Hagerty et al. and the subcontract support from the USGS Astrogeology Science Center, Flagstaff, which was awarded to Auburn University. I would also like to thank the USGS Astrogeology Science Center, Flagstaff for the creation and organization of the Flynn Creek drill-core collection, and in the present study, providing images, data, documents, and many other forms of assistance (e.g., sampling). Additionally, I was helped tremendously by my undergraduate apprentice, Sam Warren. My committee was all tireless in their ability to get edits back to me quickly and answer any questions that I may have. I'd like to thank Dr. King personally for his mentorship over the last two years. Lastly, I'd like to thank my dog, Scooter, who was always there to cheer me up when the stress ever became a bit too much.

Table of Contents

List of Figures

Introduction

The Flynn Creek crater is a marine-target impact structure of approximately 3.8-km apparent diameter, located approximately at 36° 17' N; 85° 40' W, which is within what is now the Eastern Highland Rim physiographic province of Jackson County, Tennessee (Roddy, 1968; Adrian et al., 2018). Currently the most accurate age constraints place the timing of impact at ~ 382 million years ago, making it a Late Devonian event (Schieber and Over, 2005; De Marchi et al., 2019b). Other noteworthy features found within the Flynn Creek impact structure are a centrally located mound previously interpreted as a central uplift, a terraced crater rim that was formed by several concentric slump features, a crater bowl-filling stratigraphic unit, marine resurge deposits, parautochthonous breccias below the crater bowl, and a post-impact crater-filling deposit (the Chattanooga Shale). We can see these different features within the USGS collection of 21 different drill cores, which have been recovered from various points around the crater. My primary area of focus will be centered on the crater's subsurface stratigraphy (the crater-bowl filling unit and the parautochthonous breccias below the crater bowl), where varying segments of impact-related breccia and intercalated undeformed bedrock can be found.

The original target stratigraphy of the area at the time of impact was principally flat-lying, therefore any deformation noted in outcrop or drill core can be interpreted to have been caused by the impact itself (Roddy, 1979). Said target stratigraphy is comprised mostly of Ordovician carbonates, which include, in stratigraphic order, the Knox Group, Stones River Group, and Catheys-Leipers Formation. All these stratigraphic units are represented within a small area of strongly localized deformation, which defines the Flynn Creek crater. The uppermost target layer is thought to have been a very thin bed of Upper Devonian Chattanooga

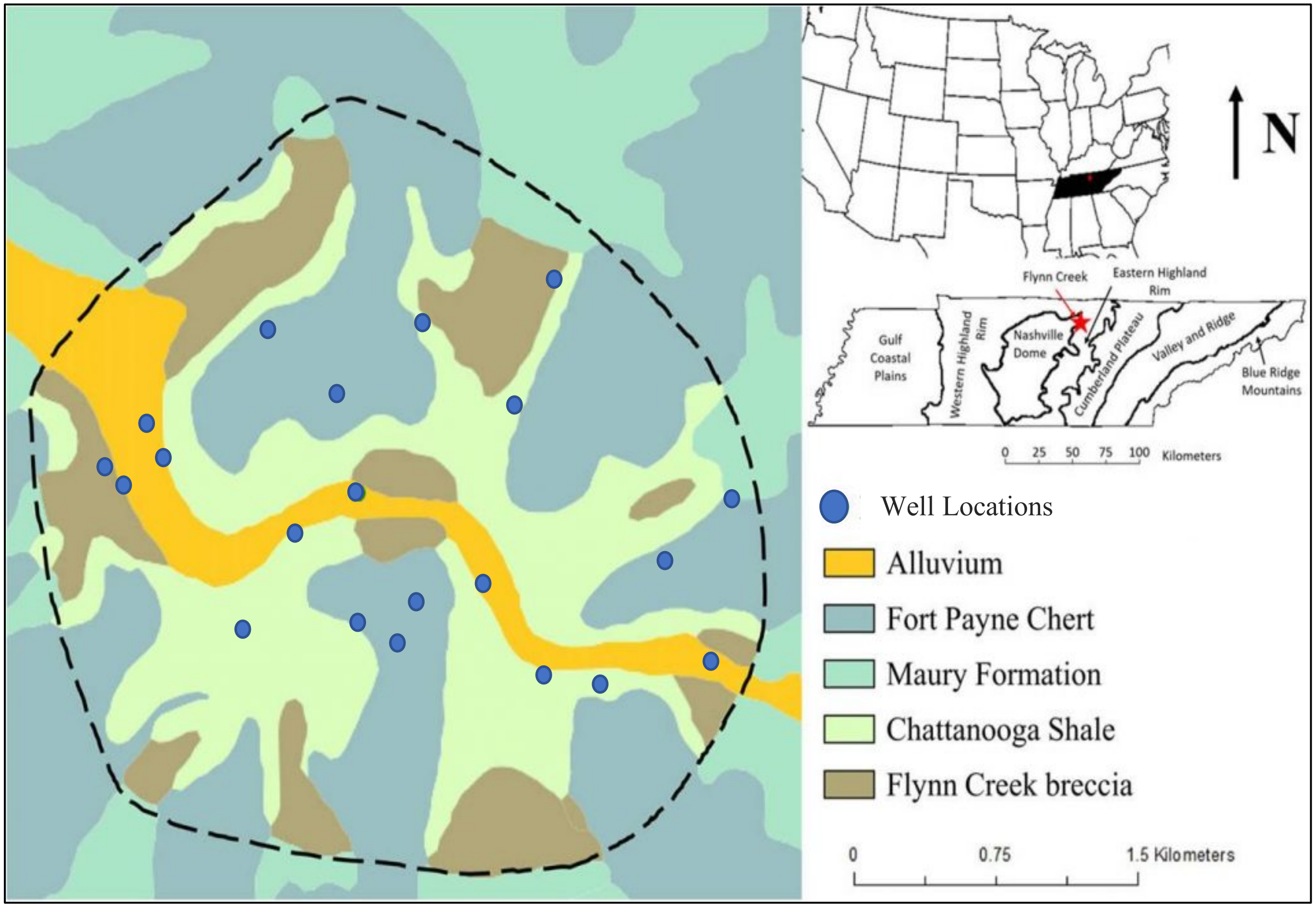

Figure 1: Flynn Creek crater area geologic map with all drill core locations marked (after Adrian et al., 2018).

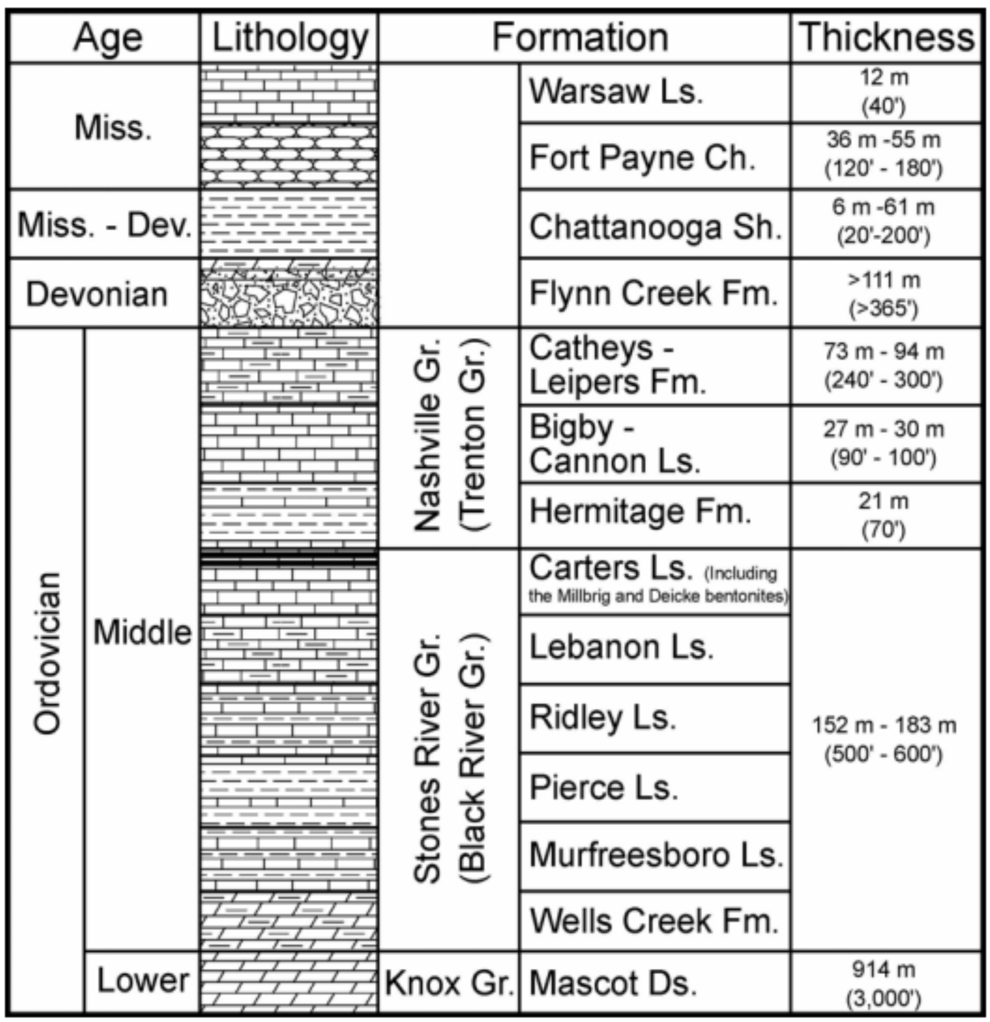

Figure 2: Gainesborough Quadrangle stratigraphy of the Flynn Creek study area (from Evenick, 2007).Please note that theFlynn Creek is referred to here as a “formation,” but in fact it is an informal unit called ‘Flynn Creek breccia’ (Adrian et al., 2018). The Flynn Creek’s stratigraphic relationship above is schematic. The Maury Formation, shown in Figure 1, is included in this present study as the basal unit of the Ft. Payne Chert.

shale that was lying upon a thin, weathered debris layer that was, in turn, lying atop the eroded Ordovician stratigraphic section (De Marchi et al., 2019b). A stratigraphic column of the Gainesborough Quadrangle is provided in Figure 2 to better understand the age order and thicknesses of the aforementioned, and younger, units as they exist in the Jackson County area.

Post-impact deposition/erosion cycles have obscured many expected features and structures that are typically found at terrestrial impact structures such as Flynn Creek. However, there is still much field evidence to be found upon close examination. Uplift near the Nashville Dome has yielded an increase in erosion of the Flynn Creek area, which has helped to expose several outcrops that were key to identifying the structure at Flynn Creek as one of impact origin (Roddy, 1968; 1979). One of the more interesting facets of this crater is the fact that some of the target strata have been locally displaced. For example, there are several outcrops within the crater exhibiting completely overturned strata, with younger layers under older layers (Roddy, 1968). Additionally, there are several small sites with well-known shatter cones, which are well developed in some of the finer limestone beds within the crater's interior area (Roddy, 1966).

The late David Roddy spent considerable time over much of his career with the USGS studying Flynn Creek. Many of his ideas were considered controversial at a time when impact crater studies were few and there were no well-accepted hypotheses or terminologies for classification. Despite this, he went on to establish the Flynn Creek structure as one of the first six recognized impact craters on Earth. Having been such a hotbed of both controversy and scientific research, there is certainly valuable information to be gained from continued research of an area with many key questions left unanswered.

The aim of this research is to shed some light on previously unexamined aspects of the impact structure at Flynn Creek by providing an in-depth analysis for a part of the area that has been relatively unexplored, specifically the subsurface aspects of the crater-bowl filling unit and the parautochthonous breccias below the crater bowl. David Roddy expedited Flynn Creek core drilling and carefully collected and archived the drill cores. In his early papers and in his subsequent work on this structure, he provides a wealth of information to examine in light of new theories for crater formation. However, no study has ever included analysis of all 21 drill cores at Flynn Creek, which were examined in the present study. Four of the drill cores penetrate below Flynn Creek's crater bowl and into the realm of the parautochthonous breccias, and thus provide insight into sub-crater rock deformation. The present work provides a thorough examination of each of the 21 drill cores via high-resolution imagery, to provide new and unique insight as to the chaotic nature of the crater's subsurface as a whole. As is typical of many impact craters, little attention has been given to deeper crater features that underlie the crater bowl of Flynn Creek, even though it makes sense that these catastrophic impact effects would profoundly alter these rocks. Thus, re-examination of Flynn Creek work to provide a more thorough assessment of features surrounding its crater bowl will be useful to studies of similar impact features in general.

Previous Work

Over the past 90 years, there has been much controversy surrounding the study and classification of the Flynn Creek structure. This is to be expected as the study of impact geology is relatively young, Roddy's work was in the vanguard, and the hypotheses and theories of crater formation have been evolving constantly since it was first imagined. Much interest has been garnered within the scientific community about Flynn Creek since it was initially studied by Lusk (1927), who interpreted it as a giant sink hole after he noted the extreme differences in shale thickness in the area. Following this, a research team comprised of Wilson and Born (1936) argued that “all the data accumulated indicates a crypto-volcanic origin of the structure.” Interestingly, the unusual features of Flynn Creek were noticed even before Lusk’s day, namely in Safford’s *Geology of Tennessee* (1869), but was written off as merely an enigmatic disturbance in the local geology (Ford et al., 2013). Despite having been recognized and preliminarily studied for several decades, the structure went through several more mistaken classifications until, in 1946, Robert Dietz, a key researcher who helped pioneer the field of impact research, publicly disagreed with the many previous workers and argued that the area more closely resembled a small lunar crater than any sort of structure such as a crypto-volcano or karstic sinkhole (Ford et al., 2013; Dietz, 1963).

Study of the Flynn Creek crater saw no real advancement past Dietz’s suppositions, until USGS geologist David Roddy (1966) revisited Jackson County during the 1960s and continued to work in the area periodically over the ensuing 20 years. Eventually, he presented convincing evidence and thus classified the structure as a meteorite impact crater (Roddy, 1968; 1979; Evenick et al., 2004; Ford et al., 2013; Adrian et al., 2018). Once the site was identified as such in peer-reviewed literature, Flynn Creek attracted much more attention as one of the (then) six known impact craters on Earth. Today, it is one of the approximately 200 known impact structures worldwide and one of the two presently verified impact structures located in Tennessee. Roddy, along with the help of several other geologists, gathered many drill cores for later study, while at the same time conducting extensive field work. In total, there were 21 complete cores taken from the Flynn Creek study site; six during 1967, three during 1977, and twelve over the course of 1978 and 1979, all of which are examined for the research presented in this paper. All but one was usable for the present study.

Figure 1 shows the location of the drill cores used in the present study. This drill-core collection is presently at the USGS office in Flagstaff, Arizona, where it has been archived and photographed for scientific access (Hagerty et al., 2013; Gaither et al., 2015).

In the early days of Roddy's study of Flynn Creek, as he was completing his 1966 dissertation on Flynn Creek at the California Institute of Technology, he was focused on the shallow deformation of the rocks at and just below the crater floor, and the structural properties of the crater floor itself. His aim was more towards classification as an impact structure versus a deeper understanding of Flynn Creek's origins. During this phase of Roddy's study, the outcropping sedimentary fill of the crater was also well described with much of the reworking of the bedded breccias into non-bedded breccias being attributed to resurge processes, which reinforced an influence of a shallow marine setting (Roddy, 1966; 1968).

During the late 1970s, however, a newer round of drill cores completed in the area provided access to more than 500 meters of unseen stratigraphy from below the crater floor, allowing for access to geologic features from deeper than any of the earlier drilling programs (Roddy, 1979; Roddy, 1980). The data retrieved from the cores permitted Roddy to classify the structure holistically as a complex, shallow-marine-target impact crater (Roddy, 1979; De Marchi et al., 2019b). Additionally, he was able to create a shallow stratigraphic cross-section of the stratigraphy of the crater fill and near-surface geology (Fig. 3). Despite having these deeper cores, the focus at that time was on developing his model for rim, crater moat, and what he interpreted as a central peak, which left the deeper subsurface descriptions from below the crater floor for another time. As such, beyond describing the stratigraphy as "essentially flat-lying with minor brecciation", except for the central area, there was not much more information provided as to the deeper subsurface characteristics and potential correlations.

Following David Roddy's death in 2002, the drill cores were at risk of loss to the impact community until Justin Hagerty, John McHone, and Tenielle Gaither at the USGS, Flagstaff, started a project to preserve them. With the support of the USGS, the aforementioned group of scientists "rescued" the cores and had them shipped to Flagstaff so that future generations of scientists would be allowed the opportunity to study and learn from them (Hagerty et al., 2013; Gaither et al., 2015). It was not until Jonathan Evenick and his colleagues re-examined the field area in preparation for the 2005 Meteoritical Society meeting in Knoxville, Tennessee, and related Flynn Creek field trip (Evenick et al., 2004; Evenick and Hatcher, 2007) that interest in the site really began to increase once again. Recently, another field trip to the area, this time sponsored by the Southeastern Section of the Geological Society of America, in connection with the annual meeting held during 2018 in Knoxville, Tennessee, helped revive interest in the area (Jaret and King, 2018).

Geologic Setting

As is typical of western and central Tennessee geology, many of the sedimentary rocks exposed at the Flynn Creek site and the surrounding areas consist of flat-lying Paleozoic limestones and dolostones with much smaller amounts of shale and sandstone present within the area (Conant and Swanson, 1961; Roddy, 1966). More specifically, the rocks located at the site of impact deformation are a very thick section of Lower Paleozoic limestone and dolomites overlying a crystalline basement layer (Gaither et al., 2015), most of which was unaffected by the impact's deformation. Many of the older rocks found at or near the surface are limestones and dolomites that include the Ordovician Knox Group and some overlying Ordovician

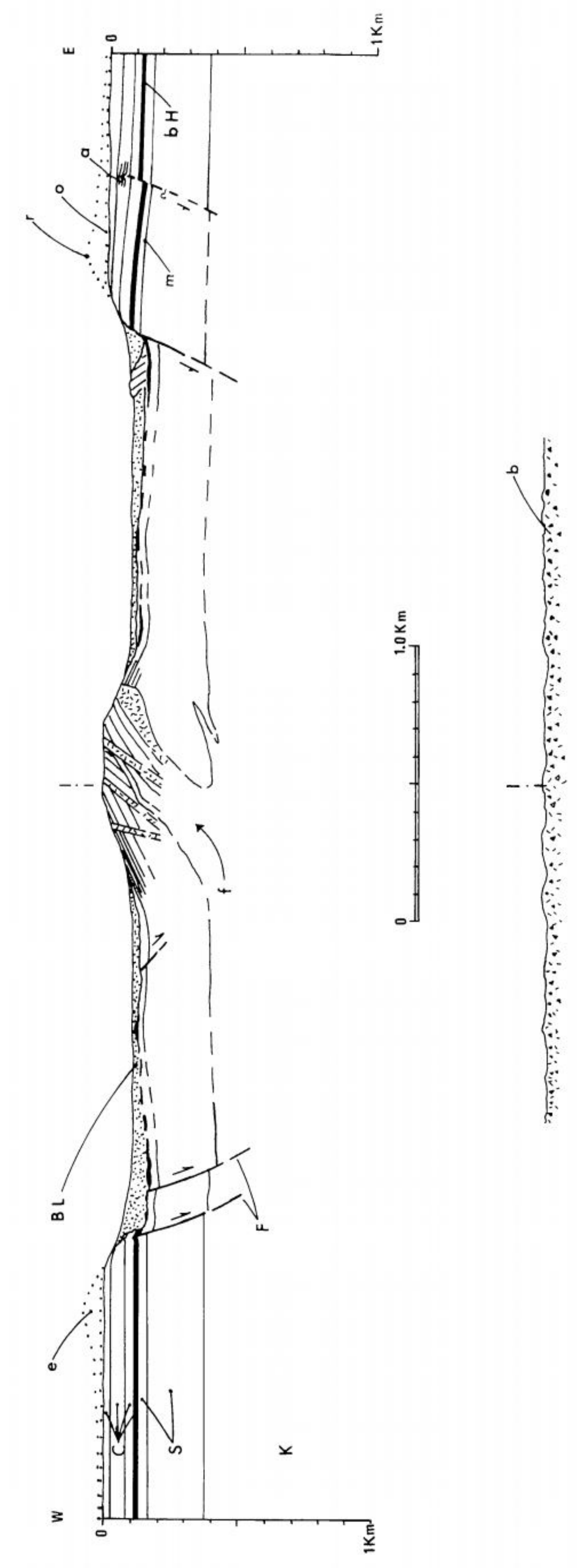

Figure 3: Detailed geologic cross-section of the Flynn Creek impact structure based upon extensive surface mapping and a long-running drill core operation of the area, as compiled by Roddy (1979). There is no vertical exaggeration and the symbology as depicted by Roddy is as follows: C = carbonate section of limestone and argillaceous limestone; S = Stones River Group of carbonates; K = Knox Group of carbonates; b = crystalline basement; BL = breccia lens; bH = base of the Hermitage Formation; a = asymmetric anticline; f = flow direction of Knox rocks in central uplift; F = single faults to show regions of extensive faulting; m = a marker bed; o = pre-impact original ground level; and r = estimated rim crest. Note that the location of drill cores that may have constrained this cross-section model are not marked, suggesting that the cross section is largely based on surface exposures. Taken from Roddy (1979).

carbonate units. Because the Knox Group in the crater area is approximately one-kilometer thick, major target deformation is not thought to extend below this layer (Roddy, 1966; 1968).

Starting from the top, the mappable stratigraphy of the crater area consists of about 50 meters of Fort Payne Chert, including a basal unit (Maury Formation) of a few meters thickness that consists of shale and limestone. This is underlain, in reverse stratigraphic order, by the Chattanooga Shale (up to 60 m within the impact structure but typically 10 m or less outside the structure), the Flynn Creek breccia (up to 175 m in thickness according to Adrian et al, 2018), and the locally brecciated Ordovician limestones and dolostones discussed earlier (Conant and Swanson, 1961; Roddy, 1966). The Chattanooga Shale, which was just beginning to be deposited at the time of impact, consists of a lower member that fills the Flynn Creek impact structure and an upper member covers the whole of the area (Schieber and Over, 2015; De Marchi et al., 2019b). The informal Flynn Creek breccia, which consists of all the fragmental materials that fill the crater bowl and moat and that surround and cover parts of what Roddy called the central uplift. Grain sizes in this impact breccia include particles ranging from clay-sized to mega-blocks that are several meters across. Studies of this unit have found a paucity of very minute shale clasts within the breccia, which are interpreted as fragments of lowermost Chattanooga Shale (discussed by De Marchi et al., 2019b). It was from these few clay particles that Schieber and Over (2015) were able to retrieve Devonian conodonts in order to determine the most accurate biostratigraphic age estimate of the time of impact, which is ~ 382 m. y. ago.

Methodology

As with recent studies of the Flynn Creek impact structure, namely work by Adrian et al. (2018), Adrian et al. (2019), and De Marchi et al. (2019b), the present research has revolved around the study and analysis of the USGS Flynn Creek drill core collection and sedimentological and structural information that can be obtained from those drill cores. Both Adrian et al. (2018; 2019) and De Marchi et al. (2019b) provided in-depth analysis for one and two drill cores respectively, however, the present work includes a review and characterization of drill cores in the Flynn Creek area, utilizing all twenty-one drill cores available in the USGS collection. Adrian et al. (2018) studied the apparent central uplift with the core FC77-1, and De Marchi et al. (2019b) focused on resurge deposits within the crater moat area using cores FC77-3 and FC67-3. Adrian et al. (2019) focused on the marine resurge gullies and overall marine-target morphology of the crater. All previous studies, including those of Roddy (1968; 1979) and Schieber and Over (2005), focused only on the shallow reaches of the crater, not the deeper subsurface realm. The present research differs from these also because it includes an examination of all drill cores including the four deeper drill cores, which penetrate the entire crater-bowl filling unit and into sub-crater rocks (i.e., the parautochthonous breccias).

The present research has two phases: phase one is a study of the drill cores using high-resolution core-box photographs and phase two is a petrographic study of some deep-seated Flynn Creek impact breccias from the sub-crater (parautochthonous) breccia lens. For the first phase, approximately 1500 high-resolution core-box photographs were analyzed and classified for the purposes of correlation and interpretation. For the second phase, a total of 33 thin sections (covered and uncovered) were prepared from samples in sub-crater breccia zones. Upon request, the USGS office in Flagstaff, Arizona, provided hand-cut, half-core segments that were used for petrographic thin-section making at a commercial laboratory. Thin sections were chosen on an individual basis after carefully examining the returned samples from one of the deeper drill cores (namely, core number FC77-3). These thin sections were analyzed for their petrologic characteristics and elemental composition.

Phase One – Drill-Core Analysis

Using USGS-provided high-resolution imagery, each box of core from each of these drill cores have been carefully analyzed and coded in the present research according to the nature and amount of breccia and bedded target rock observed in each core. Bedded target rock was considered as either horizontally oriented or inclined. Breccia was coded according to the average coarseness of texture. Furthermore, intervals of shale were noted in the upper sections of some drill cores which are likely the Chattanooga Shale. i.e., the post-impact crater-filling unit. Flynn Creek breccias were subdivided into four standard size categories of fine (average clast diameter, or ACD = 2-6mm), medium (ACD = 6-20mm), coarse (ACD = 20-60mm), and very coarse (ACD >60mm). This was done for the shallow, moat-filling resurge breccias as well as crater-bowl filling breccias. Figure 4 shows the results from an initial attempt at core-box coding for lithology, including breccia textures. These results lead to the inference that that there are many levels of breccia within the impact structure, and that a more detailed study, employing all drill cores is warranted. Multiple investigators, working together at the same time, were engaged in the drill-core analysis phase, which ensured accuracy and consistency in lithological identification.

After a methodical review of all Flynn Creek drill-cores at a fine-scale, the present study was able to help define selected intra-crater features such as (1) base of the crater bowl, (2) variations in texture within the crater-bowl filling unit, (3) top of the crater-bowl filling unit (or the “crater floor” according to Roddy (1968;1979)), and (4) base of the Chattanooga Shale (i.e., the base of the post-impact unit).

After completion of the core-box coding of the all the drilled subsurface strata, lithological findings were combined with a digital elevation model to produce a three-dimensional representation of the crater’s subsurface realm, detailing the depths and breccia content of each of the cores relying on my previous interpretations. This was accomplished by downloading the digital elevation model of the Gainesborough (Tennessee) quadrangle from an on-line database (Lakes Environmental Software, 2019) and converting it into a topographic map using free online software known as Quantum Geographic Information System (QGIS). Then, it was possible to convert this topographic map into a three-dimensional representation of the surface surrounding the crater and then overlay it onto an existing geologic map of the crater by matching up point of equal latitude and longitude using free online software known as SketchUp (Schell, 2000). The combination of these two parts allows a clearer view of the breccia distribution within the crater-bowl filling unit and in the sub-crater (parauthochthonous) breccia lens.

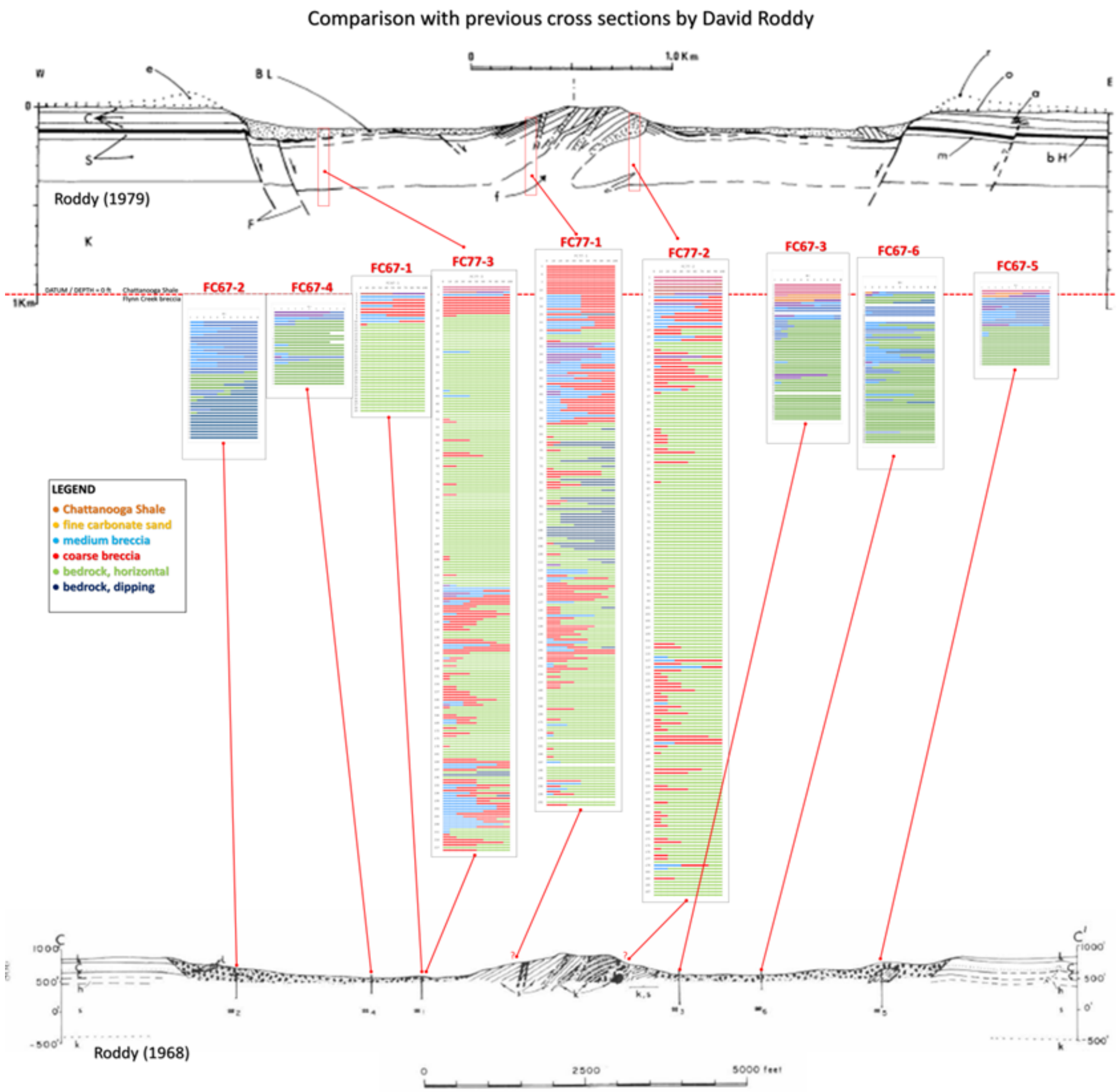

Figure 4: Initial drill-core box coding done by King et al. (2017), which compared David Roddy's cross-sections (1979) above and 1968 below) with subsurface data for selected drill cores. Color code for breccia textures, horizontal bedrock, and dipping bedrock are shown at left. Each horizontal line in each core-box histogram plot is one core box or about 10 feet (3.3 m) of section. Figure from King et al. (2017).

Phase Two - Petrographic Analysis

The petrographic analysis is broken down into two parts with the primary objective being the observation and classification of selected thin-sectioned intervals taken from drill core FC77-3. This drill core was determined to be generally representative of the parautochthonous (sub-crater bowl) breccias, and thus was the focus of this phase of the present study (see core box photo in Figure 5). Most of the thin sections that were made for the present study were taken from a swath of breccia situated at a depth of 512.6 to 626.2 meters in this drill core. In addition, the present study included, a few other selected thin sections that portrayed interesting textures and possible melt content were chosen from drill core FC77-3. Melt particles, that were previously reported as rare in some crater-moat breccias (as noted by Adrian et al., 2018; De Marchi et al., 2019b), were found to be rather common within deeper thin sections used in the present study.

Selected thin sections were further examined on a JEOL-8600 Microprobe at the Auburn University Electron Microprobe Analysis Lab (AU_EMPA), which includes four separate spectrometers. This was undertaken to evaluate the potential differences between melt types observed within sections. Additionally, one thin section was sent to Steven Jaret at the American Museum in New York, in order to better assess the potential temperature of formation of the Flynn Creek melts. He used additional analytical techniques including Fourier Transform Infrared Spectrometry (FTIR) and Raman spectroscopy at Stony Brook University, to provide data in this regard that has been used in the present study (Jaret et al., 2019).

By using standard petrographic analyses with a standard Nikon microscope and associated camera with the NIS-Elements imaging software, high definition images of each thin section were obtained and used to determine the area percent of melt, clasts, and matrix, which permitted a basic characterization of the petrology of the breccia intervals in question.

Furthermore, the microprobe allowed for retrieval of several pieces of important information via both quantitative and qualitative analysis. Quantitatively, it was possible to perform spot analysis on various mineral grains and melt clasts in order to establish the oxide weight composition and therefore determine the exact difference between different types of melt observed (grey and amber). Na and Mg were measured on the thallium acid pthalate (TAP) crystal and standardized with Amelia Albite and Olivine respectively. Al and Si were measured with the TAP 2 crystal and were standardized with Anorthite and Amelia Albite. Lastly, Ca and K were measured on the pentaerythritol (PET) crystal and were standardized with Anorthite and Microcline respectively. The qualitative portion of this work revolved mostly around back-scattered electron imagery (BSE), and elemental x-ray mapping after determining the primary elements within the melt makeup. In addition to this, energy dispersive x-ray spectroscopy (EDS) was employed to detect elements present within the samples.

Figure 5: Core box photo examples showing two of the areas where samples for thin sections were requested from the USGS, Flagstaff. The letter A is part of the thin-section number, which will include the drill core number and core box number as well. These core box photos are from the USGS Astrogeology Center collections.

Results

Objective Classification

Detailed examination of the core-box photographs of drill cores collected from Flynn Creek yielded three distinct impact-related lithic units within the crater bowl: a resurge unit, a slide unit, and a unit that fills the crater bowl (consisting of alternating breccia and bedrock (horizontal and dipping) intervals. Below the bowl of the crater lies the sub-crater parautochthonous breccia, which is the focus of petrographic study in the present research. Each of these units have distinct characteristics that made makes them relatively easy to separate from one another according to their relative position

The main purpose of reviewing images of all drill-cores was to understand their textures and structures, so it made sense to assign each core box a percentage according to several basic rock types: (1) Bedrock: Dipping and Undeformed, (2) Shale, and (3) Breccias of several different average grain sizes. After all core boxes were coded as to basic rock type (percentages of each box), it was determined that the most commonly occurring rock type in each of the cores was undeformed (i.e., horizontal) bedrock. However, the box coding also allowed a determination of where intercalated breccia is situated in relation to the undeformed bedrock. Appendix A contains all the collected data from all core boxes examined in the present study.

Once the core-box coding data were obtained, those data were input into a three-dimensional, made to-scale model that would depict the cores expanding downward from their positions in relation to the surface topography (Fig. 6). Then, it was possible to utilize this

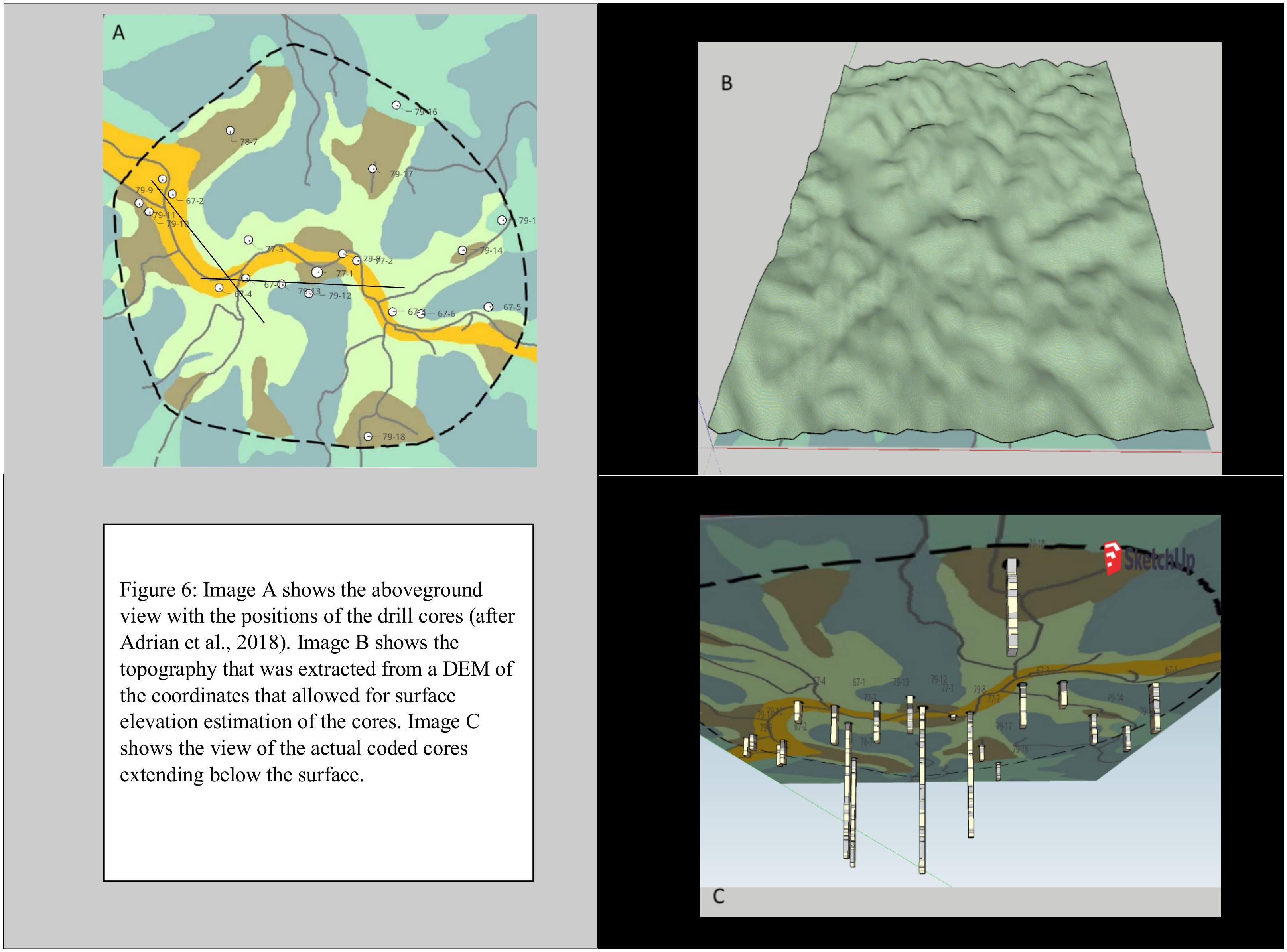

Figure 6: Image A shows the aboveground view with the positions of the drill cores (after Adrian et al., 2018). Image B shows the topography that was extracted from a DEM of the coordinates that allowed for surface elevation estimation of the cores. Image C shows the view of the actual coded cores extending below the surface.

information to more accurately position the exact location of each core on the x, y, and z axes. With this model, the present study was better able to draw correlations between the various occurrences of bedrock and intercalated breccia layers within the subsurface filling of the impact structure.

The core depths varied widely from box to box with the shallowest, FC79-10, reaching only 73.2 meters, whereas the longest, FC77-1, reached a depth of 698.9 meters. The shallower drill cores at Flynn Creek are the norm, and thus only four cores out of twenty-one extend below 500 meters. As such, the present understanding of deeper reaches of the subsurface was determined almost entirely from the four deep cores, which were drilled between 1977 and 1979. In the three 1977 cores, there are distinct zones observed in the subsurface. The first zone, an interval of approximately 150 meters of more, is a chaotic breccia that occurs near the top of the core. The second zone, just below the first, consists of approximately 200 meters of relatively undisturbed bedrock with only a very few zones of breccia within. This is followed by a thick breccia zone that persists to the bottom of the core.

The first solid model utilized to better visualize the subsurface was generated in Rockware ® from boxes of the core that displayed more than 50% breccia. This method was used as a more conservative way of understanding the vertical and lateral occurrence of the crater-filling breccias. Using fence diagrams to cut out pieces of said model allowed for an enhanced view of how the breccias might appear in the span between the cores, and essentially throughout the entire crater subsurface area. Because the geographic location of the drill-core sites are arranged somewhat in a linear order going across two transects, in the present study, these areas

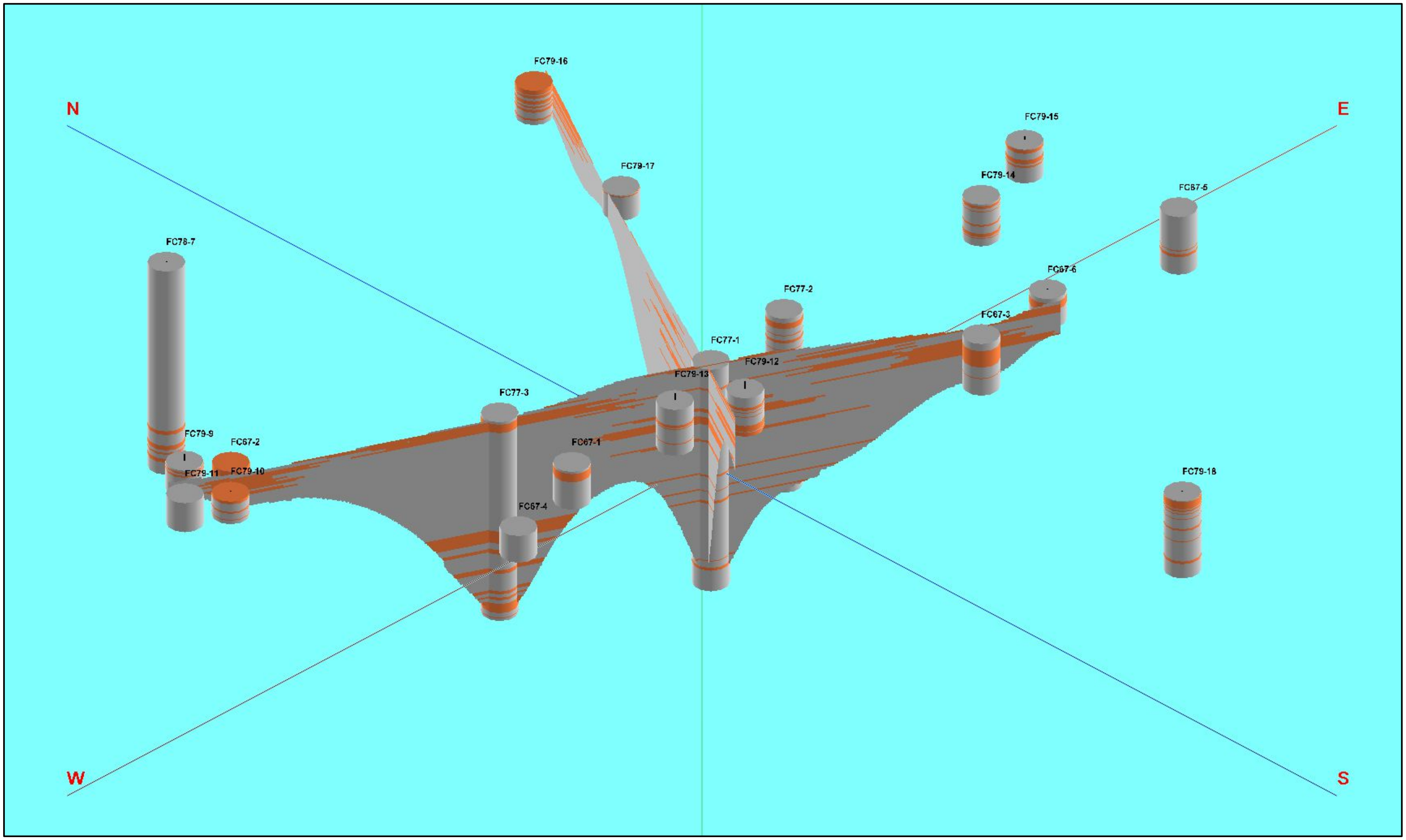

Figure 7: A labeled fence diagram depicting the breccia (orange) zones within the bedrock (grey) along the linear path that acts as the best fit line between the cores in question. The large gap area on the left side of the lower part is an artifact of the modeling algorithm which draws data from the nearest lateral core. Generated by Rockware ®.

were deemed as suitable to run the fence software with the intention of manually creating a projected stratigraphic column to compare reality to the model (Fig 7).

Genetic Classification

In looking for a rational correlation among the different breccias, it became important to separate these units by something more definite than simple grain size or structural attitude. Visually, we can make a genetic distinction between several types of Flynn Creek breccia, including graded resurge units, deformed and internally broken slide units, breccias in distinct beds (or lenses) within the crater bowl, and the underlying (sub-crater) melt-bearing parautochthonous breccias. In the list above, these breccias are listed in order from shallow to deep within the impact structure (Fig 8). With these distinct breccia units defined, they can then be correlated with the impact structure. This correlation provides a genetic interpretation of the steps in the crater's formation.

The resurge unit (a graded breccia) can be seen in six of the 21 cores. Five of these drill cores with resurge at the top are found within the crater bowl, and one drill core (FC67-2) lies near the northwestern margin of the crater. Breccia found in the resurge unit is very distinctive because the notable size grading (fining upward) does not occur in any of the other breccia units of Flynn Creek crater. This unit is known to fine upward due to the nature of its deposition by a tidal resurgence during the modification stage of impact (De Marchi et al., 2019a, b). It should be noted that the resurge breccia unit defined here also includes a basal section of a few meters in thickness that derives from pre-resurge slumping, as interpreted by De Marchi et al. (2019b).

The unit below the resurge breccia is the slide unit, which is distinct in that the stratified target bedrock is folded, broken, and then chaotically reorganized. The slide unit is associated with post-impact slumping of the outer transient crater rim, which sent large masses of target rock sliding into the crater bowl under the pressure of pore waters and the pull of gravity. The breccia of the slide unit is therefore an autobreccia, having formed by internal brittle deformation during mass movement and during collisions between mobile slump blocks.

The breccia below the slide unit is the crater bowl-filling unit, which consists mostly of target bedrock blocks that have been broken in place during impact or moved into position by slumping. Impact breccia in this crater bowl-filling unit is situated between or within thick sections of horizontal or dipping target bedrock. This unit, which is the main mass of material that fills the Flynn Creek crater bowl, therefore consists of large bedrock blocks that are intercalated with impact breccia, which is not graded and that generally does not contain melt particles. The crater-bowl filling unit has a distinctive and well-defined base. The base of the crater bowl, which is also the top of melt-bearing parautochthonous breccias, occurs in four deep drill cores. This boundary is marked by the occurrence of relatively prolific melt particles, in the parautochthonous breccia, and apparent absence of similar particles in the overlying crater-bowl filling unit. In a stratigraphic correlation of the crater subsurface (Fig. 9), the present study shows where the boundaries of the genetic units described above occur, and this enables a new picture of the subsurface structure of Flynn Creek crater to be drawn. Importantly, the bowl depicted in the first image, and partially in the second, is the inner crater bowl which has a diameter of 2 km. The second portion of Figure 9 shows where the inner crater transitions into the apparent crater, with the shallower bowl near the right side. The two transects used for this cross-sectional analysis can be seen overlain on the area map in Figure 6.

Resurge	Fining upward breccia sequence that fills the crater moat	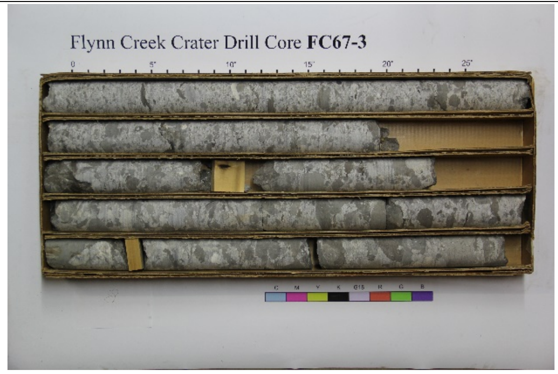
Slide	Very chaotic and broken autobreccia that was slumped from the expanding crater rim.	
Crater-Bowl Filling Breccia	Breccia that is intercalated with bedrock intervals in the crater bowl	
Parautochthonous Breccia	Breccia that is below the crater bowl; contains melt.	

<table>
<tr><td>Horizontal Bedrock</td><td>Bedrock unit in a more-or-less undisturbed state</td><td>
</td></tr>
<tr><td>Dipping Bedrock</td><td>Bedrock unit that has been shifted or tilted</td><td>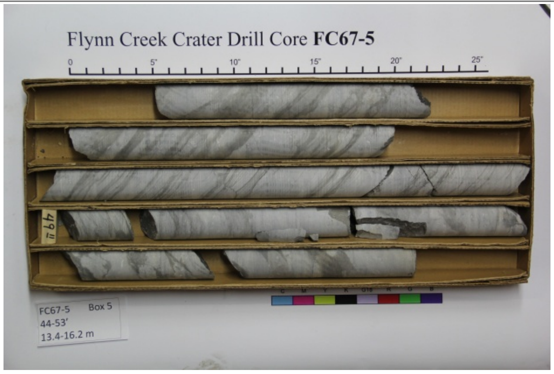
</td></tr>
</table>

Figure 8: Selected examples of core-box photos of the genetic crater units, as discussed in the text.

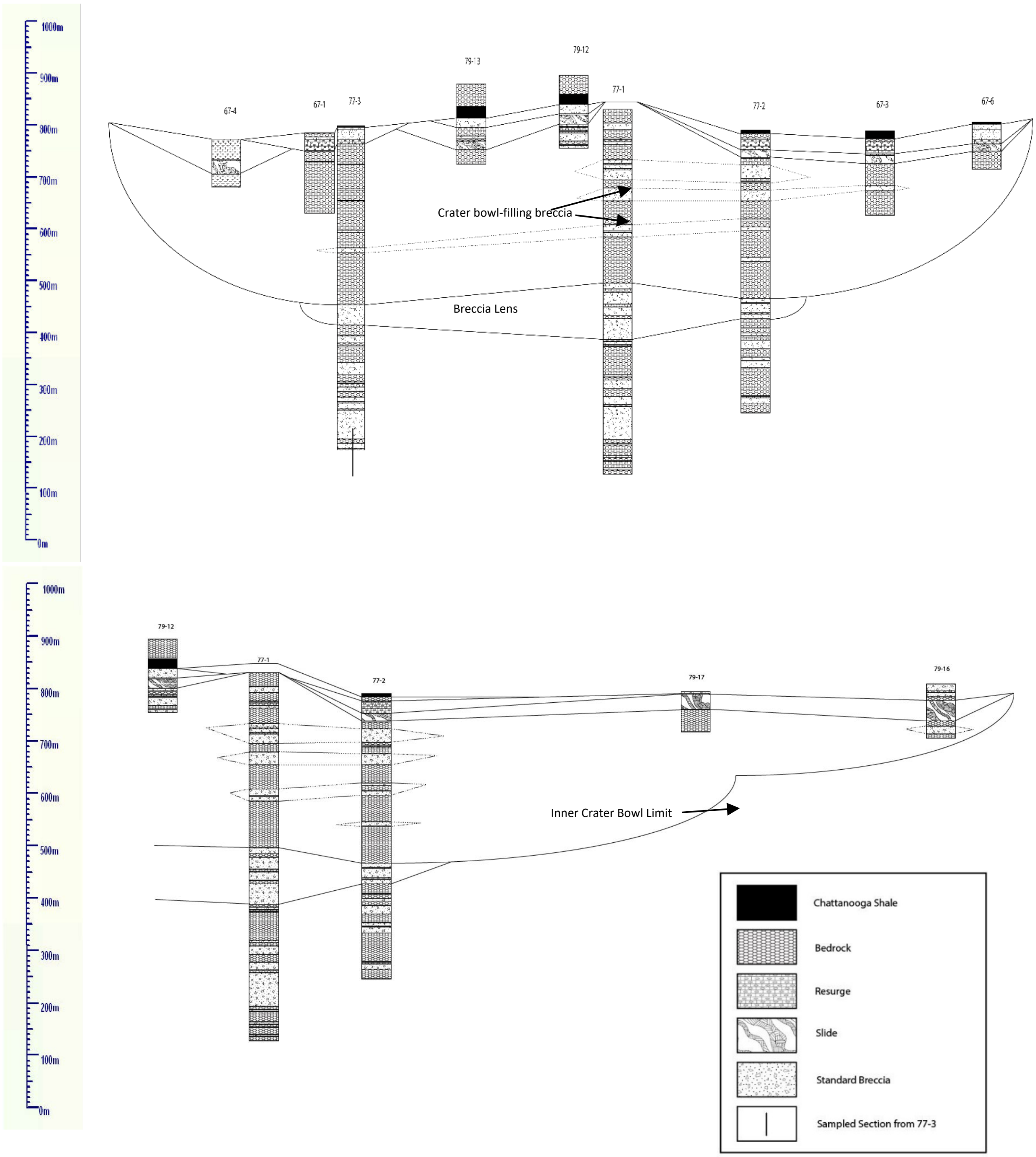

Figure 9: Two projected cross-sectional views of different crater transects, both of which depict the various breccia units observed within the impact structure. The inset map in Figure 6 shows where these cross sections were taken.

Petrographic Analysis

Thirty-three thin-sections were made from hand samples from various locations in the lower part of drill core 77-3. First, a group of nine samples were obtained and sent for thin-sectioning to assess whether the breccia at this level was of interest for the present study. Once it was determined that the breccias were of interest (specifically, melt fragments were found within these samples), an additional twenty-four samples were obtained and thin-sectioned. Of the 33 thin sections studied from the lower part of drill core 77-3, twenty-four were found to have melt or melt-like particles in various volume percentages (data in Appendix B). Dolomite, calcite, quartz, chert, and fossil fragments were found in many of the thin sections, but the characterization of the breccias soon turned to the more interesting aspects of the melt particles. Two separate melt types were observed within these thin sections, a grey and an amber melt type. Each was predominantly silica though the difference lies in the trace elemental composition of the two (see appendix C). The two melt types appear immiscible and though they are quite distinct in plain light, look strikingly similar when the polarizers are crossed (Fig. 10). Of note here is that the fact that melt is common only in the parautochthonous breccias at Flynn Creek. While melt clasts have been found in smaller numbers within other studies done at Flynn Creek, by far the highest concentration can be located within the parautochthonous breccias

Both melts appear with two distinct textures. The first being a distinctive flow pattern that can occur as small stringers or seemingly with less flow features as the matrix for the area of a whole thin section, with non-melted grains of dolomite, calcite, or quartz located within. Additionally, they have both been observed as more solid clasts without the distinctive flow textures that were seen during our first discovery of the melts. The former type appears mostly within cores that contained thick intervals of breccia, whereas the latter seems to be more common within smaller breccia veins, although both in some instances appear in both locations.

These clasts range widely in size throughout the thin sections from barely 1 mm wide to some as large as 15 mm with some thin sections being comprised of 95% melt, whereas others as little as 5%. Choosing several of these thin sections to be put to work on the microprobe was necessary to find out the compositional differences between the two melt types. Each were predominantly silica though the difference lies in the trace elemental composition of the two. The grey melt was found to be comprised almost entirely of silica whereas the amber melt had trace amounts of other elements, namely potassium, magnesium, and aluminum. Two locations of the melts are provided in Figure 10 along with thin-section location from within the core so that placement and interaction can be seen at various depths, which are provided on the actual drill-core box.

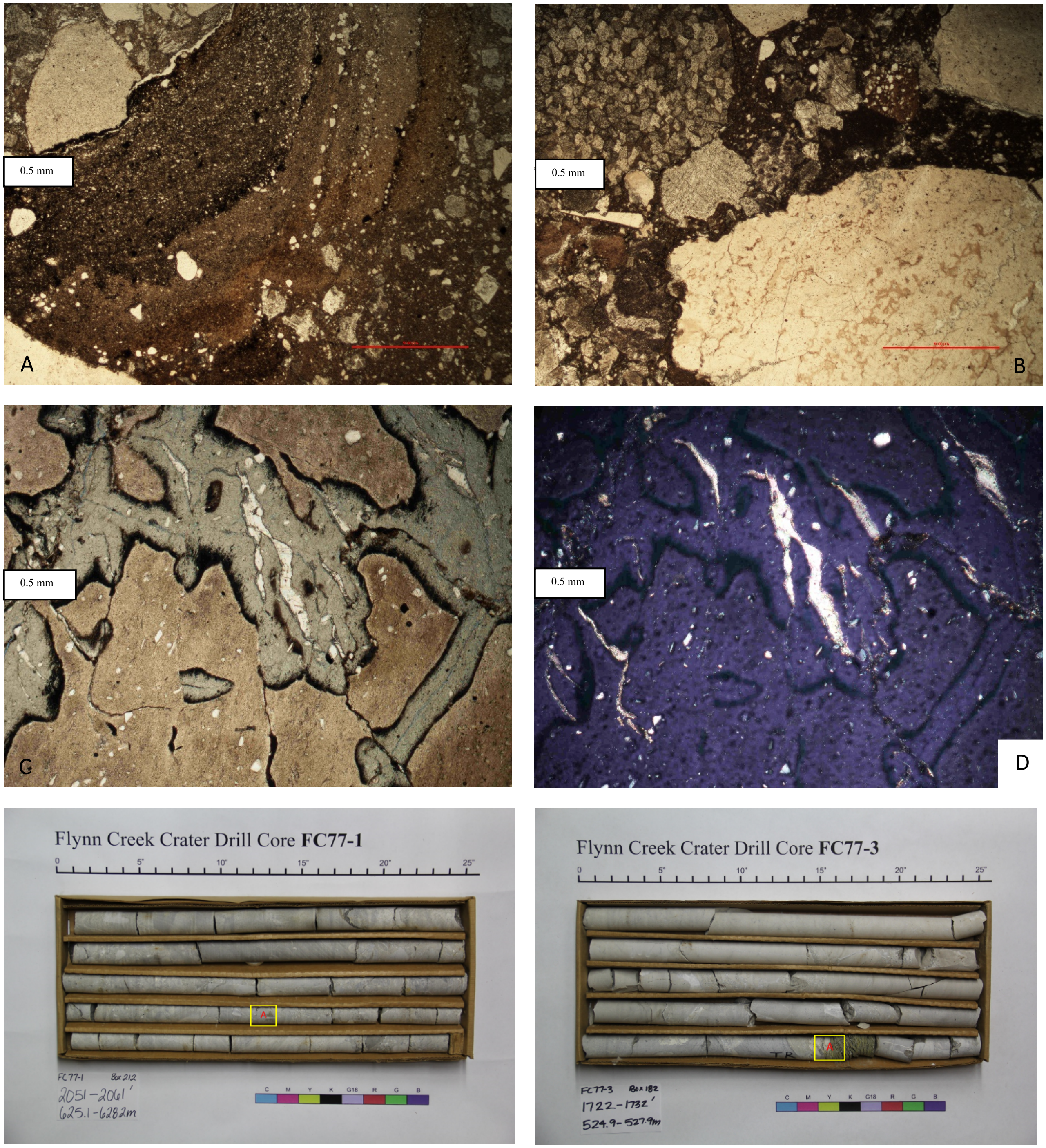

Figure 10: These images depict the melt particles found within several thin sections. Top left and right show the amber and grey melt respectively. The middle two show the interactions between the melt in both plain and polarized light. The bottom two images show examples of cores that contained melt within them. Photomicrograph scale bar is equal to 0.5 mm in each of the samples. The locations of the samples within the core are depicted at the bottom. A and B came from box 212 of drill-core FC77-1 whereas C and D (same image) was sourced from box 182 of drill core FC77-3.

Discussion

The onset of the present research into the Flynn Creek impact structure began with a question: what does the deep subsurface realm of Flynn Creek crater look like as viewed from the 21 drill cores available for this structure? Having so many drill cores for one impact structure is uncommon, and because these drill cores had not been carefully studied, there was a great opportunity for discovery. For proper comparative analysis to be done, it followed that the present study should examine at all the Flynn Creek drill cores in the same way. Hence, the data found in Appendix A were developed by the box-coding method noted earlier. For correlations, a genetic interpretation was added that helped constrain a newly developed picture of the subsurface of Flynn Creek impact structure, which is presented here. This broad scope gave unique insight into the subsurface characteristics and the styles of impact deformation exhibited within. In addition, the deeper part of drill core FC77-3 was selected for taking samples of breccias in the deepest part of the sub-crater realm. It was from thin sections of these samples that the presence of two separate melt types, which characterize the parautochthonous breccia at Flynn Creek, was discovered. Further interpretations of the various other sorts of impact breccias at Flynn Creek allowed us to challenge the previous interpretations of crater morphology as we more solidly defined certain sub-crater lithic boundaries.

Understanding of the Flynn Creek impact structure dates from the period of David Roddy's research (1966-1979). Except for the paper by Schieber and Over (2015), which established the biochronostratigraphic age of Flynn Creek, but otherwise reiterated Roddy's conclusions, there has been little written about the process of this impact structure's origin and nothing about its deeper subsurface structure. Recently, Bray et al. (2019) presented new modeling research for Flynn Creek that involved hydrocode simulation of this marine impact.

This new simulation model of the impact could be interpreted to contradict the earlier complex crater classification given to the structure by essentially all previous workers. One of the most prominent differences between a simple and a complex crater is the presence of a central peak, which expresses itself as a structurally uplifted area near the center of the crater. Flynn Creek has a central mound feature with deformed rocks, and that feature has been interpreted as a central uplift since the early work by Roddy (1966). The new modeling by Bray et al. (2019) suggests that there is no central uplift. In fact, the hydrocode model could be interpreted to depict a central mound being formed from the collision of rim-derived lithic slump blocks as they moved back into the crater bowl during an early phase of modification of the impact crater. The convergence of Bray et al.'s work and the present study of Flynn Creek's subsurface points to a new interpretation of this impact structure.

In terrestrial impact craters, both on dry land and in the marine realm, at the initial point of meteoritic impact, there will be an explosion causing flaps of material to rise upward and outward (Melosh, 1989). In the new hydrocode model, these flaps are then depicted as sliding into the bowl potentially coalescing into a mass near the center. Figure 11 shows Roddy's structure contour map of Flynn Creek, which he constructed on the contact between the Chattanooga Shale and underlying rocks (i.e., Flynn Creek breccia and the target Ordovician carbonates). The central collision zone between slump blocks (and other possible collisional mounds) are shown in this view. The outward expanding scars of large slump block are suggested by the scalloped rim. The inner crater bowl diameter of about 2 km as suggested by Bray et al. (2019) and the present study is shown in red.

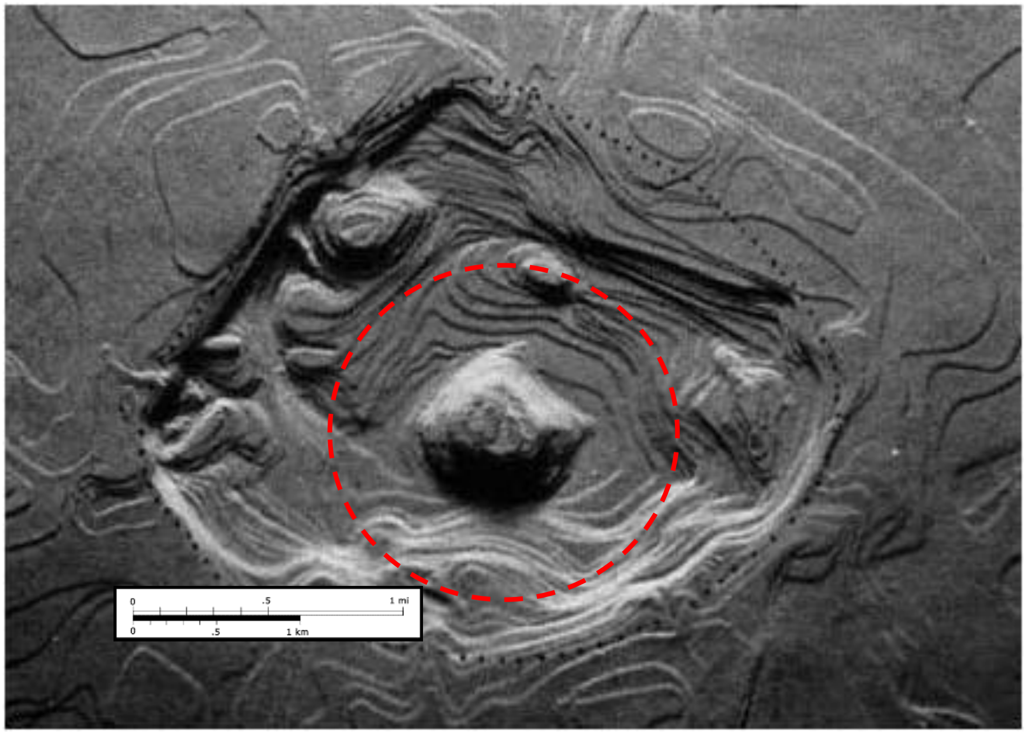

Figure 11: Roddy's (1968) structure contour map with the proposed approximate inner crater-bowl boundary outlined in red. Scale is from Roddy's original figure.

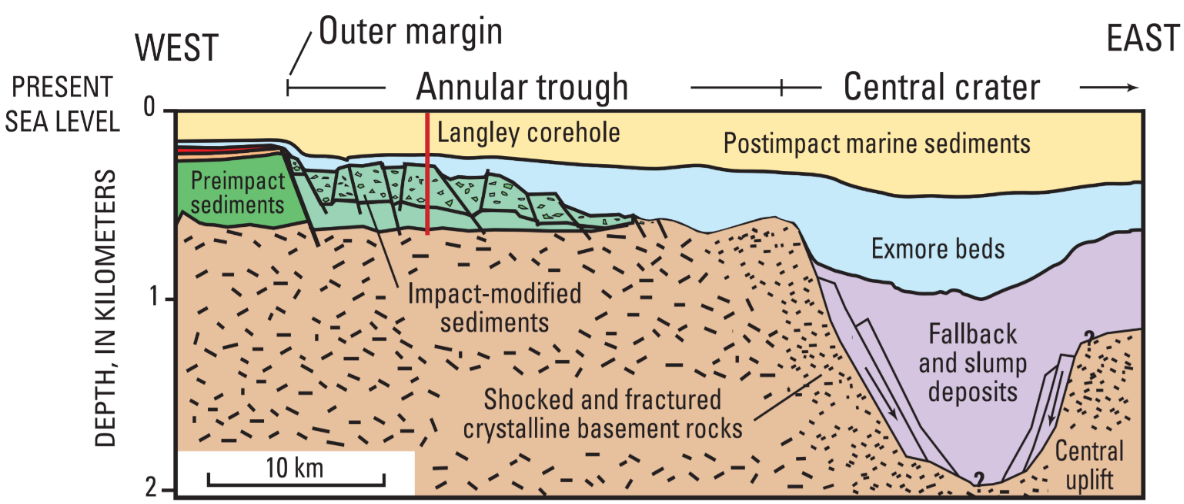

Figure 12: Half-crater cross-section of the Chesapeake Bay impact structure. Cross-section is based on seismic lines and core drillings (from Horton et al., 2006). The annular trough and inner central crater are suggested here as analogues for the much smaller Flynn Creek impact structure's features as noted in the text.

By assuming that Flynn Creek could be a simple crater instead of the previously held notion of a complex structure, opened several possible new interpretations and helped provide a better understanding of what was emerging in the new crater cross-sections of the present study (Fig. 9). The diameter of this inner crater is consistent with subsurface correlations, as noted earlier.

This new original diameter of ~2 km matches with the standard simple crater depth-to-diameter ratio of 1:6 (Melosh, 1989). If the estimated size and placement is correct, the image seems to show a delineation between the inner and outer portions of the impact crater (Fig. 11). The inner circular ring is the true, simple crater rim and the outer limits of the whole structure include the modification stage slump zones that attend the original, inner crater itself. Material around the edge of the rim succumbed to gravity, detached, and slide inward, first filling the crater bowl, and later sliding across the surface of the crater bowl filling unit. The slumping much expanded the diameter of the final structure, which was about 2 km following impact, but is now about 3.8 km.

There is precedent to this type of impact structure such that it exhibits an outwardly progressive modification rim and a characteristic "inverted sombrero" shape (when viewed in cross-section): the best example, even though it is much larger in diameter, is the Chesapeake Bay impact structure and its crater bowl filling unit and overlying Exmore breccia (Horton et al., 2005). The concept of the "inverted sombrero" (including that specific term) and its origins during the modification stage of impacts into wet targets was originally described by Melosh (1989; page 140) in his widely cited impact geology textbook.

Few marine impact structures are as well studied as Chesapeake Bay due to the burial, erosion, and deformation that takes place over millions of years, depending on the crater. The

Chesapeake Bay structure is the largest crater in the United States and has therefore received the attention of many scholars over the years, leaving it to be one of the more thoroughly researched marine target impacts (Gohn et al., 2006). One of the main influences of crater morphology when dealing with marine targets is, unsurprisingly, the way the pore water interacts with the post-impact material. From the crater shape and breccia deposition alone, there is an apparent correlation between this crater and Flynn Creek, but on a vastly different scale.

Fallback and slump deposits at Chesapeake Bay (Fig. 12) are analogous to the crater bowl filling unit at Flynn Creek, and the Exmore beds are analogous to the latter slump deposits and the resurge breccias of Flynn Creek. Chesapeake Bay has a large central uplift (owing to its greater size), which Flynn Creek does not have. In Figure 11, slump blocks are shown at far left, which have not moved to the crater bowl, and these are analogous to the slumps interpreted at Flynn Creek. Post-impact sediments in the cross section above are analogous to the Chattanooga Shale at Flynn Creek.

As previously mentioned, the genetic classification (Figure 8) assigned to the various breccias within the crater subsurface ultimately gave insight as to what a smaller crater bowl might look like with the inclusion of the annular trough. The textural differences noted between the different breccias as well as the gap between the crater-bowl filling breccia lens and the parautochthonous breccias allowed us to revise the definition of the crater floor, which was then instrumental in getting the appropriate depth for the depth-to-diameter ratio necessary for the revised diameter calculation. The second image in Figure 9 displays an approximation of where the crater bowl may end, and the annular trough begins.

Another structure that bears a strong resemblance to Flynn Creek in several ways is the Alamo Crater in Nevada (Warme et al., 2008). Whereas orders of magnitude larger (>200km), this structure is another example of a carbonate-target, marine impact which is also Late Devonian. Interestingly, there is only about one million years (or less) difference in age between the Flynn Creek and Alamo events.

Some of the most important similarities to note between the two impact structures were the lithologies present in both places and the interpreted method of emplacement of some of the breccias seen at Flynn Creek and at the Alamo structure. Warme and Sandberg (1996) describe monomict and polymict breccias as fallback material, which could help explain some of the Flynn Creek breccia lenses found between and within large sections of either horizontal or dipping target strata. It should be noted that Flynn Creek breccia lenses in the crater-bowl filling unit are monomict, as far as the present study can determine, and polymict breccias at Flynn Creek are in the domain of parautochthonous breccia only. Warme et al. (2008) goes on to mention that melts are present in several of the breccia units and though the amount of pressure at Flynn Creek must have been much less than that of the Alamo event, there are many similarities in both composition and texture between the melt clasts that were observed under a petrographic scope.

An in-depth analysis via standard microscope and the use of both micro-Raman spectroscopy and FTIR (Fourier Transform Infrared) spectroscopy was able to demonstrate that these were cryptocrystalline materials of original melt origin (Adrian et al., 2018; Jaret et al., 2019). At a very small scale, the melt appears to be composed of extremely fine-grained clasts of calcite and dolomite within a cryptocrystalline quartz matrix (Jaret et al., 2019). The reason for defining these as cryptocrystalline rather than glassy lies within the small-scale textures of the melts. Where glass is more fluidic at small scale, cryptocrystalline materials are made up of extremely fine-grained crystals with a much more rigid texture. Said classification wasn’t initially obvious as the melts appear isotropic under microscope despite being composed of many micro-crystals. It is important to mention at this point that despite minor differences in trace elemental composition, both melt types are crystallographically considered to be quartz.

Figure 13 depicts X-Ray mapping of several areas within analyzed thin sections that were examined more closely with the AU-EMPA JEOL JXA-8600 Microprobe. Several different elements were mapped with the most significant being Si due to the nature of the clasts and zones that we were exploring. For the most part, we are seeing quartz and dolomite within these sections given that the highest percentage of elements seen were Si, Ca, Mg, and K in order from most to least. It is interesting to note these minerals in such close proximity to determined melt clasts. These images clearly help portray how microscopic the "cryptocrystalline" material is when examined on such a small scale.

Additionally, several of the textures mentioned within Warme's paper as confirmation of melt status is apparent within the Flynn Creek melts as well (Fig. 13). While the Alamo breccia studied by Warme et al. is another much larger example, they discuss partial breccia melts and the associated textures (i.e feathered dolomite, quenched melt, cryptocrystalline melt, etc.) that can easily be tied to similar findings from Flynn Creek (Pinto and Warme, 2008). Each of the factors combined to enforce the fact that all of the melt recovered from Flynn Creek is highly concentrated within the breccia lens of the crater despite trace particles also being observed in resurge deposits (De Marchi et al., 2019a) and on the central mound (Adrian et al., 2018).

The feathered dolomite texture is strong evidence to further the accurate classification of melt as this type of texture is closely associated with carbonate melt (Osinski et al., 2008). The temperature of formation of these melts was determined by Jaret et al. (2019) to be between 623°C and 950°C based on the high concentrations of Ti and Al within the quartz. Whereas there

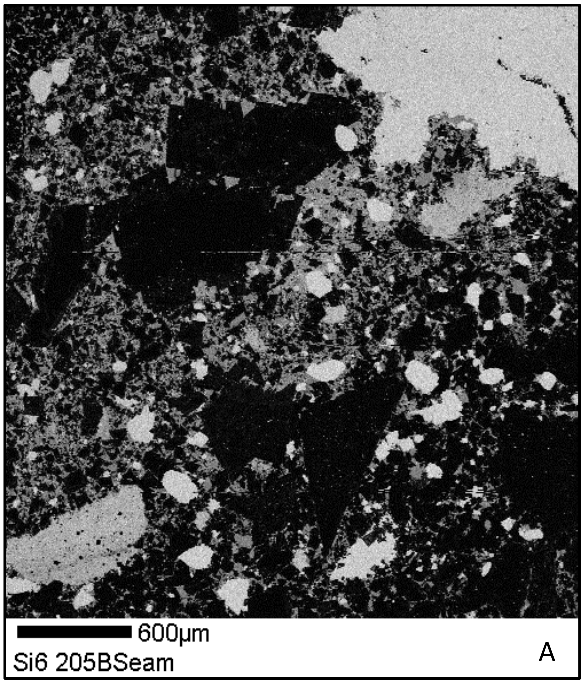

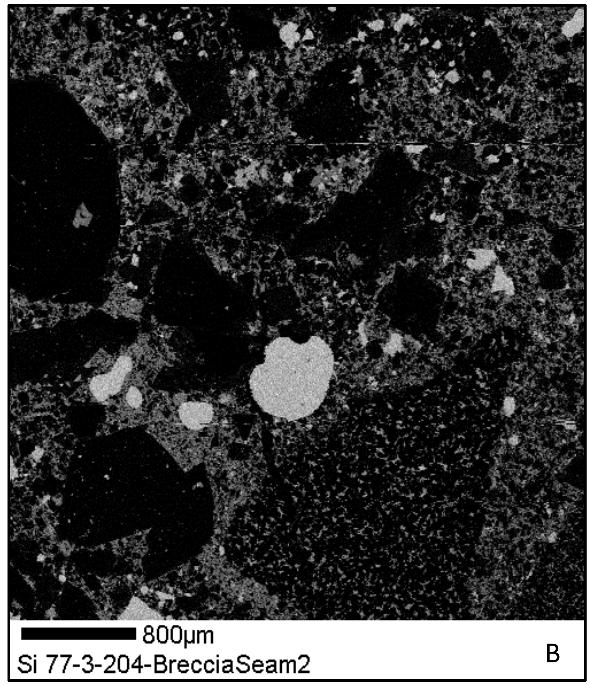

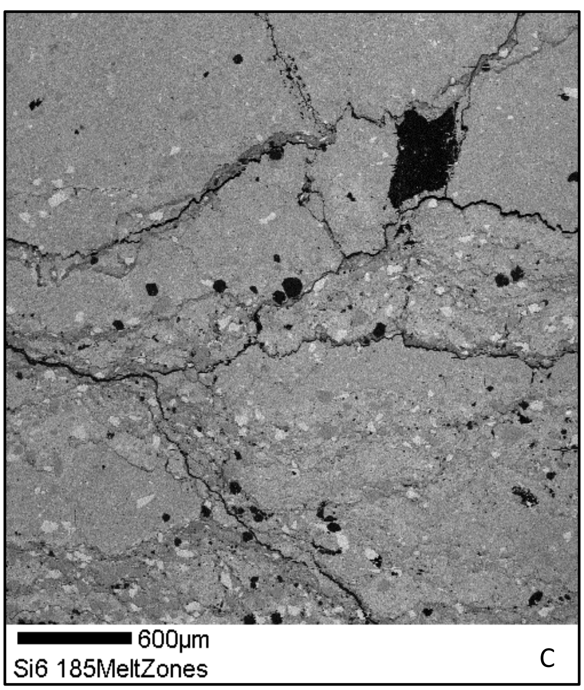

Figure 13: Images A and B both come from a small seam of breccia located at around 590m of depth within drill core 77-3. Image C comes from the same drill core but at a shallower depth of 535m. All images are X-Ray mapping of silica done with the JEOL-8600 Microprobe.

may be two separate melts positively identified within, it may be that they are two phases of the same melt, which would explain why they are commonly present in the same samples. The amber melt predominantly displays flow textures in the background matrix melt, whereas the grey melt more commonly occurs as hardened clasts. That they are essentially the same substance only becomes apparent as the two become nearly indistinguishable under cross-polarization.

Looking again at Figure 10, we can see how the two melts interact by viewing how they had solidified in conjunction with one another. In most cases where the melts interact, cross-cutting relationships suggest the amber melt was formed initially, with the grey melt often upwelling in seams between the amber, bisecting it. Additionally, at most places where the grey melt appears to cross-cut the amber there will be a small crack in the center of the mass where dolomite seems to be crystallizing. Given the similarities of locations found as well as composition, it appears that the melts crystallized rapidly one after the other, with the amber melt coming first followed closely by the grey. It may be that the compositional difference between the silica-rich amber melt and the inclusion of Ti, Al, and K in the grey melt can account for the slight deviation in timing. Given the different modes of expression within the melts, there must have been at least a slight deviation of timing of formation or crystallization. With the melts being so similar both compositionally and texturally, the only main difference that could lead to this diversion would likely have to be the slight variation in trace elemental composition.

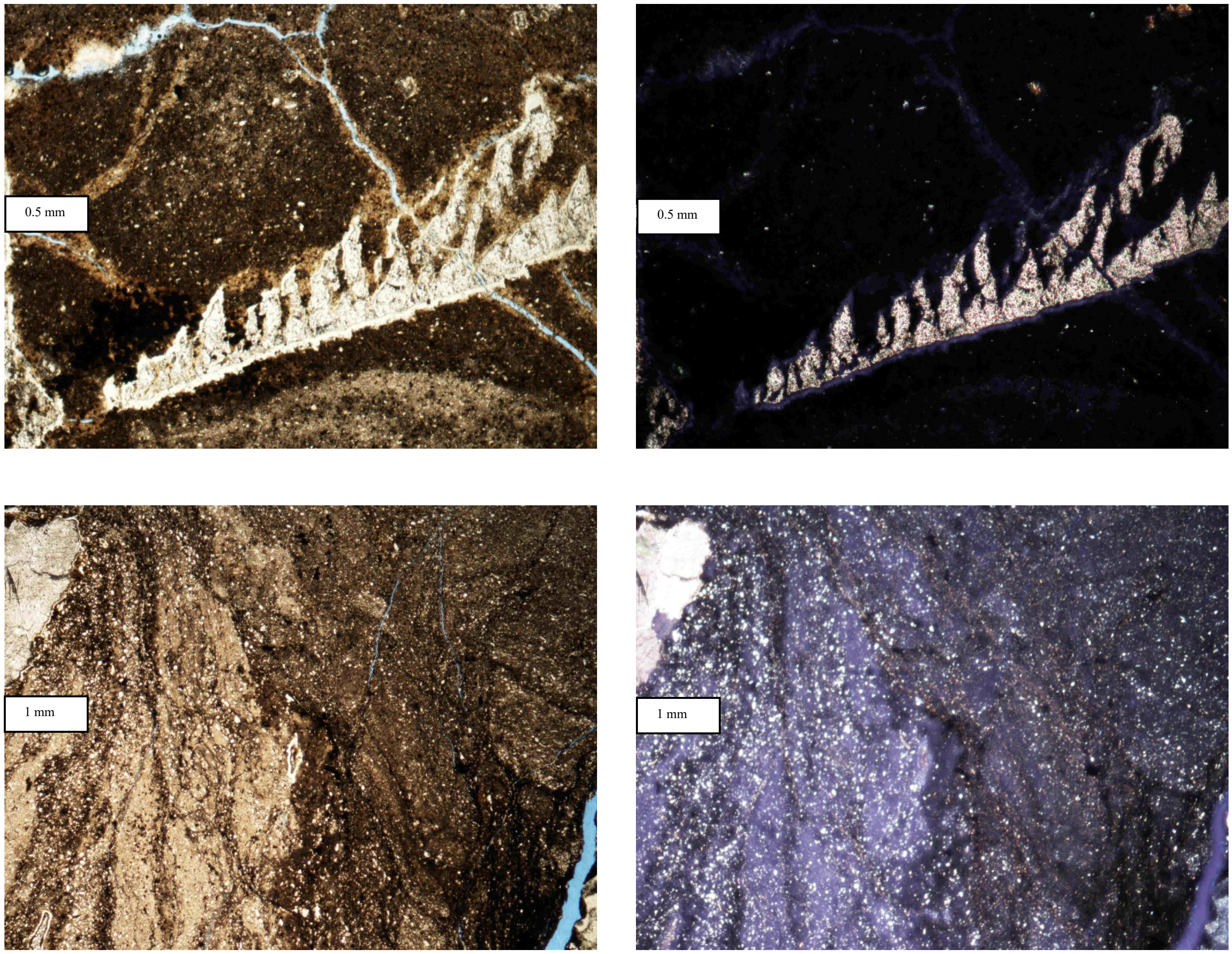

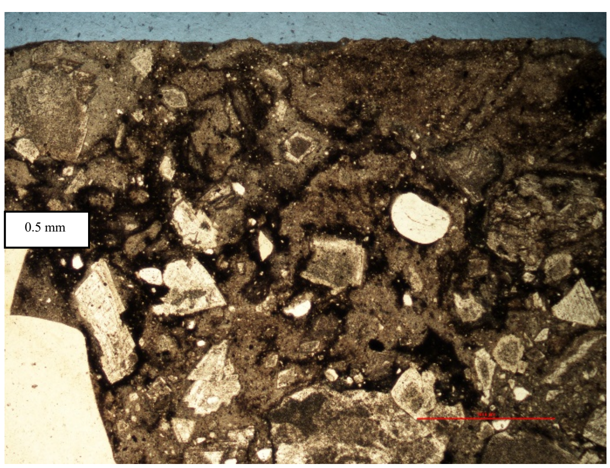

Figure 14: The upper images show feathered dolomite in a melt matrix in both plane and polarized light, the middle images depict flow textures seen in the different melt types, and the bottom left image shows dolomite, calcite, and quartz clasts “floating” in a melt matrix. Scale is 1 mm. Upper and middle images are from thin section FC77-3-200-B and the lower image is from FC77-3-192-A.

Conclusions

The Flynn Creek impact structure is a known marine target event that was previously determined to have a diameter of 3.8 km. The present interpretation of new data presented herein suggests that the structure may actually be much smaller, nearer to a diameter of 2 km. The disparity between the two suspected sizes can be explained by copious slumping of the crater rim following the impact event itself, which greatly increased the apparent diameter of the crater as viewed from outcrop. Said slumping events are supported by the folded and broken slump breccia layer atop the crater-bowl filling unit and the presence of collisional mounds on the crater floor (including the central collisional mound, which has been called a central uplift up to this point). Having a smaller bowl that previously thought reconciles quite well with many other variables that have been uncovered throughout this study. For example, the bottom of the crater bowl (contact between the crater bowl filling unit and the parautothonous breccia) is consistent with a known depth to diameter ratio for most simple craters. Additionally, the potential reclassification of Flynn Creek as a simple crater rather than a complex impact structure fits remarkably well when you consider the fact that there is no central uplift at Flynn Creek.

Furthermore, the asymmetrical shape of the crater can be explained by the aforementioned changes to the crater morphology. Where there is now an irregular "pear-shaped" structure due to slumping along concentric faults, the initial structure would have likely been more circular, which is expected based on crater formation in homogenous targets. The strange shape that we see today is likely the result of rim failures around the crater, leaving deep gouges where the material had slumped in. Given that the topography appears much shallower around the apparent rim, it can be said that Flynn Creek has the classic "inverted sombrero" cross-sectional morphology (Horton et al., 2005).

Whereas it was previously known that there was a resurge deposit, the genetic classification set down in this study allowed for the recognition of a new breccia type within the structure that was labeled as a slump deposit. Other classifications of specific breccia morphologies allowed interpretive definition of boundaries between standard crater-filling breccia, the breccia lens, and the parautochthonous breccia below the crater floor. Combing through all twenty of the usable drill cores allowed for the production of a clearer picture of the crater subsurface in cross-section. Finally, the melt found in the samples taken from deep in drill core FC77-3 has been determined to be characteristic of Flynn Creek's parautochthonous breccias almost exclusively, which was somewhat of a surprise due to the fact that melts of these types sometimes occur elsewhere in the crater bowl. The method of emplacement of these melts has been attributed to the thermal energy along the transient crater surface and thus melting a very minor silica content within the target carbonates.

References

Adrian D.R., King Jr. D.T., Jaret S.J., Ormö J., Petruny L.W., Hagerty J.J., and Gaither T.A, 2018. Sedimentological and petrographic analysis of drill core FC77-1 from the flank of the central uplift, Flynn Creek impact structure, Tennessee: *Meteoritics and Planetary Science*, v. 53, p. 857-873.

Adrian D.R., King Jr. D.T., and Ormö J. 2019. Resurge gullies and "inverted sombrero" morphology, Flynn Creek impact structure, Tennessee: *Meteoritics and Planetary Science*, v. 54, p. 2758-2768.

Bray V., Hagerty J., Collins G., King Jr. D.T., and Jaret S.J. 2019. Hydrocode simulation of the Flynn Creek impact, Tennessee (abstract #3038). 50th Lunar and Planetary Science Conference.

Conant L.C. and Swanson V. E. 1961. Chattanooga shale and related rocks of central Tennessee and nearby areas. *Geological Survey Professional Paper* 357:12-48

Dalwigk I. von, and Ormö J. 2001. Formation of resurge gullies at impacts at sea: the Lockne crater, Sweden. *Meteoritics and Planetary Science* 36:359-369.

De Marchi L., Ormö J., and King Jr. D.T. 2019. Sedimentological analysis of two drill cores through the crater moat-filling breccia, Flynn Creek impact structure, Tennessee: *Meteoritics and Planetary Science*. Published on line Oct. 7, 2019. https://doi/org/10.1111/maps.13393

De Marchi L., Agrawal V., and King Jr. D.T. 2019a. Hyrdrocode Simulations of Wetumpka impact crater. *Lunar and Planetary Science L*: 2644.

De Marchi. L., Ormö J., King Jr. D.T., Adrian D.R., Hagerty J.J., and Gaither T.A. 2019b. Sedimentological analysis of two drill cores through the crater moat-filling breccia, Flynn Creek impact structure, Tennessee. *Meteoritics and Planetary Science,* v. 54, p. 2864-2878.

Dietz, R.S., 1963. Cryptoexplosion structures: a discussion. *American Journal of Science*, 261:650-664.

Evenick, J. and Hatcher, R.D. (2007). *Geologic map and cross sections of the Flynn Creek impact structure, Tennessee*.

Evenick J., Lee P., and Deane B. 2004. Flynn Creek impact structure: New insights from breccias, melt features, shatter cones, and remote sensing (abstract#1131). 35th Lunar and Planetary Science Conference.

Ford J., Orchiston W., and Clendening R. 2013. The Flynn Creek meteorite impact site and changing views on impact cratering. *Journal of Astronomical History and Heritage* 16(2), 127-183

Gaither T., Hagerty J., and Bailen M. 2015. The USGS Flynn Creek crater drill core collection: progress on a web-based portal and online database for the planetary science community (abstract#2089). 46th Lunar and Planetary Science Conference.

Gohn, G., Koeberl C., Miller K., Reimold W., Cockell C., Horton J., Sanford W., and Voytek M. 2006. Chesapeake Bay Impact Structure Drilled. *EOS Vol. 87. Iss. 35*, 349-354

Hagerty J., McHone J., and Gaither T. 2013. The Flynn Creek crater drill core collection at the USGS in Flagstaff, Arizona (abstract#2122). 44th Lunar and Planetary Science Conference.

Horton J., Powars D., and Gohn G. 2005. Studies of the Chesapeake Bay impact structure—The USGS-NASA Langley corehole, Hampton,Virginia, and related coreholes and geophysical surveys,U.S. Geological Survery Professional Paper, 1688

Jaret S.J., and King Jr. D.T. 2018. Revisiting the Flynn Creek impact structure, Jackson County, Tennessee, in Engel, A.s., and Hatcher R.D., Jr., eds., Geology at Every Scale: Field Excursions for the 2018 GSA Southeastern Section Meeting in Knoxville, Tennessee: Geological Society of America Field Guide 50, p. 75-79. https://doi.org/10.1130/2018.0050(05)

Jaret S.J., King Jr. D.T., Tailby N., Adams M., and Ebel D. 2019. Impact melt clasts from the Flynn Creek impact structure, Tennessee – Temperature constraints from titanium-in-quartz thermometry (abstract #3170). 50th Lunar and Planetary Science Conference.

Melosh, H.J. 1989. Impact cratering: a geological process, in Research Supported by NASA. New York, Oxford University Press. *Oxford Monographs on Geology and Geophysics, No.11.* p.11

Milam K.A., and Deane B. 2005. Petrogenesis of central uplifts in complex terrestrial impact craters (abstract#3089). 36th Lunar and Planetary Science Conference.

Osinski G., Spray J., and Grieve R. 2008. Impact melting in sedimentary target rocks: An assessment. *The Geological Society of America*. Special Paper 437

Pinto, J.A., and Warme, J.E. 2008, Alamo Event, Nevada: Crater stratigraphy and impact breccia realms, in Evans, K.R., Horton, J.W., Jr., King, D.T., Jr., and Morrow, J.R., eds., The sedimentary record of meteorite impacts: *Geological Society of America Special Paper* 437:99-137

Roddy D. J. 1966. The Paleozoic crater at Flynn Creek, Tennessee. Ph. D. thesis, *California Institute of Technology*.

Roddy D. J. 1968. The Flynn Creek crater, Tennessee. *Shock Metamorphism of Natural Materials,* edited by Bevan M. French: American Association for the Advancement of Science. pp. 291–322.

Roddy D. J. 1977. Pre-impact conditions and cratering processes at the Flynn Creek Crater, Tennessee in Roddy, D.J., Pepin, R.O., and Merrill, R.B., eds. *Symposium on Planetary Cratering* p. 277-308

Roddy D. J. 1979. Structural deformation at the Flynn Creek impact crater, Tennessee: a preliminary report on deep drilling. *Lunar and Planetary Science* 10:2519-2534.

Schieber J., and Over J. D. 2005. Sedimentary fill of the Late Devonian Flynn Creek crater: a hard target marine impact. Edited by Over D. J., Morrow J. R., and Wignall P. B. Understanding Late Devonian and Permian-Triassic Biotic and Climatic Events: Towards an Integrated Approach. *Elsevier*. pp. 51-69.

Stöffler D. 1981. Terrestrial impact breccias. *Lunar and Planetary Institute.* 82-02: p.139.

Warme J. E., and Sandberg C. A. 1996. Alamo Megabreccia: Record of a Late Devonian Impact in Southern Nevada. *GSA Today*, v. 6, no. 1, p. 1-7.

Warme J., Morrow J., Sandberg C. 2008. Devonian carbonate platform of eastern Nevada: Facies, surfaces, cycles, sequences, reefs, and cataclysmic Alamo Impact Breccia. In: Field Guide to Plutons, Volcanoes, Faults, Reefs, Dinosaurs, and Possible Glaciation in Selected Areas of Arizona, California, and Nevada, edited by Ernest M. Duebendorfer, Eugene I. Smith: The Geological Society of America. pp. 215-247.

Appendix

Appendix A: List of all of the coded drill cores mentioned. TD = Top Depth, BD = Bottom Depth, MI = Missing, SH = Shale, FS = Fine Sand, BRh = Horizontal Bedrock, BRd = Dipping Bedrock, VCB = Very Coarse Breccia, CB = Coarse Breccia, MB = Medium Breccia, and FB = Fine Breccia. The standard measurement for breccia was used to split it into the various types, where fine falls between 2-6mm, medium 6-20mm, coarse 20-60mm, and very coarse being greater than 60mm. Numbers in red indicate inferred depth due to the lack of recorded information on the core boxes.

A: Core Box Coding

FC67-1													
Box	TD (ft)	BD (ft)	TD (m)	BD (m)	MI	SH	FS	BRh	BRd	VCB	CB	MB	FB
1	12.5	23	3.8	7	10	0	60	0	0	0	0	0	30
2	23.75	30	7	9.1	40	0	0	0	0	0	20	40	0
3	30	41	9.1	12.5	10	0	0	0	0	10	70	10	0
4	41	50	12.5	15.2	10	0	0	0	0	60	30	0	0
5	50	60	15.2	18.2	0	0	0	0	0	20	30	50	0
6	60	72	18.2	21.9	0	0	0	0	0	20	70	10	0
7	72	83	21.9	25.2	0	0	0	0	0	60	30	10	0
8	83	91	25.2	27.6	10	0	0	0	0	10	50	20	10
9	91	102	27.6	31	10	0	0	0	0	0	10	40	40
10	102	110	31	33.4	20	0	0	0	10	0	30	20	20
11	110	120	33.4	36.5	0	0	0	80	0	0	20	0	0
12	120	130	36.5	39.5	20	0	0	80	0	0	0	0	0
13	130	139	39.5	42.2	20	0	0	80	0	0	0	0	0
14	139	147	42.2	44.7	30	0	0	70	0	0	0	0	0
15	147	154	44.7	46.8	40	0	0	60	0	0	0	0	0
16	154	163	46.8	49.5	30	0	0	70	0	0	0	0	0
17	163	172	49.5	52.3	20	0	0	80	0	0	0	0	0
18	172	182	52.3	55.3	20	0	0	50	0	0	0	20	10
19	182	192	55.3	58.3	20	0	0	80	0	0	0	0	0
20	192	201	58.3	61.1	30	0	0	70	0	0	0	0	0
21	201	213	61.1	64.9	10	0	0	90	0	0	0	0	0

22	213	223	64.7	67.7	20	0	0	80	0	0	0	0	0
23	223	231	67.7	70.2	20	0	0	80	0	0	0	0	0
24	231	241	70.2	73.2	10	0	0	90	0	0	0	0	0
25	241	251	73.2	76.3	10	0	0	90	0	0	0	0	0
26	251	263	76.3	79.9	10	0	0	90	0	0	0	0	0
27	263	272	79.9	82.6	20	0	0	80	0	0	0	0	0
28	272	283	82.6	86	10	0	0	90	0	0	0	0	0
29	283	292	86	89	20	0	0	80	0	0	0	0	0
30	292	302	89	91.7	10	0	0	90	0	0	0	0	0
31	302	312	91.7	94.8	20	0	0	80	0	0	0	0	0
32	312	322	94.8	97.8	10	0	0	90	0	0	0	0	0
33	322	332	97.8	100.9	10	0	0	90	0	0	0	0	0
34	332	342	100.9	103.9	10	0	0	90	0	0	0	0	0
35	342	352	103.9	106.9	20	0	0	80	0	0	0	0	0
36	352	361	106.9	109.7	20	0	0	80	0	0	0	0	0
37	361	372	109.7	113	10	0	0	90	0	0	0	0	0
38	372	382	113	116.1	20	0	0	80	0	0	0	0	0
39	382	392	116.1	119.5	10	0	0	90	0	0	0	0	0

FC67-2														
Box	**TD (ft)**	**BD (ft)**	**TD (m)**	**BD (m)**	**MI**	**SH**	**FS**	**BRh**	**BRd**	**VCB**	**CB**	**MB**	**FB**
1	26.25	36	8	11	10	0	0	0	0	30	30	20	10
2	36	45	11	13.7	10	0	0	0	0	40	20	30	0
3	45	56	13.7	17.1	10	0	0	0	0	40	10	40	0
4	56	68	17.1	20.7	10	0	0	0	0	10	50	30	0
5	68	78	20.7	23.8	10	0	0	0	0	70	20	10	0
6	78	87	23.8	26.5	20	0	0	0	0	70	10	0	0
7	87	98	26.5	29.9	10	0	0	0	0	80	10	0	0
8	98	106	29.9	32.3	30	0	0	0	0	50	20	0	0
9	106	114	32.3	34.7	10	0	0	0	0	60	20	10	0
10	114	123	34.7	37.5	20	0	0	0	0	40	10	30	0
11	123	133	37.5	40.5	10	0	0	90	0	0	0	0	10
12	133	144	40.5	43.9	10	0	0	80	0	0	0	10	0
13	144	154	43.6	46.9	10	0	0	80	0	0	10	0	0
14	154	164	46.9	50	10	0	0	50	0	0	10	30	0
15	164	174	50	53	10	0	0	0	40	0	30	10	10
16	174	182	53	55.5	30	0	0	0	0	50	10	10	0
17	182	193	55.5	58.8	10	0	0	20	0	30	30	10	0

18	193	202	58.8	61.6	20	0	0	60	20	0	0	0	0
19	202	212	61.6	64.6	10	0	0	60	20	0	0	10	0
20	212	222	64.6	67.6	10	0	0	70	10	0	0	10	0
21	222	232	67.7	70.7	10	0	0	40	40	10	0	0	0
22	232	242	70.7	73.8	20	0	0	0	70	0	0	10	0
23	242	251	73.8	76.5	10	0	0	20	30	30	10	0	0
24	251	261	76.5	79.6	10	0	0	0	60	0	10	20	0
25	261	269	79.6	82	20	0	0	30	40	0	10	0	0
26	267	277	82	84.4	10	0	0	0	80	0	0	10	0
27	277	287	84.4	87.5	10	0	0	60	20	0	0	0	10
28	287	295	87.5	89.9	20	0	0	50	30	0	0	0	0
29	295	304	89.9	92.7	20	0	0	40	10	0	0	0	30
30	304	313	92.7	95.4	20	0	0	60	10	0	0	0	10
31	313	323	95.4	96.9	10	0	0	70	20	0	0	0	0
32	323	333	96.9	99.9	20	0	0	50	30	0	0	0	0
33	Missing												
34	343	353	104.5	107.6	20	0	0	70	10	0	0	0	0
35	353	362	107.6	110.3	10	0	0	90	0	0	0	0	0
36	362	372	110.3	113.4	10	0	0	90	0	0	0	0	0
37	372	382	113.4	116.4	10	0	0	90	0	0	0	0	0
38	382	392	116.4	117.6	20	0	0	80	0	0	0	0	0

FC67-3													
Box	**TD (ft)**	**BD (ft)**	**TD (m)**	**BD (m)**	**MI**	**SH**	**FS**	**BRh**	**BRd**	**VCB**	**CB**	**MB**	**FB**
1	6	17	1.8	5.2	10	90	0	0	0	0	0	0	0
2	17	27	5.2	8.2	10	90	0	0	0	0	0	0	0
3	27	37	8.2	11.3	10	90	0	0	0	0	0	0	0
4	37	50	11.7	15.2	0	100	0	0	0	0	0	0	0
5	50	57	15.2	17.4	10	20	70	0	0	0	0	0	0
6	57	67	17.4	20.4	10	0	90	0	0	0	0	0	0
7	67	75	20.4	22.9	20	0	40	0	0	0	0	40	0
8	75	86	22.9	26.2	0	0	0	0	0	0	60	40	0
9	86	95	26.2	29	20	0	0	0	0	30	20	30	0
10	95	104	29	31.7	20	0	0	0	0	50	10	20	0
11	104	114	31.7	34.7	10	0	0	0	0	50	30	10	0
12	Missing												
13	124	132	37.8	40.2	40	0	0	0	0	0	0	40	20
14	132	142	40.2	43.3	10	0	0	0	0	0	0	50	40
15	142	153	43.3	46.6	0	0	0	90	0	0	0	10	0

16	153	163	46.6	49.7	20	0	0	70	0	0	10	0	0
17	163	173	49.6	52.7	10	0	0	60	0	0	20	10	0
18	173	183	52.7	55.8	10	0	0	60	0	0	0	10	20
19	183	194	55.8	59.1	10	0	0	80	0	0	0	10	0
20	194	204	59.1	62.2	20	0	0	70	0	0	0	10	0
21	204	214	62.2	65.2	20	0	0	70	0	0	10	0	0
22	214	224	65.2	68.3	10	0	0	80	0	0	10	0	0
23	224	234	68.3	71.3	20	0	0	70	0	0	0	10	0
24	234	244	71.3	74.4	0	0	0	90	0	0	0	0	10
25	244	254	74.4	77.4	10	0	0	80	0	10	0	0	0
26	254	263	77.4	80.2	10	0	0	80	0	10	0	0	0
27	263	272	80.2	82.9	10	0	0	80	0	10	0	0	0
28	272	282	82.9	86	20	0	0	80	0	0	0	0	0
29	282	293	86	89.3	0	0	0	100	0	0	0	0	0
30	293	302	89.3	92	20	0	0	80	0	0	0	0	0
31	302	312	92	95.1	10	0	0	90	0	0	0	0	0
32	312	322	95.1	98.1	0	0	0	100	0	0	0	0	0
33	322	334	98.1	101.8	0	0	0	100	0	0	0	0	0
34	334	344	101.8	104.9	10	0	0	90	0	0	0	0	0
35	344	354	104.9	107.9	10	0	0	90	0	0	0	0	0
36	354	363	107.9	110.6	20	0	0	10	0	0	0	0	70
37	363	374	110.6	114	10	0	0	60	0	0	0	0	30
38	374	385	114	117.3	0	0	0	100	0	0	0	0	0
39	385	394	117.3	120.1	10	0	0	80	0	0	0	10	0
40	394	403	120.1	122.8	20	0	0	80	0	0	0	0	0
41	403	413	122.8	125.9	10	0	0	90	0	0	0	0	0
42	413	426	125.9	128.9	0	0	0	100	0	0	0	0	0
43	Missing												
44	434	445	132.3	135.6	20	0	0	60	20	0	0	0	0
45	445	454	135.6	138.4	20	0	0	50	30	0	0	0	0
46	454	465	135.6	138.4	0	0	0	100	0	0	0	0	0
47	465	475	141.7	144.8	10	0	0	90	0	0	0	0	0
48	475	485	144.8	147.8	20	0	0	80	0	0	0	0	0
49	485	494	147.8	150.6	30	0	0	70	0	0	0	0	0
50	494	504	150.6	153.6	10	0	0	90	0	0	0	0	0
51	504	514	153.6	156.7	20	0	0	80	0	0	0	0	0
52	514	524	156.7	159.7	20	0	0	80	0	0	0	0	0
53	524	534	159.7	162.8	20	0	0	80	0	0	0	0	0

FC67-4

Box	TD (ft)	BD (ft)	TD (m)	BD (m)	MI	SH	FS	BRh	BRd	VCB	CB	MB	FB
1	19	30	5.8	9.1	0	0	0	100	0	0	0	0	0
2	30	41	9.1	12.5	30	0	0	70	0	0	0	0	0
3	41	51	12.5	15.5	20	0	0	80	0	0	0	0	0
4	51	61	15.5	18.6	30	0	0	70	0	0	0	0	0
5	61	72	18.6	21.9	10	0	0	90	0	0	0	0	0
6	72	81	21.9	24.7	20	0	0	80	0	0	0	0	0
7	81	90	24.7	27.4	20	0	0	80	0	0	0	0	0
8	90	102	27.4	31.1	20	0	0	60	20	0	0	0	0
9	102	111	31.1	33.8	10	0	0	70	20	0	0	0	0
10	111	120	33.8	36.6	0	0	0	100	0	0	0	0	0
11	120	131	36.6	39.9	0	0	0	100	0	0	0	0	0
12	131	141	39.9	43	10	0	0	90	0	0	0	0	0
13	141	150	43	45.7	30	0	0	70	0	0	0	0	0
14	150	161	45.7	49.1	0	0	0	100	0	0	0	0	0
15	161	171	49.1	52.1	10	0	0	80	0	0	0	0	10
16	171	182	52.1	55.5	0	0	0	70	0	0	0	0	30
17	182	193	55.5	58.8	0	0	0	80	0	0	0	0	20
18	193	202	58.8	61.6	10	0	0	90	0	0	0	0	0
19	202	212	61.6	64.6	10	0	0	90	0	0	0	0	0
20	212	222	64.6	67.7	10	0	0	90	0	0	0	0	0
21	222	233	67.7	71	0	0	0	100	0	0	0	0	0
22	233	243	71	74.1	0	0	0	100	0	0	0	0	0
23	243	254	74.1	77.4	0	0	0	100	0	0	0	0	0
24	254	265	77.4	80.8	0	0	0	100	0	0	0	0	0
25	265	276	80.8	84.1	0	0	0	100	0	0	0	0	0

FC67-5													
Box	**TD (ft)**	**BD (ft)**	**TD (m)**	**BD (m)**	**MI**	**SH**	**FS**	**BRh**	**BRd**	**VCB**	**CB**	**MB**	**FB**
1	6	17	1.8	5.2	10	0	0	90	0	0	0	0	0
2	17	26	5.2	7.9	10	0	0	90	0	0	0	0	0
3	26	36	7.9	11	10	0	0	70	20	0	0	0	0
4	36	44	11	13.4	30	0	0	20	50	0	0	0	0
5	44	53	13.4	16.2	20	0	0	0	80	0	0	0	0
6	Missing												
7	53	73	16.2	22.3	20	0	0	50	0	0	20	10	0
8	73	82	22.3	25	10	0	0	60	0	0	10	20	0
9	82	90	25	27.4	30	0	0	40	0	0	0	30	0
10	90	98	27.4	29.9	30	0	0	60	0	0	0	10	0
11	Missing												
12	Missing												
13	118	128	36	39	20	0	0	40	0	0	10	30	0

14	128	139	39	42.4	0	0	0	80	0	0	0	10	10
15	139	149	42.4	45.4	20	0	0	50	0	0	20	10	0
16	149	159	45.4	48.5	0	0	0	0	20	20	30	30	0
17	159	168	48.5	51.2	20	0	0	0	60	0	0	20	0
18	168	177	51.2	53.9	20	0	0	0	70	0	0	10	0
19	177	187	53.9	57	10	0	0	0	90	0	0	0	0
20	187	197	57	60	0	0	0	80	20	0	0	0	0
21	197	205	60	62.5	20	0	0	60	10	0	0	10	0
22	205	216	62.5	65.8	10	0	0	0	0	20	20	40	20
23	216	225	65.8	68.6	20	0	0	60	0	0	0	0	10
24	225	236	68.6	71.9	0	0	0	20	0	0	20	50	10
25	236	246	71.9	75	10	0	0	0	60	0	0	30	0
26	246	255	75	77.7	10	0	0	40	0	0	10	20	20
27	255	265	77.7	80.8	20	0	0	30	0	0	10	30	10
28	265	275	80.8	83.3	10	0	0	40	0	0	10	20	20
29	275	285	83.8	86.9	10	0	0	50	0	0	20	0	20
30	285	294	86.9	89.6	20	0	0	30	0	0	10	20	20
31	294	304	89.6	92.7	20	0	0	50	0	0	10	20	0
32	303	314	92.4	95.7	10	0	0	60	0	0	10	10	10
33	314	326	95.7	99.4	0	0	0	80	0	0	10	10	0
34	326	334	99.4	101.8	30	0	0	70	0	0	0	0	0
35	334	346	101.8	105.5	10	0	0	90	0	0	0	0	0
36	346	357	105.5	108.8	0	0	0	80	0	0	10	0	0
37	346	357	105.5	108.8	10	0	0	50	0	0	10	10	20
38	370	379	112.8	115.5	0	0	0	80	0	0	0	10	10
39	379	386	115.5	117.7	40	0	0	50	0	0	0	0	10
40	386	396	117.7	120.7	10	0	0	50	0	0	10	10	20
41	396	406	120.7	123.7	20	0	0	50	0	0	10	20	0
42	406	415	123.7	126.5	20	0	0	20	0	10	10	20	20
43	415	424	126.5	129.2	10	0	0	90	0	0	0	0	0
44	424	436	129.2	132.9	0	0	0	50	40	0	10	0	0
45	436	446	132.9	135.9	20	0	0	60	20	0	0	0	0
46	446	456	135.9	139	10	0	0	90	0	0	0	0	0
47	456	466	139	142	20	0	0	80	0	0	0	0	0
48	466	474	142	144.5	40	0	0	60	0	0	0	0	0
49	474	483	144.5	147.2	30	0	0	70	0	0	0	0	0
50	483	491	147.2	149.7	20	0	0	80	0	0	0	0	0
51	491	502	149.7	153	40	0	0	30	30	0	0	0	0
52	502	513	153	156.4	10	0	0	90	0	0	0	0	0
53	513	522	156.4	159.1	20	0	0	90	0	0	0	0	0
54	522	533	159.1	162.5	10	0	0	90	0	0	0	0	0

55	533	542	162.5	165.2	20	0	0	80	0	0	0	0	0
56	542	553	165.2	168.6	10	0	0	80	0	0	0	0	10
57	553	564	168.6	171.9	0	0	0	70	0	0	0	0	30
58	564	575	171.9	175.3	10	0	0	70	0	0	0	10	10
59	575	584	175.3	178	30	0	0	60	0	0	0	0	10
60	584	595	178	181.4	10	0	0	90	0	0	0	0	0
61	595	596	181.4	181.7	90	0	0	10	0	0	0	0	0

FC67-6														
Box	**TD (ft)**	**BD (ft)**	**TD (m)**	**BD (m)**	**MI**	**SH**	**FS**	**BRh**	**BRd**	**VCB**	**CB**	**MB**	**FB**
1	9.5	20.5	2.9	6.2	0	100	0	0	0	0	0	0	0
2	20.5	31.5	6.2	9.6	10	30	0	30	0	0	0	20	10
3	31	42	9.4	12.8	0	0	0	70	0	0	20	10	0
4	42	52	12.8	15.8	10	0	0	20	0	0	40	30	0
5	52.3	62.5	15.9	19.1	10	0	0	0	0	0	10	80	0
6	62	71	18.9	21.6	20	0	0	0	0	10	20	30	20
7	71	81	21.6	24.7	10	0	0	0	0	20	10	40	20
8	81.5	92.5	24.8	28.2	0	0	0	0	0	40	60	0	0
9	92	103	28	31.4	10	0	0	0	0	0	20	50	20
10	130	114	31.4	34.7	0	0	0	0	0	0	10	40	50
11	114.2	122.3	34.8	37.3	30	0	0	0	0	10	10	30	20
12	122	132	37.2	40.2	10	0	0	70	0	0	0	0	20
13	132	141	40.2	43	20	0	0	70	0	0	0	0	10
14	141	151	43	46	20	0	0	60	0	0	0	0	20
15	151	160	46	48.8	20	0	0	80	0	0	0	0	0
16	160	170	48.8	51.8	10	0	0	90	0	0	0	0	0
17	170	179	51.8	54.6	10	0	0	80	0	0	0	0	10
18	179	190	54.6	57.9	10	0	0	90	0	0	0	0	10
19	190	200	57.9	61	30	0	0	70	0	0	0	0	0
20	200	210	61	64	20	0	0	80	0	0	0	0	0

21	210	220	64	70.1	0	0	0	100	0	0	0	0	0
22	220	230	67.1	70.1	20	0	0	80	0	0	0	0	0
23	230	240	70.1	73.2	0	0	0	90	10	0	0	0	0
24	240	249	73.2	75.9	20	0	0	70	0	0	0	0	10
25	249	258	75.9	78.6	30	0	0	70	0	0	0	0	0
26	258	269	78.6	82	10	0	0	90	0	0	0	0	0
27	269	280	82	85.3	0	0	0	100	0	0	0	0	0
28	280	290	85.3	88.4	10	0	0	90	0	0	0	0	0
29	290	301	88.4	91.7	0	0	0	100	0	0	0	0	0

FC77-1													
Box	TD (ft)	BD (ft)	TD (m)	BD (m)	MI	SH	FS	BRh	BRd	VCB	CB	MB	FB
1	5	10	1.5	3	0	0	0	100	0	0	0	0	0
2	10	20	3	6.1	0	0	0	70	30	0	0	0	0
3	20	30	6.1	9.1	0	0	0	80	20	0	0	0	0
4	30	40	9.1	12.2	0	0	0	60	40	0	0	0	0
5	40	50	12.2	15.2	0	0	0	60	40	0	0	0	0
6	50	59	15.2	18	0	0	0	60	80	0	0	10	0
7	59	69	18	21	0	0	0	60	30	0	10	0	0
8	69	78	21	23.8	0	0	0	100	0	0	0	0	0
9	78	87	23.8	26.5	0	0	0	60	30	0	0	0	10
10	87	97	26.5	29.6	0	0	0	90	0	0	10	0	0
11	97	107	29.6	32.6	0	0	0	70	0	0	20	10	10
12	107	116	32.6	35.4	0	0	0	80	0	0	0	10	10
13	116	125	35.4	38.1	0	0	0	70	0	0	10	10	10
14	125	135	38.1	41.1	0	0	0	90	0	0	0	10	0
15	135	144	41.1	43.9	0	0	0	100	0	0	0	0	0
16	144	153	43.9	46.6	0	0	0	100	0	0	0	0	0
17	153	163	46.6	49.7	0	0	0	50	40	0	0	0	10
18	163	173	49.7	52.7	0	0	0	50	50	0	0	0	0
19	173	182	52.7	55.5	0	0	0	90	0	0	0	0	10
20	182	193	55.5	58.8	0	0	0	60	0	0	10	30	0
21	193	202	58.8	61.6	0	0	0	60	30	0	0	0	10

22	202	212	61.6	64.6	0	0	0	50	0	0	20	20	10
23	212	222	64.6	67.7	10	0	0	20	0	0	10	10	50
24	221	232	67.4	70.7	0	0	0	90	0	0	0	0	10
25	232	242	70.7	73.8	0	0	0	70	30	0	0	0	0
26	242	252	73.8	76.8	0	0	0	90	0	0	0	0	10
27	252	261	76.8	79.6	0	0	0	90	0	0	0	10	0
28	261	270	79.6	82.3	0	0	0	100	0	0	0	0	0
29	270	279	82.3	85	0	0	0	90	0	0	0	10	0
30	279	289	85	88.1	0	0	0	70	20	0	0	0	10
31	289	298	88.1	90.8	0	0	0	80	10	0	0	10	0
32	298	308	90.8	93.9	0	0	0	80	20	0	0	0	0
33	308	315	93.9	96	0	0	0	90	0	0	0	10	0
34	316	326	96.3	99.4	0	0	0	90	0	0	0	0	10
35	326	336	99.4	102.4	0	0	0	70	0	10	10	0	10
36	336	346	102.4	105.5	0	0	0	70	20	0	0	0	10
37	346	356	105.5	108.5	0	0	0	90	0	0	0	10	0
38	356	366	108.5	111.6	0	0	0	60	20	0	0	10	10
39	366	375	111.6	114.3	0	0	0	70	0	0	10	10	10
40	375	384	114.3	117	0	0	0	70	20	0	0	10	0
41	384	394	117	120.1	0	0	0	70	0	0	10	20	0
42	394	403	120.1	122.8	0	0	0	70	10	0	10	10	0
43	403	413	122.8	125.9	0	0	0	70	10	0	10	10	0
44	413	422	125.9	128.6	0	0	0	50	0	0	10	10	30
45	422	432	128.6	131.7	0	0	0	40	10	0	10	30	20
46	432	442	131.7	134.7	0	0	0	40	0	0	10	20	30
47	442	450	134.7	137.2	0	0	0	40	10	0	10	10	30
48	450	460	137.2	140.2	0	0	0	80	0	0	0	10	10
49	460	470	140.2	143.3	0	0	0	60	20	0	0	20	0
50	470	479	143.3	146	0	0	0	60	0	0	10	10	20
51	479	489	146	149	0	0	0	70	0	10	0	10	10

52	489	498	149	151.8	0	0	0	70	0	0	0	10	20
53	498	508	151.8	154.8	0	0	0	20	0	0	10	50	20
54	508	518	154.8	157.9	0	0	0	50	0	0	10	20	20
55	518	526	157.9	160.3	0	0	0	50	0	0	10	10	30
56	526	536	160.3	163.4	0	0	0	40	0	0	0	10	50
57	536	546	163.4	166.4	10	0	0	0	0	0	0	20	70
58	546	556	166.4	169.5	10	0	0	40	0	0	10	20	20
59	556	565	169.5	172.2	0	0	0	50	0	0	10	20	20
60	565	575	172.2	175.3	0	0	0	40	0	0	10	20	30
61	575	584	175.3	178	0	0	0	100	0	0	0	0	0
62	584	594	178	181.1	0	0	0	70	0	0	10	10	10
63	594	603	181.1	183.8	0	0	0	100	0	0	0	0	0
64	603	613	183.8	186.8	0	0	0	90	0	0	0	0	10
65	613	623	186.8	189.9	0	0	0	90	0	0	0	0	10
66	623	632	189.9	192.6	0	0	0	70	20	0	0	0	10
67	632	641	192.6	195.4	0	0	0	30	70	0	0	0	0
68	641	651	195.4	198.4	0	0	0	30	60	0	0	0	10
69	651	661	198.4	201.5	0	0	0	10	80	0	0	0	10
70	661	670	201.5	204.2	0	0	0	70	20	0	0	0	10
71	670	680	204.2	207.3	0	0	0	70	20	0	0	0	10
72	680	689	207.3	210	0	0	0	90	0	0	0	0	10
73	689	699	210	213.1	0	0	0	90	10	0	0	0	0
74	699	708	213.1	215.8	0	0	0	60	40	0	0	0	0
75	708	718	215.8	218.8	0	0	0	90	0	0	0	0	10
76	718	728	218.8	221.9	0	0	0	90	0	0	0	0	10
77	728	737	221.9	224.6	0	0	0	80	0	0	10	10	0

78	737	747	224.6	227.7	0	0	0	20	0	0	10	20	50
79	747	757	227.7	230.7	0	0	0	30	0	0	10	10	50
80	757	766	230.7	233.5	0	0	0	80	0	0	0	10	10
81	766	776	233.5	236.5	0	0	0	90	10	0	0	0	0
82	776	786	236.5	239.6	0	0	0	80	10	0	0	10	0
83A	786	795	239.6	242.3	0	0	0	60	20	0	10	10	0
83B	795	805	242.3	245.4	0	0	0	50	20	0	0	10	20
84	805	815	245.4	248.4	0	0	0	50	20	0	10	10	10
85	815	824	248.4	251.2	0	0	0	90	0	0	0	10	0
86	824	834	251.2	254.2	0	0	0	60	30	0	0	0	10
87	834	843	254.2	256.9	0	0	0	20	70	0	0	0	10
88	843	853	256.9	260	0	0	0	70	20	0	0	10	0
89	853	863	260	263	0	0	0	60	30	0	0	0	10
90	863	872	263	265.8	0	0	0	90	10	0	0	0	0
91	872	882	265.8	268.8	0	0	0	20	70	0	0	0	10
92	882	892	268.8	271.9	0	0	0	60	30	0	0	0	10
93	892	901	271.9	274.6	0	0	0	20	70	0	0	10	0
94	901	910	274.6	277.4	0	0	0	20	70	0	0	0	10
95	910	920	277.4	280.4	0	0	0	50	40	0	0	10	0
96	920	929	280.4	283.2	0	0	0	20	70	0	0	0	10
97	929	939	283.2	286.2	0	0	0	30	60	0	0	0	10
98A	939	949	286.2	289.3	0	0	0	20	70	0	0	0	10
98B	949	958	289.3	292	0	0	0	10	80	0	0	0	10
99	958	968	292	295	0	0	0	30	60	0	0	10	0
100	968	978	295	298.1	0	0	0	20	70	0	0	10	0
101	978	987	298.1	300.8	0	0	0	30	70	0	0	0	0
102	987	997	900.8	303.9	0	0	0	0	90	0	0	0	10
103	997	1007	303.9	306.9	0	0	0	20	70	0	0	0	10
104	1007	1017	306.9	310	0	0	0	20	70	0	0	0	10

105	1017	1027	310	313	0	0	0	40	60	0	0	0	0
106	1027	1037	313	316.1	0	0	0	80	20	0	0	0	0
107	1037	1045	316.1	318.5	0	0	0	80	20	0	0	0	0
108	1045	1055	318.5	321.6	0	0	0	50	40	0	0	0	10
109	1055	1064	321.6	324.3	0	0	0	60	30	0	0	10	0
110	1064	1074	324.3	327.4	0	0	0	70	20	0	0	0	10
111	1074	1083	327.4	330.1	0	0	0	70	20	0	0	10	0
112	1083	1093	330.1	333.1	0	0	0	80	20	0	0	0	0
113	1093	1103	333.2	336.2	0	0	0	40	0	10	10	30	10
114	1103	1113	336.2	339.2	0	0	0	30	0	0	20	30	20
115	1113	1123	339.2	342.3	0	0	0	70	0	0	10	20	0
116	1123	1133	342.3	345.3	0	0	0	60	0	0	10	10	20
117	1133	1142	345.3	348.1	0	0	0	80	0	0	0	10	10
118	1142	1152	348.1	351.1	0	0	0	80	10	0	10	0	0
119	1152	1162	351.1	354.2	0	0	0	70	0	0	10	10	10
120	1162	1171	354.2	356.9	0	0	0	50	10	0	0	20	20
121	1171	1180	356.9	359.7	0	0	0	70	0	0	0	20	10
122	1180	1190	359.7	362.7	0	0	0	70	0	0	0	0	30
123	1190	1200	362.7	365.8	0	0	0	60	0	0	20	0	20
124	1200	1210	365.8	368.8	0	0	0	70	0	10	10	10	0
125	1210	1219	368.8	371.6	0	0	0	70	0	0	0	10	20
126	1219	1228	371.6	374.3	0	0	0	80	0	0	0	10	10
127	1228	1238	374.3	377.3	0	0	0	50	20	0	0	30	0
128	1238	1247	377.3	380.1	0	0	0	90	0	0	10	0	0
129	1247	1257	380.1	383.1	0	0	0	80	0	0	10	10	0
130	1257	1267	383.1	386.2	0	0	0	40	0	0	20	30	10
131	1267	1276	386.2	388.9	0	0	0	80	0	0	10	10	0
132	1276	1285	388.9	391.7	0	0	0	60	0	0	20	10	10
133	1285	1295	391.7	394.7	0	0	0	80	0	0	10	10	0
134	1295	1304	394.7	397.5	0	0	0	60	0	0	10	20	10

135	1304	1314	397.5	400.5	0	0	0	90	0	0	0	0	10
136	1314	1323	400.5	403.3	0	0	0	90	0	0	0	10	0
137	1323	1332	403.3	406	0	0	0	80	0	0	10	0	10
138	1332	1342	406	409	0	0	0	80	0	0	10	0	10
139	1342	1351	409	411.8	0	0	0	70	0	0	10	10	10
140	1351	1361	411.8	414.8	0	0	0	70	0	0	20	10	0
141	1361	1371	414.8	417.9	0	0	0	60	0	0	10	10	20
142	1361	1371	414.8	417.9	0	0	0	40	0	0	10	30	20
143	1376	1389	419.4	423.4	0	0	0	20	0	10	40	10	20
144	1389	1399	423.4	426.4	0	0	0	70	0	10	0	10	10
145	1399	1409	426.4	429.5	0	0	0	80	0	0	0	0	20
146	1409	1418	429.5	432.2	0	0	0	60	0	0	20	0	20
147	1418	1428	432.2	435.3	0	0	0	80	0	0	20	0	0
148	1420	1437	432.8	438	0	0	0	70	0	0	10	10	10
149	1437	1447	438	441	0	0	0	70	0	0	20	10	0
150	1447	1457	441	444.1	0	0	0	70	0	0	10	10	10
151	1457	1468	444.1	447.4	0	0	0	90	0	0	0	10	0
152	1468	1475	447.4	449.6	0	0	0	100	0	0	0	0	0
153	1475	1485	449.6	452.6	0	0	0	80	0	0	10	10	0
154	1485	1495	452.6	455.7	0	0	0	90	0	0	0	10	0
155	1495	1500	455.7	457.2	0	0	0	70	0	10	10	10	0
156	1500	1510	457.2	461.2	0	0	0	90	0	0	0	10	0
157	1513	1523	461.2	464.2	0	0	0	90	0	0	0	10	0
158	1523	1533	464.2	467.3	0	0	0	100	0	0	0	0	0
159	1533	1540	467.3	469.4	20	0	0	80	0	0	0	0	0
160	1540	1550	469.4	472.4	0	0	0	90	0	0	0	10	0
161	1550	1560	472.4	475.5	0	0	0	90	0	0	0	10	0
162	1560	1570	475.5	478.5	0	0	0	90	0	0	0	0	10
163	1570	1580	478.5	481.6	0	0	0	90	0	0	0	0	10
164	1580	1588	481.6	484	0	0	0	90	0	0	0	10	0
165	1588	1598	484	487.1	0	0	0	90	0	0	0	0	10

166	1598	1608	487.1	490.1	0	0	0	90	0	0	10	0	0
167	1608	1618	490.1	493.2	0	0	0	90	0	0	0	10	0
168	1618	1627	493.2	495.9	0	0	0	90	0	0	0	0	10
169	1627	1636	495.9	498.7	0	0	0	90	0	0	0	10	0
170	1635	1645	495.9	498.7	0	0	0	90	0	0	0	0	10
171	1645	1655	501.4	504.4	0	0	0	90	0	0	0	10	0
172	1655	1665	504.4	507.5	0	0	0	90	0	0	0	10	0
173	1665	1675	507.5	510.5	0	0	0	90	0	0	0	10	0
174	1675	1684	510.5	513.3	0	0	0	70	0	0	10	10	10
175	1684	1693	513.3	516	0	0	0	70	0	0	0	10	20
176	1693	1703	516	519.1	0	0	0	90	0	0	0	0	10
177	1703	1713	519.1	522.1	0	0	0	90	0	0	0	10	0
178	1713	1722	522.1	524.9	0	0	0	70	0	0	0	10	20
179	1722	1732	524.9	527.9	0	0	0	80	0	0	0	20	0
180	1732	1742	527.9	531	0	0	0	80	0	0	10	10	0
181	1742	1751	531	533.7	0	0	0	70	0	0	10	10	10
182	1751	1761	533.7	536.8	0	0	0	80	0	0	0	0	20
183	1761	1770	536.8	539.5	0	0	0	80	0	0	0	10	10
184	1770	1782	539.5	543.2	0	0	0	90	0	0	0	0	10
185	1782	1792	543.2	546.2	0	0	0	90	0	0	0	0	10
186	1792	1802	546.2	549.2	0	0	0	90	0	0	0	10	0
187	1802	1810	549.2	551.7	0	0	0	90	0	0	0	10	0
188	1810	1820	551.7	554.7	0	0	0	60	0	0	10	30	0
189	1820	1830	554.7	557.8	0	0	0	80	0	0	0	10	10
190A	1830	1840	557.8	560.8	0	0	0	80	0	0	0	10	10
190B	1840	1850	560.8	563.9	0	0	0	80	0	0	20	0	0
191	1850	1860	563.9	566.9	0	0	0	80	0	0	0	10	10
192	1860	1869	566.9	569.7	0	0	0	60	0	0	0	30	10
193	1869	1876	569.7	571.8	0	0	0	90	0	0	0	10	0
194	1878	1888	572.4	575.5	0	0	0	70	0	0	0	20	10

195	1888	1898	575.5	578.5	0	0	0	70	0	10	0	10	10
196	1898	1908	578.5	581.6	0	0	0	80	0	0	0	0	20
197	1908	1918	5816	584.6	0	0	0	70	0	0	0	20	10
198	Missing												
199	1929	1938	588	590.7	0	0	0	60	0	0	0	30	10
200	1938	1947	590.7	593.4	0	0	0	70	0	0	0	20	10
201	1947	1957	593.5	596.5	0	0	0	80	0	0	10	10	0
202	1957	1966	596.5	599.2	0	0	0	60	0	0	10	20	10
203	1966	1976	599.2	602.3	0	0	0	70	0	0	10	10	10
204	1976	1985	602.3	605	0	0	0	50	0	0	10	20	20
205	1985	1995	605	608.1	0	0	0	60	0	0	0	10	30
206	1995	2004	608.1	610.8	0	0	0	70	0	0	0	20	10
207	2004	2014	610.8	613.9	0	0	0	70	0	0	0	10	20
208	2014	2023	613.9	616.9	0	0	0	80	0	10	0	10	0
209	2023	2033	616.6	619.7	0	0	0	60	0	0	0	20	20
210	2033	2042	619.7	622.4	0	0	0	40	20	0	10	0	30
211	2042	2051	622.4	625.1	0	0	0	40	20	0	10	10	20
212	2051	2061	625.1	628.2	0	0	0	50	0	0	20	10	20
213	2061	2070	628.2	630.9	0	0	0	50	0	0	0	30	20
214	2070	2080	630.9	634	0	0	0	50	0	10	10	20	10
215	2080	2090	634	637	0	0	0	50	0	20	0	20	10
216	2090	2098	637	639.5	0	0	0	80	0	0	10	10	0
217	2098	2108	639.8	642.5	0	0	0	90	0	0	10	0	0
218	2109	2117	642.8	645.3	0	0	0	90	0	10	0	0	0
219	2117	2127	645.3	648.3	0	0	0	80	0	10	0	10	0
220	2127	2137	648.3	651.4	0	0	0	80	0	0	10	10	0
221	2137	2146	651.4	654.1	0	0	0	90	0	0	10	0	0
222	2146	2156	654.1	657.1	0	0	0	90	0	0	0	0	10

223	2156	2166	657.1	660.2	0	0	0	100	0	0	0	0	0
224	2166	2176	660.2	663.2	0	0	0	90	0	0	0	10	0
225	2176	2186	663.2	666.3	0	0	0	90	0	10	0	0	0
226	2186	2196	666.3	669.3	0	0	0	90	0	0	0	10	0
227	2196	2206	669.3	672.4	0	0	0	70	0	10	0	10	10
228	2206	2216	672.4	675.4	0	0	0	90	0	0	0	10	0
229	2216	2224	675.4	677.9	0	0	0	90	0	0	0	10	0
230	2224	2234	677.9	680.9	0	0	0	80	0	0	0	20	0
231	2234	2244	680.9	684	0	0	0	90	0	0	0	10	0
232	2244	2254	684	687	0	0	0	90	0	0	0	10	0
233	2254	2263	687	689.8	0	0	0	90	0	0	0	10	0
234	2263	2273	689.8	692.8	0	0	0	90	0	0	0	10	0
235	2273	2283	692.8	695.9	20	0	0	60	0	0	10	10	0
236	2283	2293	695.9	698.9	70	0	0	30	0	0	0	0	0

FC77-2													
Box	TD (ft)	BD (ft)	TD (m)	BD (m)	MI	SH	FS	BRh	BRd	VCB	CB	MB	FB
1	0	14	0	4.3	30	70	0	0	0	0	0	0	0
2	14	20	4.3	6.1	20	80	0	0	0	0	0	0	0
3	20	29	6.1	8.8	0	90	10	0	0	0	0	0	0
4	29	39	8.8	11.9	0	0	100	0	0	0	0	0	0
5	39	49	11.9	14.9	0	0	100	0	0	0	0	0	0
6	49	59	14.9	18	0	0	10	20	0	0	0	20	50
7	59	69	18	21	0	0	0	0	0	0	20	50	30
8	69	78	21	23.8	0	0	0	0	0	20	30	40	10
9	78	87	23.8	26.5	0	0	0	0	0	0	10	20	70
10	87	97	26.5	29.6	0	0	0	20	0	0	20	20	40
11	97	108	29.6	32.9	0	0	0	20	0	0	0	60	20
12	108	115	32.9	35.1	0	0	0	60	0	0	0	10	30
13	115	125	35.1	38.1	0	0	0	60	0	0	0	20	20
14	125	134	38.1	40.8	10	0	0	60	0	0	0	20	10

15	134	144	40.8	144	0	0	0	60	0	0	10	30	0
16	144	154	43.9	46.9	0	0	0	80	0	0	0	10	10
17	154	163	46.9	49.7	0	0	0	90	0	0	0	0	10
18	163	173	49.7	52.7	0	0	0	70	0	0	0	10	20
19	173	182	52.7	55.5	0	0	0	40	0	0	0	10	50
20	182	192	55.5	58.5	0	0	0	90	0	0	0	10	0
21	192	202	58.5	61.6	0	0	0	90	0	0	0	10	0
22	202	211	61.6	64.3	0	0	0	90	0	0	0	0	10
23	211	222	64.3	67.7	0	0	0	90	0	0	0	0	10
24	222	227	67.7	69.2	0	0	0	90	0	0	0	0	10
25	227	237	69.2	72.2	0	0	0	10	0	0	0	10	80
26	237	247	72.2	75.3	10	0	0	40	0	0	0	10	40
27	247	257	75.3	78.3	0	0	0	40	0	0	20	20	20
28	257	266	78.3	81.1	0	0	0	60	0	0	10	10	20
29	266	275	81.1	83.8	0	0	0	70	0	0	0	0	30
30	275	285	83.8	86.9	0	0	0	60	0	0	0	20	20
31	285	295	86.8	89.9	0	0	0	60	0	0	10	10	20
32	295	305	89.9	93	0	0	0	60	0	0	0	20	20
33	305	314	93	95.7	0	0	0	90	0	0	0	10	0
34	314	324	95.7	98.8	0	0	0	90	0	0	0	10	0
35	324	333	98.8	101.5	0	0	0	40	0	0	10	30	20
36	333	343	101.5	104.5	0	0	0	90	0	0	0	10	0
37	343	353	104.5	107.6	0	0	0	90	0	0	0	0	10
38	353	362	107.6	110.3	0	0	0	90	0	0	0	0	10
39	362	371	110.3	113.1	0	0	0	90	0	0	0	0	10
40	371	381	113.1	116.1	0	0	0	100	0	0	0	0	0
41	31	390	116.1	118.9	0	0	0	90	0	0	0	10	0
42	390	400	118.9	121.9	0	0	0	80	0	0	0	20	0

43	400	410	121.9	125	0	0	0	80	0	0	0	0	20
44	410	419	125	127.7	0	0	0	70	0	0	0	20	10
45	419	429	127.7	130.8	0	0	0	70	0	0	0	10	20
46	429	438	130.8	133.5	0	0	0	90	0	0	0	10	0
47	438	447	133.5	136.2	0	0	0	90	0	0	0	10	0
48	447	457	136.2	139.3	0	0	0	90	0	0	0	10	0
49	457	466	139.3	142	0	0	0	90	0	0	0	10	0
50	466	475	142	144.8	0	0	0	90	0	0	0	10	0
51	475	485	144.8	147.8	0	0	0	90	0	0	0	10	0
52	485	495	147.8	150.9	0	0	0	90	0	0	0	0	10
53	495	505	150.9	153.9	0	0	0	90	0	0	0	0	10
54	505	514	153.9	156.7	0	0	0	90	0	0	0	10	0
55	514	523	156.7	159.4	0	0	0	90	0	0	0	0	10
56	523	533	159.4	162.5	0	0	0	90	0	0	0	0	10
57	533	543	162.5	165.5	0	0	0	90	0	0	0	10	0
58	543	552	165.5	168.2	0	0	0	90	0	0	0	0	10
59	552	562	168.2	171.3	0	0	0	90	0	0	0	0	10
60	562	572	171.3	174.3	0	0	0	70	0	0	0	10	20
61	572	581	174.3	177.1	0	0	0	70	0	0	10	0	20
62	581	591	177.1	180.1	0	0	0	90	0	0	0	0	10
63	591	600	180.1	182.9	0	0	0	90	0	0	0	10	0
64	600	610	182.9	185.9	0	0	0	90	0	0	0	10	0
65	610	619	185.9	188.7	0	0	0	100	0	0	0	0	0
66	619	629	188.7	191.7	0	0	0	60	0	0	0	10	30
67	629	639	191.7	194.8	0	0	0	80	0	0	0	10	10
68	639	648	194.8	197.5	0	0	0	90	0	0	0	10	0
69	648	658	197.5	200.6	0	0	0	90	0	0	0	10	0
70	658	668	200.6	203.6	0	0	0	100	0	0	0	0	0
71	668	677	203.6	206.3	0	0	0	90	0	0	0	10	0
72	677	687	206.3	209.4	0	0	0	90	0	0	0	10	0
73	687	697	209.4	212.4	0	0	0	100	0	0	0	0	0

74	697	706	212.4	215.2	0	0	0	90	0	0	0	0	10
75	706	716	215.2	218.2	0	0	0	90	0	0	0	0	10
76	716	726	218.2	221.3	0	0	0	100	0	0	0	0	0
77	726	735	221.3	224	10	0	0	90	0	0	0	0	0
78	735	745	224	227.1	0	0	0	100	0	0	0	0	0
79	745	755	230.1	233.2	0	0	0	90	0	0	0	0	10
80	755	765	233.2	236.2	0	0	0	90	0	0	0	0	10
81	765	775	236.2	239	10	0	0	80	0	0	0	0	10
82	775	784	239	241.7	0	0	0	90	0	0	0	0	10
83	784	793	239	241.7	0	0	0	90	0	0	0	0	10
84	793	803	241.7	244.8	0	0	0	90	0	0	0	0	10
85	803	813	244.8	247.8	0	0	0	90	0	0	0	0	10
86	813	822	247.8	250.5	0	0	0	60	0	0	0	0	40
87	822	832	250.5	253.6	0	0	0	80	0	0	0	10	10
88	832	841	253.6	256.3	0	0	0	90	0	0	0	0	10
89	841	850	256.3	259.1	0	0	0	90	0	0	0	10	0
90	850	860	259.1	262.1	0	0	0	100	0	0	0	0	0
91	860	870	262.1	265.2	0	0	0	90	0	0	0	10	0
92	870	880	265.2	268.2	0	0	0	90	0	0	0	10	0
93	880	889	268.2	271	0	0	0	90	0	0	0	0	10
94	889	899	271	274	0	0	0	90	0	0	0	10	0
95	899	908	274	276.8	0	0	0	90	0	0	0	0	10
96	909	917	277	280	0	0	0	90	0	0	0	0	10
97	917	927	279.5	282.5	0	0	0	100	0	0	0	0	0
98	927	937	282.5	285.6	0	0	0	90	0	0	0	10	0
99	937	947	285.6	288.6	0	0	0	90	0	0	0	10	0
100	947	956	288.6	291.4	0	0	0	90	0	0	0	10	0
101	956	966	291.4	294.4	0	0	0	100	0	0	0	0	0
102	966	975	294.4	297.2	0	0	0	90	0	0	0	10	0
103	975	985	297.2	300.2	0	0	0	70	20	0	0	10	0
104	985	994	300.2	303	0	0	0	90	0	0	0	0	10

105	994	1003	303	305.7	0	0	0	90	0	0	0	0	10
106	1003	1013	305.7	308.8	0	0	0	100	0	0	0	0	0
107	1013	1023	308.8	311.8	0	0	0	100	0	0	0	0	0
108	1022	1032	311.5	314.6	0	0	0	90	0	0	0	0	10
109	1032	1042	314.6	317.6	0	0	0	90	0	0	0	0	10
110	1042	1051	317.6	320.3	0	0	0	90	0	0	0	0	10
111	1051	1065	320.3	324.6	0	0	0	90	0	0	0	10	0
112	1065	1075	324.6	327.7	0	0	0	70	0	0	0	20	10
113	1075	1085	327.7	330.7	0	0	0	70	0	0	0	20	10
114	1085	1095	330.7	333.8	0	0	0	90	0	0	0	0	10
115	1095	1105	333.8	336.8	0	0	0	60	0	0	0	20	20
116	1105	1115	336.8	339.9	0	0	0	70	0	0	0	20	10
117	1115	1125	336.8	339.9	0	0	0	50	0	0	10	20	20
118	1125	1135	339.9	342.9	0	0	0	80	0	0	10	10	0
119	1135	1143	345.9	348.4	0	0	0	60	0	0	0	10	30
120	1143	1153	348.4	351.4	0	0	0	70	0	0	10	10	10
121	1153	1163	351.4	354.5	0	0	0	90	0	0	0	10	0
122	1163	1172	354.5	357.2	0	0	0	90	0	0	0	10	0
123	1172	1182	357.2	360.3	0	0	0	80	0	0	10	10	0
124	1182	1192	360.3	363.3	0	0	0	70	0	0	20	10	0
125	1192	1200	363.3	365.8	0	0	0	90	0	0	0	10	0
126	1200	1210	365.8	368.8	0	0	0	90	0	0	0	10	0
127	1210	1220	368.8	371.9	0	0	0	100	0	0	0	0	0
128	1220	1229	371.9	374.6	0	0	0	90	0	0	0	10	0
129	1229	1239	374.6	377.6	0	0	0	90	0	0	0	10	0
130	1239	1248	377.6	380.4	0	0	0	90	0	0	0	10	0
131	1248	1258	380.4	383.4	0	0	0	70	0	10	20	0	0
132	1258	1268	383.4	386.5	0	0	0	90	0	0	10	0	0
133	1268	1277	386.5	389.2	0	0	0	90	0	0	0	10	0
134	1277	1286	389.2	392	0	0	0	100	0	0	0	0	0
135	1286	1296	392	395	0	0	0	80	0	0	0	10	10
136	1296	1305	395	397.8	0	0	0	80	0	0	0	10	10

137	1305	1315	397.8	400.8	0	0	0	90	0	0	0	0	10
138	1315	1324	400.8	403.6	0	0	0	90	0	0	10	0	0
139	1324	1333	403.6	406.3	0	0	0	100	0	0	0	0	0
140	1333	1343	406.3	409.3	0	0	0	60	0	0	20	10	10
141	1343	1353	409.3	412.4	0	0	0	60	0	0	10	30	0
142	1353	1363	412.4	415.4	0	0	0	70	0	0	0	10	20
143	1363	1371	415.4	417.9	0	0	0	80	0	0	10	10	0
144	1371	1381	417.9	420.9	0	0	0	80	0	0	10	10	0
145	1381	1391	420.9	424	0	0	0	90	0	0	0	10	0
146	1391	1401	424	427	0	0	0	90	0	0	0	10	0
147	1401	1409	427	429.5	0	0	0	90	0	0	0	0	10
148	1409	1419	429.5	432.5	0	0	0	90	0	0	0	0	10
149	1419	1428	432.5	435.3	0	0	0	90	0	0	0	10	0
150	1428	1438	435.3	438.3	0	0	0	90	0	0	0	10	0
151	1438	1448	438.3	441.4	0	0	0	70	0	0	10	20	0
152	1448	1457	441.4	444.1	0	0	0	80	0	0	0	20	0
153	1457	1466	444.1	446.8	0	0	0	100	0	0	0	0	0
154	1466	1476	446.8	449.9	0	0	0	80	0	0	10	10	0
155	1476	1486	449.9	452.9	0	0	0	80	0	0	10	10	0
156	1486	1496	452.9	456	0	0	0	80	0	0	10	10	0
157	1496	1506	456	459	0	0	0	60	0	0	20	10	10
158	1506	1516	459	462.1	0	0	0	100	0	0	0	0	0
159	1516	1525	462.1	464.8	0	0	0	90	0	0	0	10	0
160	1525	1535	464.8	467.9	0	0	0	90	0	0	0	0	10
161	1535	1544	470.6	473	0	0	0	90	0	0	0	0	10
162	1544	1554	473.7	476.4	0	0	0	90	0	0	0	0	10
163	1554	1563	473.7	476.4	0	0	0	90	0	0	0	10	0
164	1563	1573	476.4	479.5	0	0	0	100	0	0	0	0	0
165	1573	1583	482.5	485.2	0	0	0	90	0	0	0	10	0
166	1583	1592	485.2	488	0	0	0	90	0	0	0	0	10
167	1592	1601	485.2	488	0	0	0	90	0	0	0	0	10
168	1601	1611	488	491	0	0	0	90	0	0	0	0	10
169	1611	1620	491	493.8	0	0	0	100	0	0	0	0	0
170	1620	1630	493.8	496.8	0	0	0	90	0	0	0	10	0

171	1630	1639	496.8	499.6	0	0	0	90	0	0	0	10	0
172	1639	1649	499.6	502.6	0	0	0	90	0	0	0	10	0
173	1649	1659	502.6	505.7	0	0	0	100	0	0	0	0	0
174	1659	1668	505.7	508.4	0	0	0	90	0	0	0	10	0
175	1668	1677	508.4	511.1	0	0	0	90	0	0	0	10	0
176	1677	1687	511.1	514.2	0	0	0	70	0	0	0	20	10
177	1687	1697	514.2	517.2	0	0	0	90	0	0	0	10	0
178	1697	1704	517.2	519.4	10	0	0	90	0	0	0	0	0
179	1705	1715	519.5	522.7	0	0	0	70	0	0	10	20	0
180	1715	1725	522.7	525.8	0	0	0	80	0	0	10	10	0
181	1725	1735	525.8	528.8	0	0	0	80	0	0	0	10	10
182	1735	1744	528.8	531.6	0	0	0	90	0	0	0	10	0
183	1744	1754	531.6	534.6	0	0	0	90	0	0	10	0	0
184	1754	1764	531.6	534.6	0	0	0	90	0	0	0	10	0
185	1764	1773	540.4	543.5	0	0	0	90	0	0	0	10	0
186	1773	1783	540.4	543.5	0	0	0	90	0	0	0	10	0
187	1783	1792	543.5	546.2	0	0	0	90	0	0	0	10	0
188	1792	1800	546.2	548.6	20	0	0	70	0	0	0	10	0

FC77-3													
Box	**TD (ft)**	**BD (ft)**	**TD (m)**	**BD (m)**	**MI**	**SH**	**FS**	**BRh**	**BRd**	**VCB**	**CB**	**MB**	**FB**
1	0	18	0	5.5	20	80	0	0	0	0	0	0	0
2	18	25	5.5	7.6	0	100	0	0	0	0	0	0	0
3	25	35	7.6	10.7	0	10	40	0	0	0	0	20	30
4	35	45	10.7	13.7	0	0	0	0	0	0	30	60	10
5	45	55	13.7	15.2	0	0	0	0	0	20	50	30	0
6	55	65	16.8	19.8	0	0	0	0	0	20	40	20	20
7	65	74	19.8	22.6	0	0	0	0	0	10	30	40	20
8	74	83	22.6	25.3	0	0	0	20	0	10	20	20	30
9	83	93	25.3	28.3	0	0	0	50	0	0	10	20	20
10	93	103	28.3	31.4	0	0	0	40	0	10	20	10	20
11	103	113	31.4	34.4	0	0	0	10	0	10	30	30	20
12	113	124	34.4	37.8	0	0	0	80	0	0	0	20	0
13	124	134	37.8	40.8	0	0	0	90	0	0	0	10	0
14	134	145	40.8	44.2	0	0	0	90	0	0	0	0	10
15	145	155	44.2	47.2	0	0	0	90	0	0	0	10	0
16	155	164	47.2	50	0	0	0	90	0	0	0	10	0
17	164	173	50	52.7	0	0	0	90	0	0	0	0	10
18	173	183	52.7	55.8	0	0	0	100	0	0	0	0	0
19	183	193	55.8	58.8	0	0	0	100	0	0	0	0	0
20	193	202	58.8	61.6	0	0	0	100	0	0	0	0	0

21	202	212	61.6	64.6	0	0	0	90	0	0	0	0	10
22	212	222	64.6	67.7	0	0	0	100	0	0	0	0	0
23	222	231	67.7	70.4	0	0	0	90	0	0	0	0	10
24	231	241	70.4	73.5	0	0	0	90	0	0	0	0	10
25	241	251	73.5	76.5	0	0	0	90	0	0	0	10	0
26	251	260	76.5	79.2	0	0	0	70	0	0	0	10	20
27	260	270	79.2	82.3	0	0	0	90	0	0	0	10	0
28	270	279	82.3	85	0	0	0	90	0	0	0	0	10
29	279	289	85	88.1	0	0	0	90	0	0	0	10	0
30	289	299	88.1	91.1	0	0	0	90	0	0	0	0	10
31	299	308	91.1	93.9	0	0	0	90	0	0	0	10	0
32	308	318	93.8	96.9	0	0	0	90	0	0	0	10	0
33	318	327	96.9	99.7	0	0	0	90	0	0	0	10	0
34	327	336	99.7	102.4	0	0	0	90	0	0	0	10	0
35	336	346	102.4	105.5	0	0	0	100	0	0	0	0	0
36	346	356	105.5	108.5	0	0	0	100	0	0	0	0	0
37	356	365	105.5	108.5	0	0	0	90	0	0	0	10	0
38	365	375	111.3	114.3	0	0	0	90	0	0	0	10	0
39	375	385	114.3	117.3	0	0	0	90	0	0	0	10	0
40	385	395	117.3	120.4	0	0	0	90	0	0	0	10	0
41	395	404	120.4	123.1	0	0	0	90	0	0	0	10	0
42A	413	423	125.9	128.9	0	0	0	100	0	0	0	0	0
42B	404	413	123.1	125.9	0	0	0	60	0	0	0	20	20
43	423	433	128.9	132	0	0	0	100	0	0	0	0	0
44	433	442	132	134.7	0	0	0	100	0	0	0	0	0
45	442	452	134.7	137.8	0	0	0	100	0	0	0	0	0
46	452	462	137.8	140.8	0	0	0	90	0	0	0	0	10
47	462	471	140.8	143.6	0	0	0	90	0	0	0	10	0
48	471	481	143.6	146.6	0	0	0	80	0	0	0	10	10
49	481	491	146.6	149.7	0	0	0	90	0	0	0	0	10
50	491	500	149.7	152.4	0	0	0	90	0	0	0	0	10
51	500	510	152.4	155.4	0	0	0	90	0	0	10	0	0
52	510	520	155.4	158.5	0	0	0	90	0	0	0	10	0
53	520	530	158.5	161.5	0	0	0	90	0	0	0	10	0
54	530	539	161.5	164.3	0	0	0	90	0	0	0	10	0
55	539	549	164.3	167.3	0	0	0	90	0	0	0	0	10
56	549	559	167.3	170.4	0	0	0	90	0	0	0	0	10
57	559	568	170.4	173.1	0	0	0	100	0	0	0	0	0
58	568	578	173.1	176.2	0	0	0	100	0	0	0	0	0
59	578	588	176.2	179.2	0	0	0	90	0	0	0	0	10
60	588	598	179.2	182.3	0	0	0	100	0	0	0	0	0
61	598	607	182.3	185	0	0	0	100	0	0	0	0	0
62	607	617	185	188.1	0	0	0	90	0	0	0	0	10
63	617	627	188.1	191.1	0	0	0	90	0	0	0	10	0

64	627	637	191.1	194.2	0	0	0	90	0	0	0	10	0
65	637	646	194.2	196.9	0	0	0	100	0	0	0	0	0
66	646	656	196.9	199.9	0	0	0	100	0	0	0	0	0
67	656	666	199.9	203	0	0	0	90	0	0	0	0	10
68	666	676	203	206	0	0	0	80	0	0	0	10	10
69	676	685	206	208.8	0	0	0	80	0	0	10	10	0
70	685	695	208.8	211.8	0	0	0	100	0	0	0	0	0
71	694	704	211.5	214.6	0	0	0	90	0	0	0	0	10
72	704	714	214.6	217.6	0	0	0	90	0	0	10	0	0
73A	714	724	220.7	223.7	0	0	0	90	0	0	10	0	0
73B	724	734	220.7	223.7	0	0	0	90	0	0	0	10	0
74	734	742	223.7	226.2	0	0	0	90	0	0	10	0	0
75	742	752	226.2	229.2	0	0	0	90	0	0	0	0	10
76	752	761	229.2	232	0	0	0	90	0	0	10	0	0
77	761	770	232	234.7	0	0	0	90	0	0	0	0	10
78	770	780	234.7	237.7	0	0	0	90	0	0	0	10	0
79	780	790	237.7	240.8	0	0	0	70	0	0	0	10	20
80	790	798	240.8	243.2	0	0	0	80	0	0	0	10	10
81	798	807	243.2	246	0	0	0	80	0	0	0	10	10
82	807	817	246	249	0	0	0	70	0	0	0	20	10
83	817	827	249	252.1	0	0	0	90	0	0	0	10	0
84	827	836	252.1	254.8	0	0	0	100	0	0	0	0	0
85	836	845	254.8	257.6	0	0	0	90	0	0	0	0	10
86	845	855	257.6	260.6	0	0	0	90	0	0	0	0	10
87	855	865	260.6	263.7	0	0	0	90	0	0	0	10	0
88	865	874	263.7	266.4	0	0	0	90	0	0	0	0	10
89	874	884	266.4	269.4	0	0	0	100	0	0	0	0	0
90	884	894	269.4	272.5	0	0	0	100	0	0	0	0	0
91	894	903	272.5	275.2	0	0	0	100	0	0	0	0	0
92	903	913	275.2	278.3	0	0	0	90	0	0	0	0	10
93	913	923	278.3	281.3	0	0	0	100	0	0	0	0	0
94	923	932	281.3	284.1	0	0	0	90	0	0	0	0	10
95	932	942	284.1	287.1	0	0	0	100	0	0	0	0	0
96	942	952	287.1	290.2	0	0	0	100	0	0	0	0	0
97	952	961	290.2	292.9	0	0	0	100	0	0	0	0	0
98	961	971	292.9	296	0	0	0	100	0	0	0	0	0
99	971	981	296	299	0	0	0	100	0	0	0	0	0
100	981	990	299	301.8	0	0	0	90	0	0	0	0	10
101	990	1000	301.8	304.8	0	0	0	90	0	0	0	0	10
102	1000	1010	304.8	307.8	0	0	0	90	0	0	0	10	0
103	1010	1020	307.8	310.9	0	0	0	90	0	0	0	0	10
104	1020	1029	310.9	313.6	0	0	0	90	0	0	10	0	0
105	1029	1038	313.6	316.4	0	0	0	90	0	0	0	10	0
106	1038	1048	316.4	319.4	0	0	0	100	0	0	0	0	0

107	1048	1054	319.4	321.3	0	0	0	100	0	0	0	0	0
108	1057	1067	322.2	325.2	0	0	0	90	0	0	0	0	10
109	1067	1076	325.2	328	0	0	0	90	0	0	0	10	0
110	1076	1086	328	331	0	0	0	90	0	0	0	10	0
111	1086	1096	331	334.1	0	0	0	100	0	0	0	0	0
112	1096	1105	334.1	336.8	0	0	0	100	0	0	0	0	0
113	1105	1115	336.8	339.9	10	0	0	80	0	0	0	0	10
114	1115	1124	339.9	342.6	0	0	0	90	0	0	0	10	0
115	1124	1134	342.6	345.6	0	0	0	90	0	0	0	0	10
116	1134	1144	345.6	348.7	10	0	0	0	0	10	10	50	20
117	1144	1153	348.7	351.4	0	0	0	40	0	10	10	30	10
118	1153	1163	351.4	354.5	0	0	0	0	0	10	20	50	20
119	1163	1173	354.5	357.5	0	0	0	30	0	10	10	30	20
120	1173	1182	357.5	360.3	0	0	0	40	0	10	20	20	10
121	1182	1192	360.3	363.3	0	0	0	30	0	20	20	20	10
122	1192	1202	363.3	366.4	0	0	0	20	0	20	10	30	20
123	1200	1210	365.8	368.8	0	0	0	50	0	10	10	10	20
124	1210	1220	368.8	371.9	10	0	0	40	0	0	20	10	20
125	1220	1229	371.9	374.6	0	0	0	50	0	0	20	20	10
126	1229	1239	374.6	377.6	0	0	0	40	0	10	10	30	10
127	1239	1249	377.6	380.7	0	0	0	40	0	20	10	30	0
128	1249	1258	380.7	383.4	0	0	0	30	0	30	10	20	10
129	1258	1268	383.4	386.5	0	0	0	60	0	0	0	30	10
130	1268	1277	386.5	389.2	0	0	0	80	0	0	10	10	0
131	1277	1286	389.2	392	0	0	0	70	0	0	10	10	10
132	1286	1296	382	395	0	0	0	100	0	0	0	0	0
133	1296	1306	395	398.1	0	0	0	90	0	0	0	10	0
134	1306	1316	398.1	401.1	0	0	0	90	0	0	10	0	0
135	1316	1324	401.1	403.6	0	0	0	100	0	0	0	0	0
136	1324	1334	403.6	406.6	0	0	0	40	0	0	10	30	20
137	1334	1344	406.6	409.7	0	0	0	50	0	0	20	10	20
138	1344	1354	409.7	412.7	0	0	0	10	0	0	10	60	20
139	1354	1364	412.7	415.7	0	0	0	30	0	0	20	30	20
140	1364	1370	415.7	417.6	0	0	0	50	0	0	20	20	10
141	1370	1379	417.6	420.3	0	0	0	70	0	0	10	20	0
142	1379	1389	420.3	423.4	0	0	0	90	0	0	0	0	10
143	1389	1399	423.4	426.4	0	0	0	70	0	0	10	20	0
144	1399	1408	426.4	429.2	0	0	0	80	0	0	10	10	0
145	1408	1418	429.2	432.2	0	0	0	90	0	0	0	10	0
146	1418	1427	432.2	434.9	0	0	0	90	0	0	0	0	10
147	1427	1436	434.9	437.7	0	0	0	90	0	0	0	10	0
148	1436	1445	437.7	440.4	0	0	0	90	0	0	0	10	0
149	1445	1455	440.4	443.5	0	0	0	90	0	0	0	10	0
150	1455	1464	443.5	446.2	0	0	0	90	0	0	0	10	0

151	1464	1473	446.2	449	0	0	0	90	0	0	0	10	0
152	1473	1483	449	452	0	0	0	100	0	0	0	0	0
153	1483	1492	452	454.8	0	0	0	100	0	0	0	0	0
154	1492	1502	454.8	457.8	0	0	0	90	0	0	0	10	0
155	1502	1512	457.8	460.9	0	0	0	70	0	0	10	10	10
156	1512	1521	460.9	463.6	0	0	0	70	0	0	10	10	10
157	1521	1531	463.6	466.6	0	0	0	60	0	10	10	10	10
158	1531	1540	466.6	469.4	0	0	0	50	0	0	10	30	10
159	1540	1550	469.4	472.4	0	0	0	40	0	10	20	20	10
160	1550	1560	472.4	475.5	0	0	0	30	0	20	20	20	10
161	1560	1570	475.5	478.5	0	0	0	50	0	10	20	20	10
162	1570	1580	478.5	481.6	0	0	0	80	0	0	0	20	0
163	1580	1590	481.6	484.6	0	0	0	90	0	0	0	10	0
164	1590	1597	484.6	486.8	10	0	0	80	0	0	0	10	0
165	1597	1606	486.8	489.5	0	0	0	90	0	0	10	0	0
166	1606	1616	489.5	492.6	0	0	0	70	0	0	10	20	0
167	1616	1626	492.6	495.6	0	0	0	60	0	0	20	10	10
168	1626	1635	495.6	498.3	0	0	0	90	0	0	0	10	0
169	1635	1644	498.3	501.1	0	0	0	90	0	0	0	10	0
170	1644	1654	501.1	504.1	0	0	0	90	0	0	0	10	0
171	1654	1664	507.2	507.2	0	0	0	90	0	0	0	10	0
172	1664	1670	504.1	509	30	0	0	40	0	0	10	10	10
173	1670	1680	509	512.1	0	0	0	80	0	0	20	0	0
174	1680	1689	512.1	514.8	0	0	0	90	0	0	0	10	0
175	1689	1698	514.8	517.6	0	0	0	100	0	0	0	0	0
176	1698	1708	517.6	520.6	10	0	0	80	0	0	0	10	0
177	1708	1717	520.6	523.3	0	0	0	90	0	0	10	0	0
178	1717	1722	523.3	524.9	50	0	0	40	0	0	10	0	0
179	Missing												
180	Missing												
181	Missing												
182	1722	1732	524.9	527.9	0	0	0	80	0	0	0	10	10
183	1732	1742	527.9	531	0	0	0	80	0	0	10	10	0
184	1742	1751	531	533.7	0	0	0	70	0	0	10	20	0
185	1751	1760	533.7	536.4	0	0	0	20	0	10	20	30	20
186	1760	1769	536.4	539.2	0	0	0	50	0	0	10	20	20
187	1769	1782	539.2	543.2	10	0	0	40	0	10	20	10	20
188	1782	1792	543.2	546.2	0	0	0	70	30	0	0	0	0
189	1792	1795	546.2	547.1	70	0	0	0	20	0	0	10	0
190	1795	1805	547.1	550.2	0	0	0	70	0	10	10	10	0
191	1805	1815	550.2	553.2	0	0	0	70	0	0	10	10	10
192	1815	1823	553.2	555.7	0	0	0	40	0	20	10	20	10
193	1823	1833	555.7	558.7	0	0	0	40	0	20	10	20	10
194	1833	1843	558.7	561.7	0	0	0	50	0	0	20	20	10

195	1843	1850	561.7	563.9	0	0	0	60	0	0	0	20	20
196	1850	1860	563.9	566.9	0	0	0	50	20	0	0	20	10
197	1860	1870	566.9	570	0	0	0	60	0	10	10	0	20
198	1870	1880	570	573	0	0	0	70	0	0	10	20	0
199	1880	1889	573	575.8	0	0	0	40	0	10	20	20	10
200	1889	1899	575.8	578.8	0	0	0	30	0	10	20	20	20
201	1899	1908	578.8	581.6	0	0	0	20	0	40	10	10	20
202	1908	1918	581.6	584.6	0	0	0	50	0	0	10	20	20
203	1918	1925	584.6	586.7	0	0	0	50	0	10	20	10	10
204	1925	1937	586.7	590.4	0	0	0	50	0	0	10	20	20
205	1937	1947	590.4	593.4	0	0	0	50	0	10	10	10	20
206	1947	1956	593.4	596.2	0	0	0	30	0	10	20	30	10
207	1956	1966	596.2	599.2	0	0	0	40	0	0	10	30	20
208	1966	1975	599.2	602	0	0	0	50	0	0	10	10	30
209	1975	1985	602	905	0	0	0	100	0	0	0	0	0
210	1985	1994	605	607.8	0	0	0	90	0	0	0	10	0
211	1994	2004	607.8	610.8	0	0	0	90	0	0	0	10	0
212	2004	2013	610.8	613.6	0	0	0	90	0	0	10	0	0
213	2013	2023	613.6	616.6	0	0	0	60	0	0	10	30	0
214	2023	2032	616.6	619.4	0	0	0	20	0	20	10	20	30
215	2032	2042	619.4	622.4	0	0	0	70	0	0	10	20	0
216	2042	2050	622.4	624.8	0	0	0	100	0	0	0	0	0
217	2050	2056	624.8	626.7	20	0	0	70	0	0	0	10	0

FC78-7													
Box	TD (ft)	BD (ft)	TD (m)	BD (m)	MI	SH	FS	BRh	BRd	VCB	CB	MB	FB
1	0	6.5	0	2	50	0	0	20	0	0	10	20	0
2	6.5	11	2	3.4	50	0	0	40	0	0	0	10	0
3	11	15	3.4	4.6	60	0	0	30	0	0	0	10	0
4	15	24.5	4.6	7.5	10	0	0	50	0	0	10	20	10
5	24.5	33.5	7.5	10.2	0	0	0	60	0	0	0	20	20
6	33.5	42.5	10.2	13	0	0	0	60	0	0	0	30	10
7	42.5	50	13	15.2	0	0	0	90	0	0	0	0	10
8	50	58.5	15.2	17.8	10	0	0	50	0	0	0	30	10
9	58.5	68.2	17.8	20.8	0	0	0	90	0	0	0	10	0
10	69	77	21	23.5	10	0	0	70	0	0	0	10	10

11	77	83.5	23.5	25.5	10	0	0	70	0	0	10	0	10
12	83.5	93.5	25.5	28.5	0	0	0	70	0	0	0	10	20
13	93.5	102.6	28.5	31.3	0	0	0	80	0	0	0	10	10
14	102.6	112	31.3	34.1	0	0	0	70	0	0	0	10	20
15	112	121	34.1	36.9	0	0	0	70	0	0	0	10	20
16	121	130	34.1	36.9	10	0	0	70	0	0	10	0	10
17	130	139	39.6	42.4	0	0	0	70	0	0	10	10	10
18	139	148	42.4	45.1	0	0	0	80	0	0	0	10	10
19	148	157	45.1	47.9	0	0	0	80	0	0	0	10	10
20	157	167	47.9	50.9	0	0	0	80	0	0	10	10	0
21	167	173	50.9	52.7	20	0	0	60	0	0	10	10	0
22	173	182	52.7	55.5	0	0	0	70	0	0	10	20	0
23	182	191	55.5	58.2	10	0	0	80	0	0	0	10	0
24	191	199	58.2	60.7	10	0	0	80	0	0	0	10	0
25	199	207	60.7	63.1	10	0	0	80	0	0	0	0	10
26	207	215	63.1	65.5	0	0	0	90	0	0	0	0	10
27	215	222	65.5	67.7	10	0	0	70	0	0	0	20	0
28	222	233	67.7	71	0	0	0	80	0	0	0	10	10
29	233	242	71	73.8	0	0	0	80	0	0	0	0	20
30	242	252	73.8	76.8	0	0	0	90	0	0	0	10	0
31	252	260	76.8	79.2	10	0	0	80	0	0	0	10	0
32	260	269	79.2	82	0	0	0	90	0	0	0	10	0
33	269	278	82	84.7	10	0	0	80	0	0	10	0	0
34	278	286	84.7	87.2	10	0	0	80	0	0	0	0	10
35	286	296	87.2	90.2	10	0	0	70	0	0	0	10	10
36	296	303	90.2	92.4	10	0	0	60	0	0	0	20	10
37	303	312	92.4	95.1	10	0	0	50	0	0	0	10	30
38	312	321	95.1	97.8	0	0	0	80	0	0	0	0	20
39	321	330	97.8	100.6	0	0	0	100	0	0	0	0	0

40	330	339	100.6	103.3	0	0	0	90	0	0	0	0	10
41	339	347	103.3	105.8	0	0	0	90	0	0	0	10	0
42	347	357	105.8	108.8	0	0	0	90	0	0	0	0	10
43	357	365	108.8	111.3	0	0	0	100	0	0	0	0	0
44	365	376	111.3	114.6	0	0	0	100	0	0	0	0	0
45	376	385	114.6	117.3	0	0	0	100	0	0	0	0	0
46	385	393	117.3	119.8	20	0	0	80	0	0	0	0	0
47	393	401	119.8	122.2	20	0	0	80	0	0	0	0	0
48	401	409	122.2	124.7	10	0	0	90	0	0	0	0	0
49	409	417	124.7	127.1	20	0	0	80	0	0	0	0	0
50	417	426	127.1	129.8	10	0	0	80	0	0	0	0	10
51	426	435	129.8	132.6	10	0	0	90	0	0	0	0	0
52	435	443	132.6	135	10	0	0	80	0	0	0	0	10
53	443	452	135	137.8	0	0	0	90	0	0	0	0	10
54	401	409	122.2	124.7	0	0	0	90	0	0	0	0	10
55	409	417	124.7	127.1	10	0	0	80	0	0	0	10	0
56	417	426	127.1	129.8	0	0	0	100	0	0	0	0	0
57	478	487	145.7	148.4	0	0	0	100	0	0	0	0	0
58	487	496	148.4	151.2	0	0	0	90	0	0	0	0	10
59	496	505	151.2	153.9	0	0	0	100	0	0	0	0	0
60	505	514	153.9	156.7	10	0	0	90	0	0	0	0	0
61	514	523	156.7	159.4	0	0	0	100	0	0	0	0	0
62	523	532	159.4	162.2	0	0	0	90	0	0	0	0	10
63	532	540	162.2	164.6	10	0	0	90	0	0	0	0	0
64	540	549	164.6	167.3	10	0	0	90	0	0	0	0	0
65	549	557	167.3	169.8	10	0	0	80	0	0	0	10	0
66	557	566	169.8	169.5	10	0	0	80	0	0	0	0	10
67	566	574	172.5	175	10	0	0	80	0	0	0	10	0
68	574	584	175	178	0	0	0	90	0	0	0	0	10
69	584	592	178	180.4	10	0	0	90	0	0	0	0	0
70	592	601	180.4	183.2	10	0	0	90	0	0	0	0	0
71	601	610	183.2	185.9	0	0	0	90	0	0	0	10	0
72	610	620	185.9	189	0	0	0	90	0	0	0	0	10
73	620	629	189	191.7	0	0	0	100	0	0	0	0	0
74	629	638	191.7	194.5	0	0	0	90	0	0	0	10	0

75	638	647	194.5	199	10	0	0	80	0	0	0	10	0
76	647	656	199	199.9	10	0	0	90	0	0	0	0	0
77	656	664	199.9	202.4	10	0	0	80	0	0	0	10	0
78	664	672	202.4	204.8	0	0	0	90	0	0	0	0	10
79	672	682	204.8	207.9	0	0	0	90	0	0	0	0	10
80	682	690	207.9	210.3	10	0	0	80	0	0	0	0	10
81	690	699	210.3	213.1	0	0	0	100	0	0	0	0	0
82	699	709	213.1	216.1	0	0	0	90	0	0	0	10	0
83	709	718	216.1	218.8	10	0	0	90	0	0	0	0	0
84	718	727	218.8	221.6	0	0	0	90	0	0	0	0	10
85	727	736	221.6	224.3	10	0	0	90	0	0	0	0	0
86	736	745	224.3	227.1	0	0	0	90	0	0	0	0	10
87	745	755	227.1	230.1	0	0	0	100	0	0	0	0	0
88	755	764	230.1	232.9	10	0	0	90	0	0	0	0	0
89	764	773	232.9	235.6	10	0	0	90	0	0	0	0	0
90	773	782	235.6	238.4	0	0	0	90	0	0	0	10	0
91	782	791	238.4	241.1	0	0	0	90	0	0	0	0	10
92	791	800	241.1	243.8	0	0	0	90	0	0	0	0	10
93	800	809	243.8	246.6	0	0	0	100	0	0	0	0	0
94	809	819	246.6	249.6	0	0	0	90	0	0	0	0	10
95	819	828	249.6	252.4	0	0	0	90	0	0	0	0	10
96	828	837	252.4	255.1	0	0	0	90	0	0	0	0	10
97	837	848	255.1	258.5	0	0	0	90	0	0	0	10	0
98	848	856	258.5	260.9	10	0	0	80	0	0	0	0	10
99	856	865	260.9	263.7	0	0	0	100	0	0	0	0	0
100	865	873	263.7	266.1	0	0	0	90	0	0	0	0	10
101	873	883	266.1	269.1	0	0	0	100	0	0	0	0	0
102	883	892	269.1	271.9	0	0	0	90	0	0	0	10	0
103	892	902	271.9	274.9	0	0	0	90	0	0	0	0	10
104	902	910	274.9	277.4	10	0	0	80	0	0	0	10	0
105	910	919	277.4	280.1	0	0	0	100	0	0	0	0	0
106	919	928	280.1	282.9	0	0	0	90	0	0	0	10	0

107	928	937	282.9	285.6	0	0	0	80	0	0	0	0	20
108	937	946	285.6	288.3	0	0	0	80	0	0	0	10	10
109	946	956	288.3	291.4	10	0	0	70	0	0	0	20	0
110	956	966	291.4	294.4	0	0	0	80	0	0	0	10	10
111	966	975	294.4	297.2	0	0	0	100	0	0	0	0	0
112	975	984	297.2	299.9	10	0	0	90	0	0	0	0	0
113	984	993	299.9	302.7	0	0	0	90	0	0	0	10	0
114	993	1002	302.7	305.4	0	0	0	90	0	0	0	10	0
115	1002	1011	305.4	308.2	0	0	0	90	0	0	0	0	10
116	1011	1020	308.2	310.9	0	0	0	100	0	0	0	0	0
117	1020	1030	310.9	313.9	0	0	0	90	0	0	0	0	10
118	1030	1039	313.9	316.7	0	0	0	90	0	0	0	0	10
119	1039	1048	316.7	319.4	0	0	0	90	0	0	0	0	10
120	1048	1057	319.4	322.2	0	0	0	100	0	0	0	0	0
121	1057	1067	322.2	325.2	0	0	0	100	0	0	0	0	0
122	1067	1076	325.2	328	0	0	0	100	0	0	0	0	0
123	1076	1085	328	330.7	10	0	0	90	0	0	0	0	0
124	1085	1094	330.7	333.5	0	0	0	90	0	0	0	0	10
125	1094	1103	333.5	336.2	0	0	0	100	0	0	0	0	0
126	1103	1112	336.2	338.9	0	0	0	100	0	0	0	0	0
127	1112	1120	338.9	341.4	10	0	0	70	0	0	10	10	0
128	1120	1128	341.4	343.8	10	0	0	50	0	0	10	30	0
129	1128	1137	343.8	346.6	10	0	0	50	0	0	10	30	0
130	1137	1146	346.6	349.3	0	0	0	70	0	0	0	20	10
131	1146	1155	349.3	352	0	0	0	80	0	0	0	20	0
132	1155	1163	352	354.5	0	0	0	90	0	0	0	10	0
133	1163	1171	354.5	356.9	10	0	0	80	0	0	0	10	0
134	1171	1181	356.9	360	0	0	0	100	0	0	0	0	0
135	1181	1190	360	362.7	0	0	0	100	0	0	0	0	0
136	1190	1199	362.7	365.5	0	0	0	90	0	0	0	10	0
137	1199	1207	365.5	367.9	10	0	0	60	0	0	0	10	20
138	1207	1215	367.9	370.3	0	0	0	90	0	0	0	0	10
139	1215	1224	370.3	373.1	10	0	0	80	0	0	0	10	0
140	1224	1234	373.1	376.1	10	0	0	80	0	0	0	10	0
141	1234	1243	376.1	378.9	0	0	0	100	0	0	0	0	0

142	1243	1251	378.9	381.3	10	0	0	80	0	0	0	10	0
143	1257	1260	383.1	384	0	0	0	90	0	0	0	10	0
144	1260	1270	384	387.1	0	0	0	90	0	0	0	10	0
145	1270	1280	387.1	390.1	0	0	0	90	0	0	0	10	0
146	1280	1289	390.1	392.9	0	0	0	90	0	0	0	10	0
147	1289	1299	392.9	395.9	0	0	0	100	0	0	0	0	0
148	1299	1308	395.9	398.7	10	0	0	90	0	0	0	0	0
149	1308	1317	398.7	401.4	0	0	0	100	0	0	0	0	0
150	1317	1326	401.4	404.2	0	0	0	100	0	0	0	0	0
151	1326	1335	404.2	406.9	0	0	0	90	0	0	0	10	0
152	1335	1344	406.9	409.7	0	0	0	90	0	0	0	0	10
153	1344	1353	409.7	412.4	0	0	0	100	0	0	0	0	0
154	1353	1363	412.4	415.4	0	0	0	90	0	0	0	10	0
155	1363	1373	415.4	418.5	0	0	0	100	0	0	0	0	0
156	1373	1382	418.5	421.2	0	0	0	80	0	0	0	10	10
157	1382	1391	421.2	424	0	0	0	60	0	0	10	20	10
158	1391	1400	424	426.7	10	0	0	80	0	0	0	10	0
159	1400	1409	426.7	429.5	0	0	0	100	0	0	0	0	0
160	1409	1418	429.5	432.2	0	0	0	70	0	0	10	10	10
161	1418	1427	432.2	434.9	0	0	0	90	0	0	0	0	10
162	1427	1437	434.9	438	0	0	0	90	0	0	0	10	0
163	1437	1446	438	440.7	0	0	0	100	0	0	0	0	0
164	1446	1456	440.7	443.8	0	0	0	90	0	0	0	10	0
165	1456	1465	443.8	446.5	0	0	0	90	0	0	0	10	0
166	1465	1474	446.5	449.3	0	0	0	90	0	0	10	0	0
167	1474	1483	449.3	452	0	0	0	70	0	0	10	10	10
168	1483	1492	452	454.8	0	0	0	80	0	10	0	10	0
169	1492	1502	454.8	457.8	0	0	0	100	0	0	0	0	0
170	1503	1511	458.1	460.6	0	0	0	90	0	0	0	10	0
171	1511	1520	460.6	463.3	0	0	0	80	0	0	10	10	0
172	1520	1529	463.3	466	0	0	0	100	0	0	0	0	0
173	1529	1539	466	469.1	0	0	0	100	0	0	0	0	0
174	1539	1549	469.1	472.1	0	0	0	100	0	0	0	0	0
175	1549	1557	472.1	474.6	0	0	0	90	0	0	0	0	10
176	1557	1566	474.6	477.3	0	0	0	90	0	0	0	10	0
177	1566	1576	477.3	480.4	0	0	0	100	0	0	0	0	0
178	1576	1585	480.4	483.1	0	0	0	90	0	0	10	0	0
179	1585	1594	483.1	485.9	0	0	0	100	0	0	0	0	0

180	1594	1604	485.9	488.9	0	0	0	100	0	0	0	0	0
181	1604	1618	488.9	490.1	0	0	0	80	0	0	0	10	10
182	1618	1627	493.2	495.9	0	0	0	100	0	0	0	0	0
183	1627	1637	495.9	499	0	0	0	80	0	0	0	20	0
184	1637	1646	499	501.7	0	0	0	70	0	10	10	10	0
185	1646	1655	501.7	504.4	0	0	0	80	0	0	10	10	0
186	1655	1664	504.4	507.2	0	0	0	40	0	20	30	10	0
187	1664	1674	507.2	510.2	0	0	0	30	0	0	10	20	40
188	1674	1683	510.2	513	0	0	0	40	0	10	10	30	10
189	1683	1693	513	516	0	0	0	50	0	10	20	20	0
190	1693	1703	516	519.1	0	0	0	90	0	0	10	0	0
191	1703	1712	519.1	521.8	0	0	0	100	0	0	0	0	0
192	1712	1721	521.8	524.6	0	0	0	90	0	0	0	10	0
193	1721	1730	524.6	527.3	0	0	0	70	0	0	10	10	10
194	1730	1739	527.3	530	0	0	0	70	0	10	10	0	10
195	1739	1749	530	533.1	0	0	0	90	0	0	0	0	10
196	1749	1758	533.1	535.8	0	0	0	90	0	0	0	10	0
197	1758	1767	535.8	538.6	0	0	0	90	0	0	0	10	0
198	1767	1777	538.6	541.6	0	0	0	90	0	0	0	10	0
199	1777	1787	541.6	544.7	0	0	0	60	0	0	10	10	20
200	1787	1797	544.7	547.7	0	0	0	60	0	10	0	20	10
201	1797	1805	547.7	550.2	0	0	0	90	0	0	0	10	0
202	1805	1815	550.2	553.2	0	0	0	50	0	0	10	20	20
203	1815	1824	553.2	556	0	0	0	40	0	0	20	30	10
204	1824	1833	556	558.7	0	0	0	30	0	0	20	30	20
205	1833	1842	558.7	561.4	10	0	0	40	0	20	10	20	0
206	1842	1850	561.4	563.9	0	0	0	40	0	0	10	20	30
207	1850	1860	563.9	566.9	0	0	0	60	0	0	0	20	20
208	1860	1869	566.9	569.7	0	0	0	70	0	0	20	10	0
209	1869	1878	569.7	572.4	10	0	0	80	0	0	0	10	0
210	1878	1887	572.4	575.2	0	0	0	40	0	10	20	20	10

211	1887	1896	575.2	577.9	0	0	0	50	0	0	20	10	20
212	1896	1905	577.9	580.6	0	0	0	80	0	0	0	20	0
213	1905	1914	580.6	583.4	0	0	0	80	0	0	10	10	0
214	1914	1923	583.4	586.1	0	0	0	80	0	0	10	10	0
215	1923	1931	586.1	588.6	0	0	0	80	0	0	10	10	0
216	1931	1940	588.6	591.3	0	0	0	90	0	0	0	10	0
217	1940	1950	591.3	594.4	0	0	0	50	0	0	10	10	30
218	1950	1959	594.4	597.1	0	0	0	40	0	10	10	30	10
219	1959	1968	597.1	599.8	0	0	0	40	0	10	20	20	10
220	1968	1977	599.8	602.6	0	0	0	30	0	20	20	20	10
221	Missing												
222	1986	1995	605.3	608.1	0	0	0	80	0	0	0	10	10
223	1995	2003	608.1	610.5	0	0	0	80	0	0	0	10	10
224	2003	2013	610.5	613.6	0	0	0	70	0	0	0	20	10
225	2013	2022	613.6	616.3	0	0	0	70	0	0	10	10	10
226	2022	2031	616.3	619	0	0	0	100	0	0	0	0	0
227	2031	2041	619	622.1	0	0	0	90	0	0	0	10	0
228	2041	2050	622.1	624.8	0	0	0	90	0	0	0	10	0
229	2050	2059	624.8	627.6	0	0	0	90	0	0	10	0	0
230	2059	2068	627.6	630.3	0	0	0	100	0	0	0	0	0
231	2068	2078	630.3	633.4	0	0	0	100	0	0	0	0	0
232	2078	2087	633.4	636.1	0	0	0	100	0	0	0	0	0
233	2087	2095	636.1	638.6	0	0	0	90	0	0	0	0	10
234	2095	2102	638.6	640.7	30	0	0	70	0	0	0	0	0

FC79-9													
Box	TD (ft)	BD (ft)	TD (m)	BD (m)	MI	SH	FS	BRh	BRd	VCB	CB	MB	FB
8	73	83	22.3	25.3	0	0	0	0	100	0	0	0	0
10	91	101	27.7	30.8	0	0	0	30	0	0	20	10	40
11	101	110	30.8	33.5	0	0	0	30	0	0	10	20	40
12	110	119	33.5	36.3	0	0	0	90	0	0	0	10	0
13	119	128	36.3	39	0	0	0	80	20	0	0	0	0

14	128	137	39	41.8	0	0	0	70	0	0	0	10	20
15	137	147	41.8	44.8	0	0	0	20	0	0	0	10	70
32	297	306	90.5	93.3	0	0	0	90	0	0	0	0	10
34	315	325	96	99.1	0	0	0	70	30	0	0	0	0
35	325	334	99.1	101.8	0	0	0	70	20	0	0	10	0
36	334	344	101.8	104.9	0	0	0	30	70	0	0	0	0
37	344	353	104.9	107.6	0	0	0	40	60	0	0	0	0

FC79-10													
Box	**TD (ft)**	**BD (ft)**	**TD (m)**	**BD (m)**	**MI**	**SH**	**FS**	**BRh**	**BRd**	**VCB**	**CB**	**MB**	**FB**
1	7	16	2.1	4.9	10	0	0	30	0	10	0	20	30
2	16	25	4.9	7.6	0	0	0	20	0	0	10	0	70
3	25	35	7.6	10.7	0	0	0	0	0	0	20	30	50
4	35	46	10.7	14	0	0	0	60	0	0	10	20	10
5	46	55	14	16.8	0	0	0	70	0	0	20	10	0
6	55	65	16.8	19.8	0	0	0	90	0	0	10	0	0
7	65	74	19.8	22.6	0	0	0	90	0	0	0	10	0
8	74	84	22.6	25.6	0	0	0	90	0	0	0	0	10
9	84	92	25.6	28	0	0	0	90	0	0	0	0	10
10	92	104	28	31.7	0	0	0	90	0	0	0	10	0
11	104	114	31.7	34.7	0	0	0	100	0	0	0	0	0
12	123	123	34.7	37.5	0	0	0	40	0	0	20	30	10
13	123	132	37.5	40.2	0	0	0	50	0	20	10	20	0
14	132	141	40.2	43	0	0	0	90	0	0	0	0	10
15	141	150	43	45.7	0	0	0	70	0	0	0	10	20
16	150	159	45.7	48.5	10	0	0	90	0	0	0	0	0
17	159	169	48.5	51.5	0	0	0	90	0	0	0	10	0
18	169	178	51.5	54.3	0	0	0	90	0	0	0	10	0
19	178	187	54.3	57	0	0	0	60	0	0	0	10	30

20	187	196	57	59.7	0	0	0	60	0	0	30	10	0
21	196	205	59.7	62.5	0	0	0	20	0	60	10	10	0
22	205	215	62.5	65.5	0	0	0	70	20	0	0	0	10
23	215	224	65.5	68.3	0	0	0	40	60	0	0	0	0
24	224	232	68.3	70.7	0	0	0	0	100	0	0	0	0
25	232	240	70.7	73.2	20	0	0	60	20	0	0	0	0

FC79-11													
Box	TD (ft)	BD (ft)	TD (m)	BD (m)	MI	SH	FS	BRh	BRd	VCB	CB	MB	FB
1	20	30	6	9	30	0	0	70	0	0	0	0	0
2	30	40	9	12	50	0	0	50	0	0	0	0	0
3	40	50	12	15	10	0	0	90	0	0	0	0	0
4	50	60	15	18	0	0	0	100	0	0	0	0	0
5	60	70	18	21	10	0	0	90	0	0	0	0	0
6	70	80	21	24	0	0	0	100	0	0	0	0	0
7	80	90	24	27	0	0	0	100	0	0	0	0	0
8	90	100	27	30	20	0	0	70	0	0	0	0	10
9	100	110	30.5	33.5	0	0	0	60	0	0	0	0	10
10	110	119	33.5	36.3	0	0	0	90	0	0	0	0	10
11	119	129	36.3	39.3	0	0	0	100	0	0	0	0	0
12	129	137	39.3	41.8	0	0	0	100	0	0	0	0	0
13	137	147	41.8	44.8	0	0	0	100	0	0	0	0	0
14	147	156	44.8	47.5	0	0	0	100	0	0	0	0	0
15	156	166	47.5	50.6	0	0	0	100	0	0	0	0	0
16	166	175	50.6	53.3	0	0	0	100	0	0	0	0	0
17	175	185	53.3	56.4	0	0	0	100	0	0	0	0	0
18	185	194	56.4	59.1	0	0	0	100	0	0	0	0	0
19	194	204	59.1	62.2	0	0	0	100	0	0	0	0	0
20	204	213	62.2	64.9	0	0	0	100	0	0	0	0	0
21	213	222	64.9	67.7	10	0	0	80	0	0	0	0	10
22	222	230	67.7	70.1	10	0	0	60	0	0	0	0	30
23	230	239	70.1	72.8	0	0	0	100	0	0	0	0	0
24	239	249	72.8	75.9	0	0	0	100	0	0	0	0	0
25	249	258	75.9	78.6	0	0	0	100	0	0	0	0	0
26	258	267	78.6	81.4	0	0	0	100	0	0	0	0	0
27	267	276	81.4	84.1	0	0	0	100	0	0	0	0	0
28	276	285	84.1	86.9	0	0	0	100	0	0	0	0	0
29	285	294	86.9	89.6	0	0	0	100	0	0	0	0	0

30	294	300	89.6	91.4	50	0	0	50	0	0	0	0	0

FC79-12													
Box	TD (ft)	BD (ft)	TD (m)	BD (m)	MI	SH	FS	BRh	BRd	VCB	CB	MB	FB
1	64	85	19.5	25.9	40	0	60	0	0	0	0	0	0
2	85	90	25.9	27.4	0	0	100	0	0	0	0	0	0
3	90	100	27.4	30.5	0	0	100	0	0	0	0	0	0
4	100	110	30.5	33.5	0	0	100	0	0	0	0	0	0
5	110	119	33.5	36.3	0	100	0	0	0	0	0	0	0
6	119	129	36.3	39.3	0	100	0	0	0	0	0	0	0
7	129	138	39.3	42.1	0	100	0	0	0	0	0	0	0
8	138	148	42.1	45.1	0	100	0	0	0	0	0	0	0
9	148	157	45.1	47.9	0	100	0	0	0	0	0	0	0
10	157	167	47.9	50.9	0	100	0	0	0	0	0	0	0
11	167	176	50.9	53.6	0	60	0	0	0	0	10	10	20
12	176	184	53.6	56.1	0	0	0	0	0	0	0	10	90
13	184	194	56.1	59.1	0	0	0	0	0	0	10	10	80
14	194	204	59.1	62.2	0	0	0	0	0	10	10	20	60
15	204	215	62.2	65.5	0	0	0	0	70	0	0	20	10
16	214	223	65.2	68	0	0	0	0	70	20	0	0	10
17	223	232	68	70.7	0	0	0	0	0	20	10	20	50
18	232	242	70.7	73.8	0	0	0	0	70	10	0	0	20
19	242	250	73.8	82	10	0	0	0	80	0	10	0	0
20	250	259	76.2	78.9	0	0	0	0	100	0	0	0	0
21	259	269	78.9	82	0	0	0	0	80	0	0	10	10

Box	TD (ft)	BD (ft)	TD (m)	BD (m)	MI	SH	FS	BRh	BRd	VCB	CB	MB	FB
22	269	277	82	84.4	0	0	0	0	40	30	20	0	10
23	277	287	84.4	87.5	0	0	0	10	70	20	0	0	0
24	287	296	87.5	90.2	0	0	0	0	60	20	10	10	0
25	296	304	90.2	92.7	0	0	0	0	90	0	0	10	0
26	304	314	92.7	95.7	0	0	0	0	70	10	0	20	0
27	314	323	95.7	98.5	0	0	0	0	50	20	10	10	10
28	323	332	98.5	101.2	0	0	0	0	90	0	10	0	0
29	332	342	101.2	104.2	0	0	0	0	90	0	0	0	10
30	342	351	104.2	107	0	0	0	0	60	20	10	10	0
31	351	361	110	112.5	0	0	0	0	100	0	0	0	0
32	361	369	110	112.5	10	0	0	0	40	20	20	10	0
33	369	378	112.5	115.2	0	0	0	0	10	40	20	30	0
34	378	388	115.2	118.3	0	0	0	0	0	40	10	50	0
35	388	397	118.3	121	0	0	0	0	0	60	30	10	0
36	397	405	121	123.4	0	0	0	0	0	20	30	10	40
37	405	415	123.4	126.5	0	0	0	0	0	40	30	10	20
38	415	424	126.5	129.2	0	0	0	10	0	20	20	40	10
39	424	433	129.2	132	0	0	0	80	0	10	0	10	0
40	433	442	132	134.7	0	0	0	90	0	10	0	0	0
41	442	452	134.7	137.8	0	0	0	20	80	0	0	0	0
42	452	461	137.8	140.5	0	0	0	80	0	0	0	20	0
43	461	470	131.4	143.3	0	0	0	30	0	0	20	40	10

FC79-13													
Box	TD (ft)	BD (ft)	TD (m)	BD (m)	MI	SH	FS	BRh	BRd	VCB	CB	MB	FB
1	64	85	19.5	25.9	10	0	30	60	0	0	0	0	0
2	85	94	25.9	28.7	0	0	80	20	0	0	0	0	0
3	94	104	28.7	31.7	0	0	70	30	0	0	0	0	0
4	104	113	31.7	34.4	0	0	30	70	0	0	0	0	0
5	113	122	34.4	37.2	0	0	50	50	0	0	0	0	0

6	122	132	37.2	40.2	0	0	30	60	0	0	10	0	0
7	132	142	40.2	43.3	0	70	20	10	0	0	0	0	0
8	142	152	43.3	46.3	0	100	0	0	0	0	0	0	0
9	152	162	46.3	49.4	0	100	0	0	0	0	0	0	0
10	162	172	49.4	52.4	0	100	0	0	0	0	0	0	0
11	172	181	52.4	55.2	0	100	0	0	0	0	0	0	0
12	181	190	55.2	57.9	0	100	0	0	0	0	0	0	0
13	190	200	57.9	61	0	100	0	0	0	0	0	0	0
14	200	208	61	63.4	0	100	0	0	0	0	0	0	0
15	208	218	63.4	66.4	0	100	0	0	0	0	0	0	0
16	218	228	66.4	69.5	0	100	0	0	0	0	0	0	0
17	228	237	69.5	72.2	10	0	0	0	0	0	20	20	50
18	237	245	72.2	74.7	0	0	0	0	0	30	40	10	20
19	245	255	74.7	77.7	0	0	0	30	0	0	10	20	40
20	255	264	77.7	80.5	0	0	0	90	0	0	0	10	0
21	264	274	80.5	83.5	0	0	0	30	0	0	10	10	50
22	274	283	83.5	86.3	0	0	0	50	20	0	0	10	20
23	283	293	86.3	89.3	0	0	0	0	90	0	0	10	0
24	293	303	89.3	92.4	0	0	0	30	70	0	0	0	0
25	303	312	92.4	95.1	0	0	0	0	90	0	0	0	10
26	312	322	95.1	98.1	0	0	0	70	30	0	0	0	0
27	322	331	98.1	100.9	0	0	0	100	0	0	0	0	0
28	331	341	100.9	103.9	0	0	0	60	0	0	10	10	20
29	341	351	103.9	107	0	0	0	50	30	0	0	0	20
30	351	361	107	110	0	0	0	100	0	0	0	0	0
31	361	369	110	112.5	0	0	0	80	20	0	0	0	0
32	369	379	112.5	115.5	0	0	0	40	60	0	0	0	0
33	379	388	115.5	118.3	0	0	0	0	100	0	0	0	0

34	388	398	118.3	121.3	0	0	0	0	100	0	0	0	0
35	398	407	121.3	124.1	0	0	0	50	50	0	0	0	0
36	407	416	124.1	126.8	0	0	0	100	0	0	0	0	0
37	416	426	126.8	129.8	0	0	0	10	10	0	30	20	30
38	426	436	129.8	132.9	0	0	0	0	100	0	0	0	0
39	436	445	132.9	135.6	0	0	0	10	90	0	0	0	0
40	445	455	135.6	138.7	0	0	0	0	100	0	0	0	0
41	455	464	138.7	141.4	0	0	0	0	100	0	0	0	0
42	464	474	141.4	144.5	0	0	0	0	100	0	0	0	0
43	474	483	144.5	147.2	0	0	0	0	100	0	0	0	0
44	483	493	147.2	150.3	0	0	0	0	100	0	0	0	0
45	493	502	150.3	155.8	0	0	0	0	100	0	0	0	0
46	502	511	155.8	158.5	0	0	0	0	100	0	0	0	0
47	511	520	158.5	161.2	0	0	0	0	100	0	0	0	0
48	520	529	161.2	164	0	0	0	0	100	0	0	0	0

FC79-14													
Box	**TD (ft)**	**BD (ft)**	**TD (m)**	**BD (m)**	**MI**	**SH**	**FS**	**BRh**	**BRd**	**VCB**	**CB**	**MB**	**FB**
1	0	17	0	5.2	20	0	0	50	0	0	0	20	10
2	17	26	5.2	7.9	0	0	0	50	0	0	0	20	30
3	26	36	7.9	10.7	0	0	0	50	0	0	10	10	30
4	36	45	10.7	13.7	0	0	0	50	0	0	10	10	30
5	45	54	13.7	16.5	10	0	0	70	10	0	0	10	0
6	54	63	16.5	19.2	0	0	0	60	0	0	0	10	30
7	63	73	19.2	22.3	0	0	0	80	0	0	0	10	10
8	73	82	22.3	25	0	0	0	50	0	0	0	30	20
9	82	91	25	27.7	0	0	0	60	0	0	10	10	20
10	91	100	27.7	30.5	0	0	0	70	0	0	0	10	20
11	100	110	30.5	33.5	0	0	0	80	0	0	0	10	20
12	110	119	33.5	36.3	0	0	0	60	0	0	0	10	30

13	119	128	36.3	39	0	0	0	90	0	0	0	0	10
14	128	137	39	41.8	0	0	0	90	0	0	0	0	10
15	137	146	41.8	44.5	0	0	0	90	0	0	10	0	0
16	146	155	44.5	47.2	0	0	0	90	0	0	0	0	10
17	155	164	47.2	50	0	0	0	90	0	0	0	10	0
18	164	174	50	53	0	0	0	80	20	0	0	0	0
19	174	182	53	55.5	0	0	0	40	50	0	0	0	10
20	182	191	55.5	58.2	0	0	0	70	0	0	0	10	20
21	191	201	58.2	61.3	0	0	0	60	0	0	0	10	30
22	201	210	61.3	64	0	0	0	90	0	0	0	10	0
23	210	219	64	66.8	0	0	0	50	0	0	10	20	20
24	219	229	66.8	69.8	0	0	0	50	0	0	30	20	0
25	229	238	69.8	72.5	0	0	0	70	0	0	0	10	20
26	238	247	72.5	75.3	0	0	0	90	0	0	10	0	0
27	247	256	75.3	78	0	0	0	90	0	0	0	0	10
28	256	266	78	81.1	0	0	0	90	0	0	0	0	10
29	266	275	81.1	83.8	0	0	0	100	0	0	0	0	0
30	275	284	83.8	86.6	0	0	0	100	0	0	0	0	0
31	284	293	86.6	89.3	0	0	0	90	0	0	0	0	10
32	293	303	89.3	92.4	0	0	0	90	0	0	10	0	0
33	303	312	92.4	95.1	0	0	0	50	0	0	10	10	30
34	312	321	95.1	97.8	0	0	0	40	0	0	10	30	20
35	321	330	97.8	100.6	0	0	0	30	0	0	20	20	30
36	330	338	100.6	103	10	0	0	30	0	0	20	10	30
37	338	348	103	106.1	0	0	0	60	0	0	10	10	20
38	348	356	106.1	108.5	0	0	0	50	0	0	0	10	40
39	356	366	108.5	111.6	0	0	0	60	0	0	10	0	30

40	366	375	111.6	114.3	0	0	0	70	0	0	0	10	20
41	375	384	114.3	117	10	0	0	70	0	0	0	10	20
42	384	393	117	119.8	0	0	0	90	0	0	0	0	10
43	393	402	119.8	122.5	0	0	0	90	0	0	0	10	0
44	402	413	122.5	125.9	0	0	0	100	0	0	0	0	0
45	413	422	125.9	128.6	0	0	0	90	0	0	0	0	10
46	422	431	128.6	131.4	50	0	0	40	0	0	0	10	0

FC79-15													
Box	**TD (ft)**	**BD (ft)**	**TD (m)**	**BD (m)**	**MI**	**SH**	**FS**	**BRh**	**BRd**	**VCB**	**CB**	**MB**	**FB**
1	34	42	10.4	12.8	50	0	30	10	0	0	0	0	10
2	42	51	12.8	15.5	0	0	20	20	0	0	10	10	40
3	51	60	15.5	18.3	0	0	0	40	0	0	10	20	30
4	60	70	18.3	21.3	0	0	0	50	0	0	10	20	20
5	70	78	21.3	23.8	0	0	0	40	0	0	0	20	40
6	78	88	23.8	26.8	0	0	0	60	0	0	20	10	10
7	88	96	26.8	29.3	0	0	0	50	40	0	0	0	10
8	96	105	29.3	32	0	0	0	60	30	0	0	0	10
9	105	115	32	35.1	0	0	0	60	30	0	0	0	10
10	115	124	35.1	37.8	0	0	0	90	0	0	10	0	0
11	124	134	37.8	40.8	0	0	0	60	0	0	10	10	20
12	134	144	40.8	43.9	0	0	0	60	0	0	0	10	30
13	144	152	43.9	46.3	0	0	0	50	0	0	0	20	30
14	152	162	46.3	49.4	0	0	0	40	0	0	10	30	20
15	162	170	49.4	51.8	0	0	0	50	0	0	20	20	10

16	170	179	51.8	54.6	0	0	0	30	0	0	10	40	20
17	179	188	54.6	57.3	0	0	0	50	0	0	0	20	30
18	188	198	57.3	60.4	0	0	0	60	0	0	0	0	40
19	198	207	60.4	63.1	0	0	0	60	0	0	0	20	20
20	207	217	63.1	66.1	0	0	0	40	0	0	10	10	40
21	217	226	66.1	68.9	0	0	0	50	0	0	0	10	40
22	226	234	68.9	71.3	0	0	0	60	0	0	10	0	30
23	234	244	71.3	74.4	0	0	0	60	0	0	0	10	30
24	244	253	74.4	77.7	0	0	0	70	0	0	0	10	20
25	253	262	77.7	79.9	0	0	0	90	0	0	0	0	10
26	262	272	79.9	82.9	0	0	0	90	0	0	0	0	10
27	272	281	82.9	85.6	0	0	0	90	0	0	0	10	0
28	281	291	85.6	88.7	0	0	0	100	0	0	0	0	0
29	291	301	88.7	91.7	0	0	0	60	0	0	0	20	20
30	301	309	91.7	94.2	0	0	0	70	0	0	0	10	20
31	309	318	94.2	96.9	10	0	0	60	0	0	10	10	10
32	318	327	96.9	99.7	0	0	0	70	0	0	0	20	10
33	327	336	99.7	102.4	0	0	0	90	0	0	0	10	0
34	336	346	102.4	105.5	0	0	0	100	0	0	0	0	0
35	346	355	105.5	108.2	0	0	0	100	0	0	0	0	0
36	355	366	108.2	111.6	0	0	0	100	0	0	0	0	0
37	366	375	111.6	114.3	20	0	0	80	0	0	0	10	0
38	375	384	114.3	117	10	0	0	80	0	0	0	0	10

FC79-16													
Box	**TD (ft)**	**BD (ft)**	**TD (m)**	**BD (m)**	**MI**	**SH**	**FS**	**BRh**	**BRd**	**VCB**	**CB**	**MB**	**FB**
1	0	18	0	5.5	0	0	0	20	0	10	10	20	40
2	18	26.8	5.5	8.2	0	0	0	40	0	0	10	20	30

3	Missing												
4	36.5	46	11.1	14	0	0	0	30	0	0	10	30	30
5	46	55	14	16.8	0	0	0	90	0	0	0	10	0
6	55	65	16.8	19.8	0	0	0	40	0	0	0	20	40
7	65	74	19.8	22.6	0	0	0	20	0	0	10	20	50
8	74	83	22.6	25.3	0	0	0	40	0	0	10	10	40
9	83	92	25.3	28	0	0	0	70	20	0	0	0	10
10	92	102	28	31.1	0	0	0	90	0	0	0	0	10
11	102	110	31.1	33.5	0	0	0	20	20	20	0	10	30
12	110	120	33.5	36.6	0	0	0	20	0	20	10	10	40
13	120	128	36.6	39	10	0	0	20	20	0	20	10	20
14	128	137	39	41.8	0	0	0	10	20	0	0	20	50
15	137	145	41.8	44.2	10	0	0	10	20	10	10	10	30
16	145	154	44.2	46.9	0	0	0	0	90	0	0	10	0
17	154	163	46.9	49.7	0	0	0	30	30	0	0	10	30
18	163	172	49.7	52.4	10	0	0	30	10	0	0	20	30
19	172	182	52.4	55.5	0	0	0	20	10	0	10	20	40
20	182	190	55.5	57.9	0	0	0	50	20	0	10	10	10
21	190	200	57.9	61	0	0	0	40	20	0	0	10	30
22	200	208	61	63.4	0	0	0	0	30	0	0	10	60
23	208	217	63.4	66.1	0	0	0	0	20	0	0	10	70
24	217	227	66.1	69.2	0	0	0	40	10	0	0	20	30
25	227	236	69.2	71.9	0	0	0	80	0	0	0	20	0
26	236	245	71.9	74.7	0	0	0	90	10	0	0	0	0
27	245	255	74.7	77.7	10	0	0	80	0	0	0	10	0
28	255	264.3	77.7	80.6	0	0	0	100	0	0	0	0	0
29	264.3	273	80.6	83.2	0	0	0	40	20	0	0	30	10
30	273	282	83.2	86	0	0	0	60	0	0	0	20	20
31	282	291	86	88.7	20	0	0	50	0	0	0	20	10
32	291	301	88.7	91.7	0	0	0	40	10	0	10	30	10
33	301	310	91.7	94.5	0	0	0	50	0	0	10	30	10
34	310	319	94.5	97.2	0	0	0	60	0	0	10	30	0
35	319	328	97.2	100	0	0	0	100	0	0	0	0	0
36	328	336	100	102.4	0	0	0	100	0	0	0	0	0
37	336	345	102.4	105.2	10	0	0	90	0	0	0	0	0
38	345	354	105.2	107.9	40	0	0	60	0	0	0	0	0

FC79-17													
Box	**TD (ft)**	**BD (ft)**	**TD (m)**	**BD (m)**	**M I**	**S H**	**F S**	**BR h**	**BR d**	**VC B**	**C B**	**M B**	**F B**

1	0	10	0	3	70	0	0	0	0	0	0	30	0
2	10	21	3	6.4	20	0	0	0	20	0	20	20	20
3	21	30	6.4	9.1	0	0	0	0	90	0	0	10	0
4	21	30	6.4	9.1	10	0	0	0	90	0	0	0	0
5	30	39	9.1	11.9	20	50	0	0	30	0	0	0	0
6	39	51	11.9	15.5	0	80	0	0	20	0	0	0	0
7	51	60	15.5	18.3	10	80	0	0	10	0	0	0	0
8	60	69	18.3	21	0	0	0	80	0	0	0	0	20
9	78	87	23.8	26.5	10	0	0	0	70	0	0	20	0
10	87	96	26.5	29.3	0	0	0	80	0	0	0	0	20
11	96	105	29.3	32	0	0	0	60	0	0	0	30	10
12	105	115	32	35.1	10	0	0	70	0	0	10	0	20
13	115	124	35.1	37.8	0	0	0	60	0	0	10	20	10
14	124	133	37.8	40.5	0	0	0	70	0	0	10	10	10
15	133	143	40.5	43.6	0	0	0	50	20	0	0	20	10
16	143	152	43.6	46.3	40	30	0	0	30	0	0	0	0
17	152	160	46.3	48.8	40	60	0	0	0	0	0	0	0
18	160	169	48.8	51.5	40	40	0	0	20	0	0	0	0
19	169	180	51.5	55	50	10	0	0	40	0	0	0	0
20	181	190	55.1	57.9	0	0	0	0	100	0	0	0	0
21	191	200	58.1	60.9	0	0	0	0	100	0	0	0	0
22	200	209	61	63.8	0	0	0	0	100	0	0	0	0
23	210	219	64	66.8	10	0	0	0	90	0	0	0	0
24	220	229	66.9	69.7	0	0	0	0	100	0	0	0	0
25	229	238	69.9	72.7	0	0	0	0	100	0	0	0	0
26	239	248	72.9	75.6	0	0	0	0	100	0	0	0	0
27	249	258	75.8	78.6	0	0	0	0	100	0	0	0	0

FC79-18													
Box	**TD (ft)**	**BD (ft)**	**TD (m)**	**BD (m)**	**MI**	**SH**	**FS**	**BRh**	**BRd**	**VCB**	**CB**	**MB**	**FB**
1	0	9	0	2.7	50	0	0	10	0	0	0	20	20

2	9	19	2.7	5.7	0	10	0	10	0	0	10	20	50
3	19	29	5.7	8.7	0	0	0	50	0	10	0	10	30
4	29	39	8.7	11.7	0	0	0	30	0	0	0	10	60
5	39	48	11.7	14.4	0	0	0	20	0	0	10	20	50
6	48	57	14.4	17.1	0	0	0	20	0	10	30	20	20
7	57	66	17.1	19.8	0	0	0	30	0	10	20	0	40
8	66	76	19.8	22.8	10	0	0	20	0	0	20	10	40
9	76	86	22.8	25.8	0	0	0	50	0	0	0	10	40
10	86	95	25.8	28.5	0	0	0	70	0	0	0	0	30
11	95	104	28.5	31.2	0	0	0	30	0	0	10	10	50
12	104	114	31.2	34.2	0	0	0	40	0	0	20	30	10
13	114	124	34.2	37.2	0	0	0	90	0	0	0	10	0
14	124	133	37.2	39.9	0	0	0	90	0	0	0	0	10
15	133	143	39.9	42.9	0	0	0	40	0	0	0	10	50
16	143	152	42.9	45.6	0	0	0	60	0	0	10	20	10
17	152	161	45.6	48.3	0	0	0	90	0	0	0	10	0
18	161	171	48.3	51.3	0	0	0	60	0	0	0	30	10
19	171	182	51.3	54.6	0	0	0	80	0	0	10	10	0
20	182	190	54.6	57	0	0	0	60	0	0	0	20	20
21	190	198	57	59.4	0	0	0	60	0	0	10	30	10
22	198	207	59.4	62.1	0	0	0	90	0	0	0	10	0
23	207	217	62.1	65.1	0	0	0	90	0	0	0	0	10
24	217	226	65.1	67.8	0	0	0	90	0	0	0	10	0
25	226	236	67.8	70.8	0	0	0	90	0	0	0	10	0
26	236	246	70.8	73.8	0	0	0	90	0	0	0	10	0
27	246	255	73.8	76.5	0	0	0	100	0	0	0	0	0
28	255	265	76.5	79.5	0	0	0	60	0	0	0	30	10

29	265	274	79.5	82.2	0	0	0	80	0	0	0	20	0
30	274	284	82.2	85.2	0	0	0	80	0	0	0	10	10
31	284	294	85.2	88.2	0	0	0	70	0	0	0	10	20
32	294	303	88.2	90.9	0	0	0	30	0	0	0	30	40
33	303	313	90.9	93.9	0	0	0	40	0	0	0	10	50
34	313	322	93.9	96.6	0	0	0	50	40	0	0	0	10
35	322	332	96.6	99.6	0	0	0	80	10	0	0	0	10
36	332	341	99.6	102.3	0	0	0	80	20	0	0	0	0
37	341	350	102.3	105	0	0	0	30	70	0	0	0	0
38	350	360	105	108	0	0	0	40	60	0	0	0	0
39	360	368	108	110.4	0	0	0	100	0	0	0	0	0
40	368	378	110.4	113.4	0	0	0	40	50	0	0	10	0
41	378	389	113.4	116.7	0	0	0	60	20	0	0	10	0
42	389	396	116.7	118.8	0	0	0	90	0	0	0	0	10
43	396	406	118.8	121.8	0	0	0	80	10	0	0	10	0
44	406	414	121.8	124.2	0	0	0	100	0	0	0	0	0
45	414	423	124.2	126.9	0	0	0	100	0	0	0	0	0
46	423	433	126.9	129.9	0	0	0	90	0	0	0	10	0
47	433	442	129.9	132.6	0	0	0	100	0	0	0	0	0
48	442	450	132.6	135	0	0	0	60	0	0	0	0	40
49	450	460	135	138	0	0	0	80	0	0	0	10	10
50	460	470	138	141	0	0	0	60	0	0	0	10	30
51	470	479	141	143.7	0	0	0	60	0	0	0	10	30
52	479	485	143.7	145.5	40	0	0	40	0	0	0	10	10
53	485	493	145.5	147.9	0	0	0	90	0	0	0	10	0
54	493	502	147.9	150.6	0	0	0	100	0	0	0	0	0
55	502	512	150.6	153.6	0	0	0	100	0	0	0	0	0
56	512	521	153.6	156.3	0	0	0	100	0	0	0	0	0
57	521	530	156.3	159	0	0	0	90	0	0	0	10	0
58	530	540	159	162	0	0	0	90	0	0	0	0	10
59	540	550	162	165	0	0	0	90	0	0	0	0	10

60	550	559	165	167.7	20	0	0	70	0	0	0	0	10
61	559	466	167.7	139.8	0	0	0	80	0	0	0	20	0
62	466	574	139.8	172.2	10	0	0	60	0	0	10	0	20
63	574	583	172.2	174.9	10	0	0	90	0	0	0	0	0
64	583	592	174.9	177.6	0	0	0	90	0	0	0	10	0
65	592	602	177.6	180.6	0	0	0	100	0	0	0	0	0
66	602	611	180.6	183.3	0	0	0	90	0	0	0	10	0
67	611	622	183.3	186.6	0	0	0	70	0	0	0	20	10
68	622	633	186.6	189.9	0	0	0	80	0	0	0	10	10
69	633	642	189.9	192.6	0	0	0	50	0	0	0	10	40
70	642	651	192.6	195.3	0	0	0	50	0	0	0	10	40
71	651	661	195.3	198.3	0	0	0	40	0	0	0	0	60
72	Missing												
73	670	679	201	203.7	0	0	0	70	0	0	0	0	30
74	679	690	203.7	207	20	0	0	50	0	0	0	0	30
75	690	700	207	210	0	0	0	60	0	0	0	0	40
76	700	710	210	213	0	0	0	100	0	0	0	0	0
77	720	730	216	219	50	0	0	40	0	0	10	0	0

Appendix B: List of melt-bearing thin-sections with corresponding measurements for the melt and clast sizes

Section	GreyMelt%	AmberMelt%	Clast%	GreyMeltSize(mm)	AmberMeltSize(mm)
3-183	0	30	45	0	30
3-184	0	15	70	0	6.54
3-191	<5	5	90	2.421	4.116
3-192	20	10	60	3.613	1.403
3-194	60	30	10	19.5	4.608

3-195	40	60	0	12.438	19.4862
3-198-A	15	30	60	2.3	5.74
3-198-B	5	35	40	2.609	21.115
3-199	5	20	70	2.889	1.884
3-200-B	30	15	40	1.2534	5.293
3-201	30	5	25	10.85	5.21
3-202	40	20	35	13.476	3.024
3-204	20	30	35	8.68	4.774
3-205	5	0	85	1.426	0
3-206-A	25	5	70	7.812	5.283
3-206-B	0	15	80	0	6.118
3-207-A	40	20	25	24.7	2.965
3-207-B	0	60	35	0	25
3-211	55	5	40	14.7	1.736
3-212	40	30	20	12.32	9.46
3-213-B	10	5	80	4.86	1.3
3-216	80	0	15	21.8	0
3-217	15	20	50	1.703	2.891
3-217-B	30	25	20	14.7	15

Appendix C: List of thin sections and places within thin section that were studied by microprobe analysis, as described in the methods and results. Number are in oxide weights.

Feldspars-Oxide Weight Percents								
Sample	**Na_2O**	**MgO**	**Al_2O_3**	**SiO_2**	**K_2O**	**CaO**	**FeO**	**MnO**
77-3-174-A	0.1474	1.3087	0	0.5397	0.0282	97.82	0.0078	0.1464
77-3-174 Test	0.1816	0.0791	1.1346	98.31	0.1461	0.0195	0	0.1287
77-3-174 Test 2	0.1932	0.244	3.87	94.59	0.7847	0.0506	0.1328	0.1368
77-3-174-Melt Zone	0.0788	0.0139	2.9781	94.54	2.333	0.0148	0.034	0.012
77-3-174-Breccia Seam	0.0635	0	0	99.88	0.0247	0.0257	0	0.0061
77-3-174-Matrix	0	0.0185	0.3767	99.53	0.0596	0.0015	0.0025	0.0062
77-3-185-Amber003	0.2273	8.02	3.92	85.9	1.4676	0.3353	0.1307	0
77-3-185-Calcite	0.1344	2.1032	0.1839	0	0.0458	97.41	0.1276	0
77-3-185-Amber002	0.0716	1.1426	9.29	84.6	4.56	0.108	0.1467	0.0807
77-3-185-Calcite	0	0.8649	0.4241	0	0.03	98.47	0	0.2062
77-3-185-Grey	0.0913	0	0.3503	99.4	0.0484	0.0655	0.0183	0.0274
77-3-185-Grey003	1.723	8.8	3.39	43.43	1.0768	40.75	0.828	0

Felsic Glass-Oxide Weight Percents									
Sample	Na_2O	MgO	Al_2O_3	SiO_2	K_2O	CaO	FeO	MnO	TiO2
77-3-174-AmberMelt	0.0219	0.0173	0.6016	92.94	0.1006	0.0088	6.28	0.0154	0.0098

Pyroxene-Oxide Weight Percents									
Sample	Na_2O	MgO	Al_2O_3	SiO_2	K_2O	CaO	FeO	MnO	TiO2
77-3-185-Amber	0.1807	1.9115	7.08	88.26	2.1367	0.1105	0.1894	0.0565	0.0818
77-3-185-Grey	0.2381	1.8044	15.53	73.48	8.31	0.0428	0.3081	0	0.2846